

# **LASER SURFACE TEXTURING ON FTO COATED GLASS**

*A thesis submitted towards partial fulfillment of the requirements for the  
degree of*

**Master of Technology (M.Tech.)**

**In**

**Laser Technology**

**by**

**ANANNYA SINHA**

**Examination Roll No. : M4LST22006**

**University Registration No. : 154561 of 2020-2021**

*Under the guidance of*

**PROF. (DR.) SOUREN MITRA**

Professor, Production Engineering Department  
Jadavpur University, Kolkata– 700032

**School of Laser Science and Engineering**

*Course affiliated to*

**Faculty of Engineering and Technology**

*and offered by*

**Faculty of Interdisciplinary Studies, Law and Management**

**Jadavpur University**

188, Raja S. C. Mallick Road, Kolkata -700032

India

**2022**

**M.TECH. IN LASER TECHNOLOGY**  
Course affiliated to  
**FACULTY OF ENGINEERING & TECHNOLOGY**  
Offered by  
**FACULTY OF INTERDISCIPLINARY STUDIES, LAW & MANAGEMENT**  
**JADAVPUR UNIVERSITY**

---

**CERTIFICATE OF RECOMMENDATION**

I, HEREBY, RECOMMEND THAT THE THESIS PREPARED UNDER MY SUPERVISION BY **ANANNYA SINHA** ENTITLED **LASER SURFACE TEXTURING ON FTO COATED GLASS** BE ACCEPTED IN THE PARTIAL FULFILLMENT OF THE REQUIREMENTS FOR THE DEGREE OF MASTER OF TECHNOLOGY IN LASER TECHNOLOGY DURING THE ACADEMIC SESSION 2020-2022.

-----  
**THESIS SUPERVISOR**

**(Dr. Souren Mitra)**

**Professor, Production Engineering Department,  
Jadavpur University, Kolkata-700 032**

Countersigned

-----  
**DIRECTOR**

**(Sri Dipten Misra)**

**School of Laser Science and Engineering  
Jadavpur University, Kolkata-700 032**

-----  
**DEAN**

**Faculty of Interdisciplinary Studies, Law and Management  
Jadavpur University, Kolkata-700 032**

**JADAVPUR UNIVERSITY**

**FACULTY OF INTERDISCIPLINARY STUDIES, LAW AND MANAGEMENT**

---

**CERTIFICATE OF APPROVAL \*\***

This foregoing thesis is hereby approved as a creditable study of an engineering subject carried out and presented in a manner satisfactory to warrant its acceptance as a pre-requisite to the degree for which it has been submitted. It is understood that by this approval the undersigned do not necessarily endorse or approve any statement made, opinion expressed or conclusion drawn therein but approve the thesis only for the purpose for which it has been submitted.

-----

-----

-----

**COMMITTEE OF FINAL EXAMINATION  
FOR EVALUATION OF THESIS**

\*\* Only in case the recommendation is concurred

## **DECLARATION OF ORIGINALITY AND COMPLIANCE OF ACADEMIC ETHICS**

The author hereby declares that this thesis contains original research work by the undersigned candidate, as part of her **Master of Technology in Laser Technology** studies during academic session 2020-2022.

All information in this document has been obtained and presented in accordance with academic rules and ethical conduct.

The author also declares that as required by the rules and conduct, the author has fully cited and referred all material and results that are not original to this work.

**NAME: ANANNYA SINHA**

**EXAMINATION ROLL NUMBER: M4LST22006**

**REGISTRATION NUMBER: 154561 of 2020-2021**

**THESIS TITLE: LASER SURFACE TEXTURING ON FTO  
COATED GLASS**

**SIGNATURE:**

**DATE:**

## **ACKNOWLEDGEMENT**

I have taken immense pleasure to express my warm gratitude to everyone who has helped me to complete this thesis.

First and foremost, I would like to convey my sincere gratitude to my supervisor **Dr. Souren Mitra**, Professor, Department of Production Engineering, Jadavpur University. I am deeply grateful to him for his valuable suggestions, assiduous guidance and constant inspiration at every aspect throughout the period of the thesis work.

I express my indebtedness to **Sri Dipten Misra**, Director, School of Laser Science and Engineering, Jadavpur University for his valuable suggestions, guidance and providing me the opportunity to perform the entire work in a systematic manner.

Also I would like to thank Dr. Sachindranath Das, Assistant Professor, Department of Instrumentation Science, Jadavpur University for helping me with proper guidance.

I would like to thank **Dr. K. Paramsivam** for his indebted help and cooperation in completing the thesis work. Also I would very much thankful to **Dr. Somnath Paul** for his constant support throughout the work.

I would like to thank **Sri Souradip Paul**, **Ms. Upama Dey** and **Sri Souvik Mal** for their continuous support, encouragements and selfless help for carrying out the entire thesis work.

Lastly but obviously not the least I would like to pay my special admiration thanks to my parents for their constant support, love and faith.

My eternal gratitude goes to God.

Anannya Sinha

Examination Roll No. : M4LST22006

Registration No. : 154561 of 2020-2021

## **Table of contents**

### **Title: LASER SURFACE TEXTURING ON FTO COATED GLASS**

<b>Title Sheet</b>	<b>i</b>
<b>Certificate of Recommendation</b>	<b>ii</b>
<b>Certificate of Approval</b>	<b>iii</b>
<b>Declaration of Originality and Compliance of Academic Ethics</b>	<b>iv</b>
<b>Acknowledgement</b>	<b>v</b>
<b>List of Figures</b>	<b>viii</b>
<b>List of Tables</b>	<b>xi</b>
<b>Chapter 1: Introduction</b>	<b>1-28</b>
1.1    Laser Surface Texturing	2
1.1.1    Need for Laser Surface Texturing	4
1.2    Fundamentals of Laser Surface Texturing	4
1.2.1    Process Parameters Involved	4
1.2.2    Types of Laser Used	6
1.2.3    Types of Pattern Formation	9
1.3    Singlemode and Multimode Laser for Surface Texturing	11
1.4    Application of Laser Surface Texturing	12
1.5    Literature Survey	17
1.6    Objective of Present Research	28
<b>Chapter 2: Experimental Setup, Procedure and Materials</b>	<b>29-48</b>
2.1 Experimental Setup and Measuring Equipment	30
2.1.1 Fibre Laser Cutting Machine	30
2.1.2 Measuring Equipment	35
2.1.2.1 Optical Microscope	35
2.1.2.2 UV-Vis Spectrophotometer	36

2.1.2.3 Surftest- Surface Roughness Tester	38
2.2 Materials Investigated	40
2.2.1 FTO Coated Glass	40
2.2.2 Copper	42
2.2.3 Aluminium	44
2.2.4 Stainless Steel	45
2.3 Analysis of Results	47
<b>Chapter 3: Experimental Investigation and Analysis</b>	<b>49-86</b>
3.1 Experimental Plan	50
3.1.1 Setting Parameters Levels	52
3.1.2 Plan of Experiment	52
3.1.3 Sample Preparation	53
3.2 Experimental Procedure	54
3.3 Analysis of the Effect of Variable Parameters on Wavelength	57
3.3.1 Results for Un-textured FTO Coated Glass	58
3.3.2 Results Obtained for Textured FTO Coated Glass	59
3.3.3 Analysis of S/N Ratio Plots for Wavelength	72
3.4 Analysis of the Effect of variable parameters on Surface Roughness	78
3.4.1 Results Obtained for an Un-textured FTO Coated Glass	79
3.4.2 Results Obtained for Textured FTO Coated Glass	79
3.4.3 Analysis of S/N Ratio Plots for Surface Roughness	80
<b>Chapter 4 : General Conclusion and Future Scope of Research</b>	<b>87-89</b>
4.1 General Conclusion	88
4.2 Future Scope of Research	89
<b>Reference</b>	<b>90-93</b>
<b>Appendix</b>	<b>94-107</b>

## List of Figures

Fig 1.1 Schematic Diagram of Laser Surface Texturing	3
Fig 1.2 Schematic Diagram of a Nd:YAG Laser	7
Fig 1.3 Schematic Diagram of a Carbon-di-oxide Laser	8
Fig 1.4 Schematic Diagram of an Excimer Laser	9
Fig 1.5 Multimode and Singlemode Laser Operations	12
Fig 1.6 Adhesive Bonding by Laser Texturing	13
Fig 1.7 Mechanical Seals by Laser Texturing	13
Fig 1.8 Laser Induced Coating	14
Fig 1.9 Laser Cladding	15
Fig 1.10 Laser Texturing inducing energy absorption	15
Fig 1.11 Laser Induced Thermal Spraying	16
Fig 2.1 Fiber Laser Cutting Machine	31
Fig 2.1 a) Fiber Laser System	31
Fig 2.1 b) Console Monitor for the Laser	31
Fig 2.1 c) Chiller Unit of the Laser	32
Fig 2.1 d) Assist Gas Cylinder	33
Fig 2.1 e) Voltage Stabilizer of the Laser	33
Fig 2.1 f) Clipping Unit of the Equipment	34
Fig 2.2 Cypcut Laser Cutting Software Screen Display	35
Fig 2.3 Optical Microscope	36
Fig 2.4 UV-Vis Spectrophotometer	37
Fig 2.5 Inside view of UV-Vis Spectrophotometer	37
Fig 2.6 UV-Vis Spectrophotometer Software Screen Display	38



Fig 2.7 Surface Roughness Tester	39
Fig 2.8 Close view of a probe testing a FTO sample	39
Fig 2.9 FTO Coated Glass	40
Fig 2.10 Fluorine doped tin oxide (FTO)	41
Fig 2.11 Copper Plates (Base Material)	43
Fig 2.12 Aluminium Sheets (Base Material)	45
Fig 2.13 Stainless Steel Sheets (Base Material)	46
Fig 2.14 8 step Flowchart Diagram for Taguchi Analysis	48
Fig 3.1 Texturing of Laser on FTO Coated Glass	55
Fig 3.2 Experimentation of Textured FTO Coated Glass in Spectrophotometer	56
Fig 3.3 Graph of absorbance for un-textured FTO Coated Glass	58
Fig 3.4 FTO Coated Glass after Experimentation 1	59
Fig 3.5 Graph for absorbance after Experimentation 1	60
Fig 3.6 FTO Coated Glass after Experimentation 2	60
Fig 3.7 Graph for absorbance after Experimentation 2	61
Fig 3.8 FTO Coated Glass after Experimentation 3	62
Fig 3.9 Graph for absorbance after Experimentation 3	63
Fig 3.10 FTO Coated Glass after Experimentation 4	63
Fig 3.11 Graph for absorbance after Experimentation 4	64
Fig 3.12 FTO Coated Glass after Experimentation 5	65
Fig 3.13 Graph for absorbance after Experimentation 5	66
Fig 3.14 FTO Coated Glass after Experimentation 6	66
Fig 3.15 Graph for absorbance after Experimentation 6	67
Fig 3.16 FTO Coated Glass after Experimentation 7	68
Fig 3.17 Graph for absorbance after Experimentation 7	69

Fig 3.18 FTO Coated Glass after Experimentation 8	69
Fig 3.19 Graph for absorbance after Experimentation 8	70
Fig 3.20 FTO Coated Glass after Experimentation 9	71
Fig 3.20 Graph for absorbance after Experimentation 9	72
Fig 3.21 Residual Plot for Means	75
Fig 3.22 Residual Plots for SN Ratios	75
Fig 3.23 Main Effects Plots for Means	76
Fig 3.24 Main Effects Plot for SN Ratios	76
Fig 3.25 Main Effects Plots for Means	82
Fig 3.26 Main Effects Plot for SN Ratios	83
Fig 3.27 Residual Plots for SN Ratios	84
Fig 3.28 Residual Plots for Means	84

## **List of Tables**

Table 2.1 Specifications of the Fiber Laser Cutting Machine	32
Table 2.2 Specifications of the Surface Roughness Tester	40
Table 2.3 Comparison between ITO and FTO	42
Table 2.4 Characteristics of Copper	42
Table 2.5 Characteristics of Aluminium	44
Table 2.6 Characteristics of Stainless Steel	46
Table 3.1 Trial and Errors for experimentation	51
Table 3.2 Parameter Levels	52
Table 3.3 Plan of Experiment	53
Table 3.4 Response on Wavelength at variable parameters	57
Table 3.5 Absorbance on un-textured FTO Coated Glass	58
Table 3.5 Response for absorbance in terms of wavelength after Experimentation 1	59
Table 3.6 Response for absorbance in terms of wavelength after Experimentation 2	61
Table 3.7 Response for absorbance in terms of wavelength after Experimentation 3	62
Table 3.8 Response for absorbance in terms of wavelength after Experimentation 4	64
Table 3.9 Response for absorbance in terms of wavelength after Experimentation 5	65
Table 3.10 Response for absorbance in terms of wavelength after Experimentation 6	67
Table 3.11 Response for absorbance in terms of wavelength after Experimentation 7	68
Table 3.12 Response for absorbance in terms of wavelength after Experimentation 8	70
Table 3.13 Response for absorbance in terms of wavelength after Experimentation 9	71
Table 3.14 Analysis of Variable in terms of Wavelength	72
Table 3.15 Estimated Model Coefficients for SN ratios	73
Table 3.16 Model Summary	73
Table 3.17 Analysis of Variance for SN ratios	73
Table 3.18 Estimated Model Coefficients for Means	74
Table 3.19 Model Summary	74

Table 3.20 Analysis of Variance for Means	74
Table 3.21 Analysis of Variable in terms of Surface Roughness	78
Table 3.22 Surface Roughness for un-textured FTO Glass	79
Table 3.23 Surface Roughness for textured FTO Glass at different input parameters	79
Table 3.24 Analysis of Variable in terms of Surface Roughness (Ra)	80
Table 3.25 Estimated Model Coefficients for SN ratios	80
Table 3.26 Model Summary	80
Table 3.27 Analysis of Variance for SN ratios	81
Table 3.28 Estimated Model Coefficients for Means	81
Table 3.29 Model Summary	81
Table 3.30 Analysis of Variance for Means	81

# **Chapter – 1**

## **Introduction**

## **1. Introduction**

FTO (Fluorine doped Tin Oxide) is a transparent conducting film made over a glass substrate that is electrically conductive in nature. FTO Coated glass substrates are basically used in solar cell panels for light absorption of the sunrays and later converted to energy for use. However glass being an optically transparent and non-conducting material doesn't help much in the absorption and hence is used with FTO coating. Though FTO is conductive in nature but still most of the light gets transmitted through it. Laser Surface Texturing makes the FTO coated glass substrate surface duly uneven in nature which shortens the light paths entering in the substrate and traps them. Hence a certain part of the light does get absorbed into the material which can be later used for energy conversion.

Some of the Applications of FTO coated glass includes:

- Thin film Solar Cells
- Touch Panels
- Electroluminescent (EL) Devices
- Optical Devices
- Liquid Crystal Devices (LCDs)

### **1.1 Laser Surface Texturing**

Laser Surface Texturing is a method that alters the surface properties of any material by modifying its roughness, texture and optical properties. It is one of the most efficient methods that improve the tribological performance of a material. The laser radiation creates micro patterns like groves or dimples of any free forms of any shape and size on the material surface through laser ablation i.e. removing the layers of the surface with micrometer precision and consistent repeatability. It can be used to improve surface properties like wettability, adherence, electrical and thermal conductivity and also to prepare surface for thermal spray coating and laser cladding. Laser Surface Texturing has gained suitable interest amongst the other modification methods due to its good controllability, high flexibility and superior texturing accuracy.

By adjusting the laser parameters we will be able to control the amount of material to be removed by ablation of the significant pattern that we need to make. To reach the working material's ablation threshold, the pulsed lasers concentrate the energy from the laser beam to reach a high peak power. Usually the pulse duration is 100 nanoseconds where each pulses consists of about 0.5 to 1 mili Joules of energy. However the time required to texture the surface depends on a few factors like the material to be worked on, the desired surface roughness and the laser system's power output.

Laser Surface texturing is different from other texturing methods due to its unique nature of not using any consumables while texturing the surface of any material. Surface modification methods like chemical etching or abrasive blasting uses consumables like acid or chemicals and steel respectively to get the desired outputs.

This uniqueness of Laser Texturing results in many advantageous outcomes like low maintenance, low operating costs, less environmental wastes etc. The operators no more need to deal with any sort of chemicals and hence wear protective gears. Also Laser Surface Texturing being a non-contact process reduces chances of any kind health hazards to take place.

Laser Surface Texturing is one of the most advancing texturing methods for surface treatment of materials. The process designs of Laser Surface Texturing include direct laser ablation, laser interference, and laser shock processing. The effects of laser parameters on the texture features are highlighted. The enhanced tribological properties of LST-processed materials and their applications on various fields are reviewed. The current challenges and future directions of LST techniques include in various fields of modern technologies like energy absorption or biomedical applications.

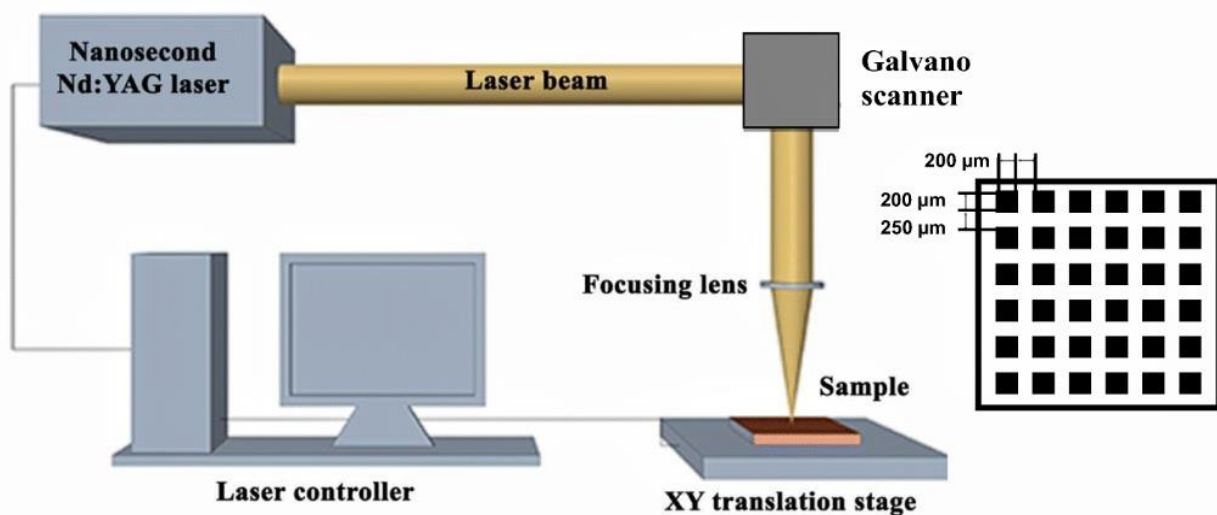


Fig 1.1 Schematic Diagram of Laser Surface Texturing

### **1.1.1 Need for Laser Surface Texturing**

1. Laser Surface Texturing can be used to improve certain properties like thermal and electrical conductivity, wettability, adherence and reduction in friction.
2. Laser Surface Texturing can also be used as surface preparation before thermal spray coating and laser cladding to improve the quality of the mechanical seals.
3. It is an efficient, reliable and repeatable process which is controlled by suitable computer mechanisms.
4. Reduces labor and Production time in comparison to other methods of texturing.
5. Laser Surface Texturing is a cost efficient method of surface modification.
6. It has a more précised method of working in comparison to other etching methods like acid etching as chemicals involved in this method cannot accurately calculate the correct depth or width of the texture.
7. Laser Texturing have a very high level of control over the microstructures produced which in return help to reduce the environmental impact of this process in comparison to the other methods.
8. It lacks the need of any chemical reagents of other consumables and thus helps in a significant reduction in waste

## **1.2 Fundamentals of Laser Surface Texturing**

### **1.2.1 Process Parameters Involved**

#### **Peak Power**

Peak power is basically the maximum optimal power that a laser pulse will attain in its period of work. It indicates the amount of energy that a laser pulse contains. A high peak power is one that has either high energy per pulse or short pulse width comparatively. Peak power can be mathematically represented as:  $\text{Peak Power (W)} = \text{Energy per pulse (J)} / \text{Pulse width (s)}$ . High power lasers are more expensive and produce more waste heat. With variation in peak power of a laser, the dimensions of the groove or dimple formed due to texturing will also vary accordingly. Deeper grooves will be formed with increase in peak power and shallow ones with decrease in peak power.

#### **Pulse Wavelength**

The laser pulse wave is a non-periodic waveform that consists of crest and valleys. Like other waveforms, a pulse has an amplitude and velocity. Pulse wavelength is the distance between two consecutive peaks or valleys. The shortest pulse wavelengths range from 10 to 400 nm to produce ultraviolet light, intermediate pulse wavelength range from 380 to 740 nm to produce visible radiation from violet to red and the longest wave range from 700nm to 1mm to produce



infrared radiation. Both infrared and UV radiations are invisible to human eye. Shorter the wavelength more précised is the texturing obtained.

### **Beam Diameter**

The beam diameter can be measured along the propagation axis. The focal spot can be very small and with it the beam size varies very rapidly along the axis of propagation. When the beam diameter is decreased, the power density increases so does the depth of the textures formed on the material surface.

### **Pulse Duration**

The pulse duration (fs to ms) is the time the laser pulse take to deliver energy to the surface of the material to be treated. They are the full width at half maximum of the laser's optical power vs time.

### **Scanning Speed**

The scan speed of the laser system is possibly how fast the laser can scan a particular area to be worked on. It can also be described in as how fast the laser head moves on the surface to give desired results. As the scanning speed increases the depth of the groves or dimples or textures formed on the material surface decreases

### **Pulse Repetition Rate**

Pulse repetition rate describes the number of pulses emitted per second. Pulse repetition rate is inversely proportional to the pulse energy and directly proportional to the average power. High repetition rates result in generation of rapid heating at the final focused spot and thus increasing the HAZ. Hence for better results at texturing the repetition rates need to be intermediate or low.

### **Surface Geometry**

The surface geometry of the material to be worked on also plays an important role in Laser Surface Texturing. The surface of the material needs to be flat for precise texturing. Uniform surfaces lead to best results, However on the rough surface the surface texturing becomes less evident.

### **Working Distance**

Working distance is the physical distance from the optical element (focusing lens) to the object or the surface to be worked on. In laser Surface texting the working range is aimed to maximize so that it doesn't produce too much of a HAZ thereby disrupting the desired texture to be formed.

## 1.2.2 Types of Lasers used

### Nd:YAG Laser

Neodymium-doped Yttrium Aluminum Garnet (Nd:YAG) laser is a solid state laser. Its formula is  $\text{Y}_{2.97}\text{Nd}_{0.03}\text{Al}_5\text{O}_{12}$ . Neodymium doping concentration is 0.725% by weight. It is a four leveled laser system which operate in both continuous and pulsed modes. This laser consists of wavelength in the near infrared region of the spectrum at 1064nm. It also operates at other wavelengths like 1440nm, 1320nm, 1120nm, 940nm.

It consists of 3 important elements namely an energy source, active medium and an optical resonator. Energy source or pump source supplies energy for population inversion. Usually laser diodes or flashtubes are used as energy sources in the laser. The active medium of the laser is made up of Yttrium Aluminum Garnet doped with the chemical element Neodymium. The electrons from lower energy states of Neodymium ion are excited to higher energy states to provide with the lasing action. The optical resonator part consists of two optically coated mirrors, one fully coated with silver and the other partially coated with silver and the Nd:YAG crystal is placed between these two mirrors.

When external pumping is given to the active medium of the laser then electrons at lower energy states gain energy and jump from lower energy states to the higher unstable energy state. Once the electrons gets exhaust of its energy in the higher state it comes to the metastable state and then population inversion is achieved. It then emits energy in form of photons and then again the electrons owing to their short lifespan over there jump back to the lower energy state.

Typical types of Nd:YAG lasers that are used are (a) Lamp pumped lasers which can operate at a very low fractional excitation of the activated ions in laser, (b) Diode pumped lasers which are made of relatively small sized crystals. For mode locking Nd:YAG lasers are less suitable because of its limited gain bandwidth.

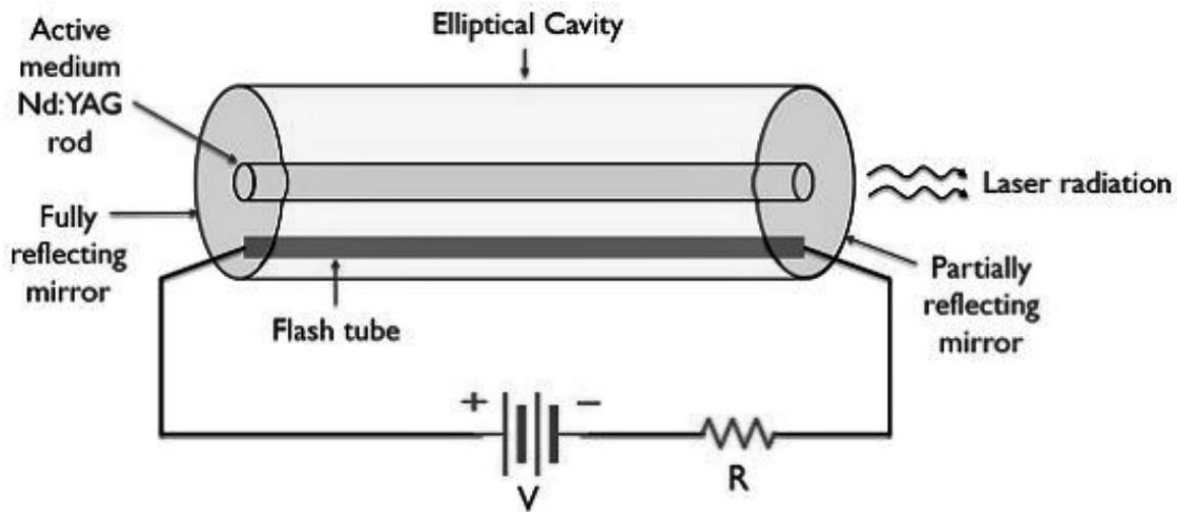


Fig 1.2 Schematic Diagram of a Nd:YAG Laser

## CO<sub>2</sub> Laser

It is one of the earliest developed lasers. It is a high power continuous wave type lasers and ablative in nature. It consists of two concave mirrors that form the resonant cavity. It produces radiations in the infrared region of the spectrum having wavelength between 9600 to 10600 nm. CO<sub>2</sub> is a symmetric molecule (O=C=O) and consists of 3 vibration modes namely: symmetric stretching, bending and asymmetric stretching.

It is very useful in industrial purpose for its high power levels. Carbon di oxide lasers are frequently used for the purpose of cutting and welding whereas as the low power lasers are used for engraving (texturing). It also finds its use in Selective Laser Sintering (SLS). It is basically used for its advantageous nature of minimal damage to the surroundings surface upon which it is worked on.

There are two type of CO<sub>2</sub> lasers used in small and medium laser machines namely DC or Glass tubes and RF or metal/ceramic lasers. The optical quality of DC is better than RF and hence produces narrower kerf and a better focus spot. However switching time of RF lasers are faster than DC laser which results in précised engraving or texturing detail and an increase in engraving speed without hampering the quality of work.

CO<sub>2</sub> laser is a mixture of Carbon di oxide and nitrogen in the ratio of 0.8:1. The mixture also consists of Helium. The CO<sub>2</sub> molecules act as the active medium and the nitrogen molecules help in achieving the population inversion. When electric discharge is allowed to pass through the

tube, electrons get emitted and they pump the nitrogen molecules to a vibrational state. This state of  $N_2$  is metastable and provides much time for collision between excited  $N_2$  molecules and  $CO_2$  molecules in ground state. Hence  $CO_2$  molecules get excited to higher energy state and population inversion achieved. As the electrons lose energy and jump back to their initial states they emit energy in form of photons in the infrared region.

Carbon di oxide lasers have high efficiency and high output power which can be further increased by increasing the length of gas tube. However the contamination of the oxygen by carbon monoxide leaves a detrimental effect on the long run of the laser action.

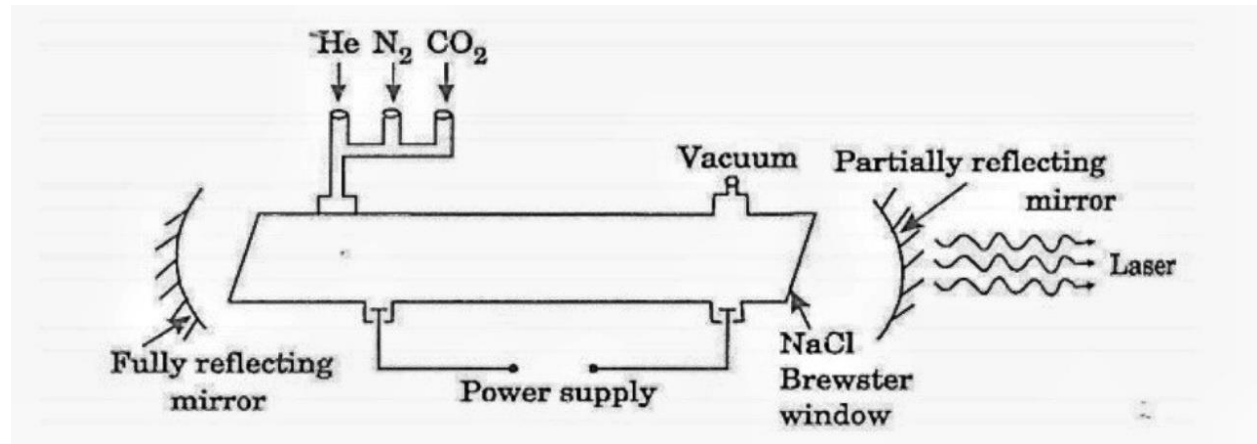


Fig 1.3 Schematic Diagram of Carbon-di-Oxide Laser

## Excimer Laser

The term excimer basically means excited dimer i.e a molecular complex of two atoms that stable only in an electronically excited state. It is an Ultraviolet (UV) laser that uses a noble gas component as its gain medium. These lasers have the ability to oscillate at exceptionally high frequency for lasers in the UV range. It is widely used in texturing of surfaces for such characteristics as well as in biomedical applications like LASIK treatments and many more.

Excimer laser consists of basically 3 components namely a pump which is the energy source, the gain medium and an optical resonator. The energy from the pump is amplified by the gain medium. This energy is converted to light and reflected by the optical resonator as the output laser beam. The laser medium (gain) is filled with mainly 3 types of gases. A noble gas, halogen gas of a buffer gas.

The Excimer laser ablation is a surface structuring technique based on interaction of the laser pulses with the working material. This results in electronic excitations which results in local ejection of the material. The presence of non-thermal reactions leads to a clean and well defined geometry of the output surface textures of desired ablated zones.

The advantages of an Excimer laser include their capability of producing a very minute and précised spot at a very low wavelength. The spot diameter produced by Excimer laser is about 40 times smaller in comparison to any other laser. Hence they are useful in laser surface texturing. They are also efficient in removing excess material through laser ablation asthey can destroy the targeted spot with little or no thermal buildup.

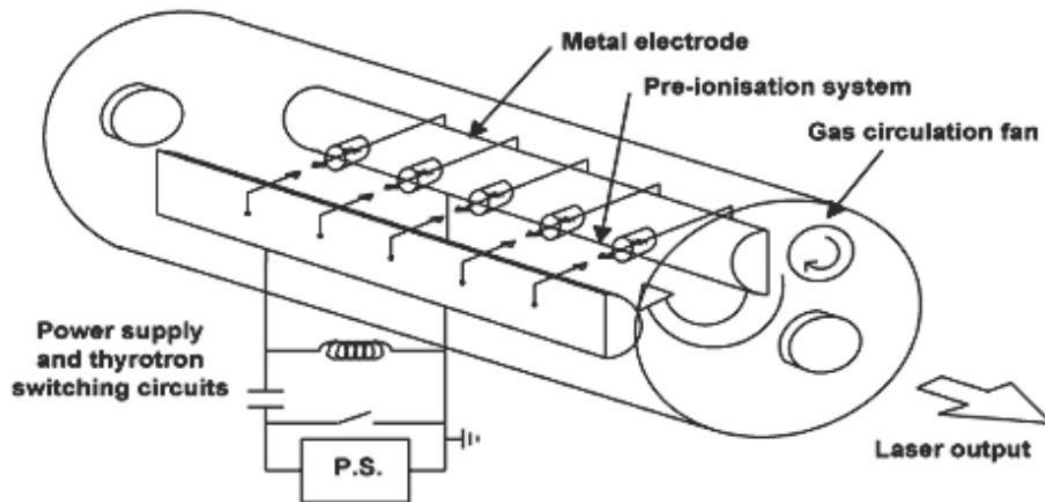


Fig 1.4 Schematic Diagram of an Excimer Laser

### 1.2.3 Types of Pattern Formations

The laser beam position with respect to the work piece is manipulated in order to get the desired patterned outputs. There are mainly three main methods of controlling the desired patterns namely direct beam method, scanning method and the use of interference methods. The method to be used depends on the geometry of pattern and scale of production.

#### Direct Beam Method

In this method the laser beam is straightaway directed to the material surface. An ablation head focuses the laser and high pressure gas blows away the melted part of material. The relative position of the ablation head can be easily manipulated along with the work piece position and duration of laser pulses to get the desired output geometry of patterns.

#### Scanning Method

Another method to control the output pattern is the scanning system where the laser beam is reflected by a series of motorized mirrors which can easily focus the laser to the micro cavity to be created. In order to check that the beam does not hit the material at an angle a flat field lens is

being used to keep in check that the beam and material surface are perpendicular to each other at point of contact.

### **Interference Patterns**

In order to create patterned grooves, optical interference patterns are used. The interference pattern covers the entire area of beam diameter and creates many micro cavities all at once. In order to create cross grooves at first the material can be oriented at a certain position and exposed to laser and then rotated 90 degrees to undergo the same exposure again.

Some other important features when working with laser includes

#### **a. Pore Geometry, Size, and Frequency**

It is not an exact science to determine the ideal micro pore patterning and shape for the best tribological features as it depends on several application-specific parameters. It is discovered that with dimple-like depressions, the precise geometry is not as important as the ratio between pore diameter and depth and the percentage of the surface area covered by pores. [1] The following application parameters can affect the ideal pore ratio and area fraction: Maximum load, Pressure, Material, Sliding Speed.

The majority of the recent research indicates that 10 to 15 percent of the pore area should be covered. Additionally, the ideal pore diameter is typically 10  $\mu$ m. The lubricating film clearance decreases and a dramatic increase in friction is observed with increasing pore sizes. LST is discovered to work best in some high pressure applications when only a portion of the contact surface is textured. The load capacity between the surfaces can be significantly increased by just texturing a portion of the surface.

#### **b. Finishing Operations**

The target material must be melted, ablated, and blown away by high pressure gas for laser surface texturing to work. Excess melt rims and slag are visible on a surface after LST has been applied to it as a byproduct of the laser processing. For the intended surface geometry to operate as expected, these melt rims and surplus re-solidified material must be eliminated through polishing. Gentle abrasives and common mechanical polishing methods can be used for this polishing.

To enhance surface properties, coatings may also be used following LST. To enhance specific surface properties like hardness and wear, films made of materials like diamond-like carbon and Ti alloys can be used.

## **1.3 Single Mode and Multimode Laser for Surface Texturing**

### **Single Mode Operation**

A single mode laser also known as a single frequency laser is a laser that operates on a single resonator mode it thus emits quasi monochromatic radiation with very low phase noise and small line width

### **Multimode Operation.**

A multimode laser is a laser beam with a single spatial mode but multiple frequencies. While monochromatic multimode beams exhibit granular intensity patterns, the polychromatic multimode beams can have smooth profiles.

### **Difference between Multimode and Singlemode Laser**

In Laser Surface Texturing the focused spot is of great significance to the quality of patterns produced. The core in case of single mode laser is comparatively thin and the quality of beam is also better than multimode. Also in single mode the energy distribution is as per Gaussian mapping where the intermediate energy density is the highest.

However the core of the multimode beam is coarser than that of single mode one. The energy distribution is smaller comparatively as well. The 3-D image of energy distribution is like an inverted cup

The 1mm thin plate texturing precision is 20% higher than multimode in single mode but from 2mm the speed advantage gradually decreases. Now if we need to decide which one is advantageous we can clearly notice that single mode finds its advantage in thin sheets of material and multimode is more advantageous in thick sheets.

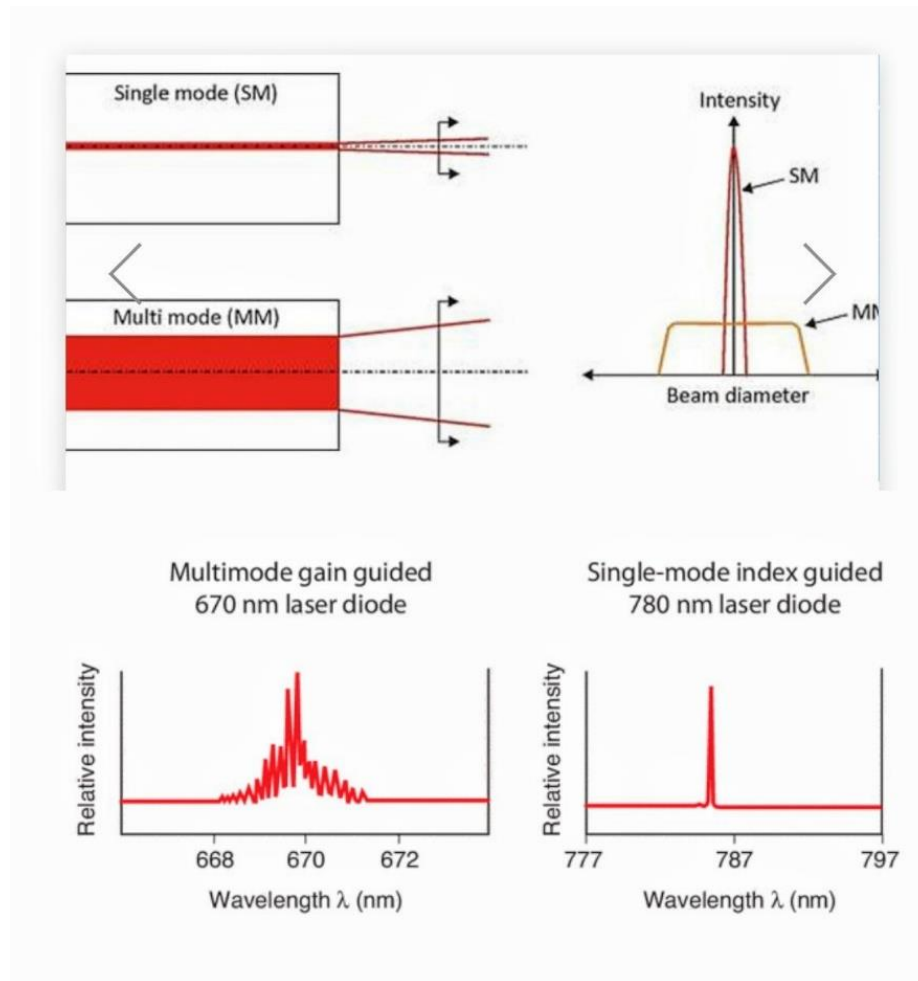


Fig 1.5 Multimode and Singlemode Laser Operations

## 1.4 Applications of Laser Surface Texturing

### Adhesive Bonding

Laser Surface Texturing can be used to produce robust and predictable bonds without causing any defects to the surface. Laser Texturing unlike other etching methods like grit blasting or acid etching do not produce any micro cracks or hinder the bond's strength. By enhancing the surface characteristics like roughness or surface area laser texturing improves the mechanical interlocking between the bonded parts. This results in an improved bond strength, wettability and porosity.



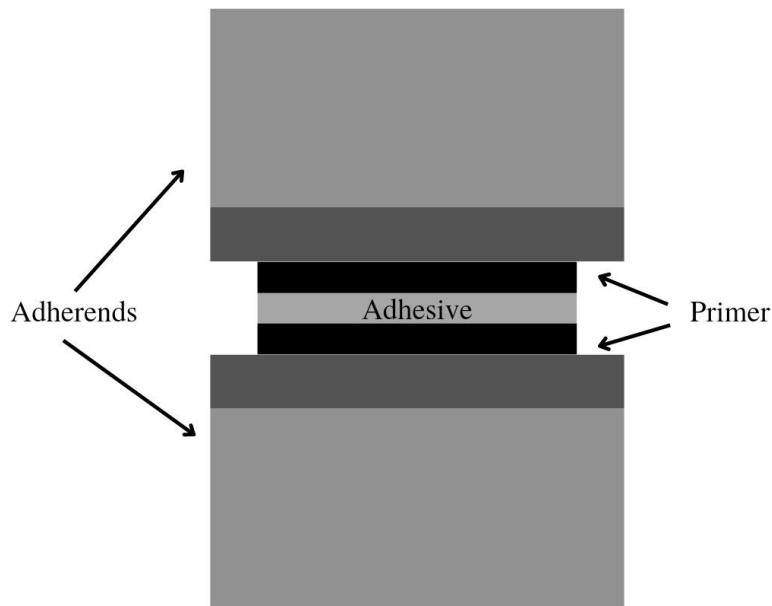


Fig 1.6 Adhesive Bonding by Laser Texturing

### Mechanical Seals

Laser Texturing enhances the adhesion of the mechanical seals which are subjected to friction and high pressure by texturing their surfaces with various patterns like that of a groove or dimple. The surface texturing significantly improves the tribological properties of the mechanical seals. The patterns (dimples and grooves) formed on the seal surface retain lubricants, thereby improving the seal's durability and reducing its friction.

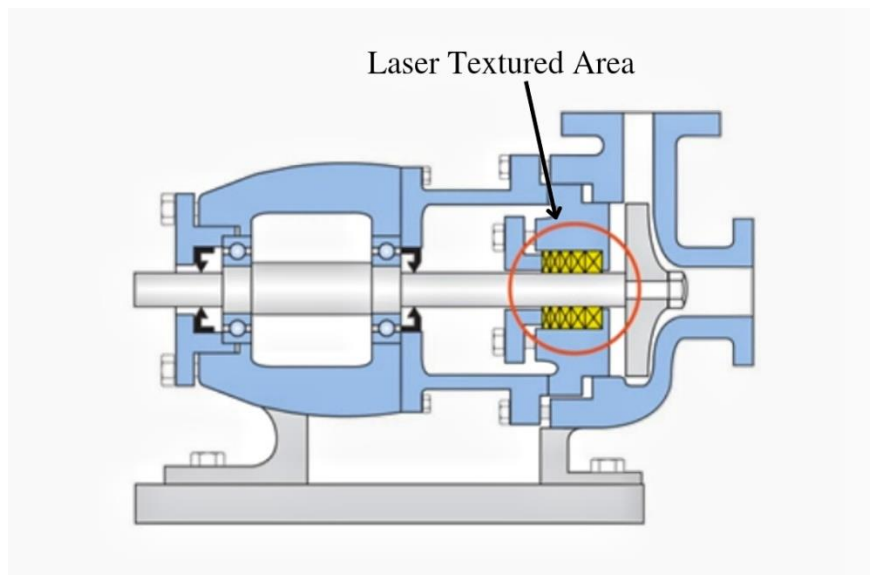


Fig 1.7 Mechanical Seals by Laser Texturing

## Paintings and Coatings

Laser Texturing can be used to prepare surfaces are more feasible for holding the paint or any sort of coating for more duration or more efficiently. Paints usually stick well to the surfaces that are clean and wavy or rough and this can be achieved by laser texturing. Laser texturing improves the surface adhesion and durability by removing any surface contamination or dirt and thereby improving the electrostatic bond between the paint and surface. This method also prevents peeling off of the paint by forming a corrosion resistant oxide layer.

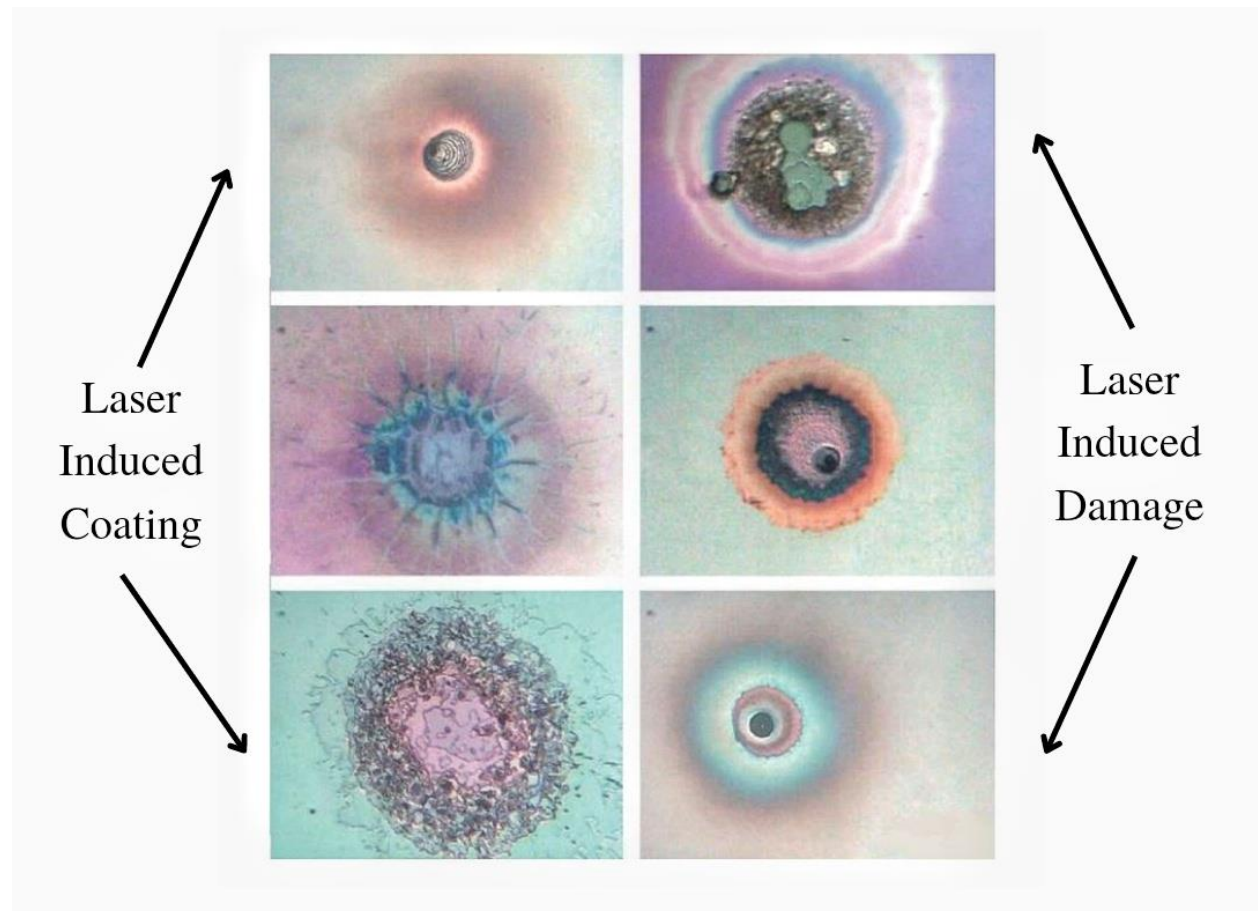


Fig 1.8 Laser Induced Coating

## Laser Cladding

Laser Texturing can be used to etch a precise and repetitive textured surface thereby preparing a better surface for laser cladding. Other surface treatment methods like abrasive blasting forms surface defects that hampers the efficiency of laser cladding No such problems arise when the surface is prepared using laser texturing method.

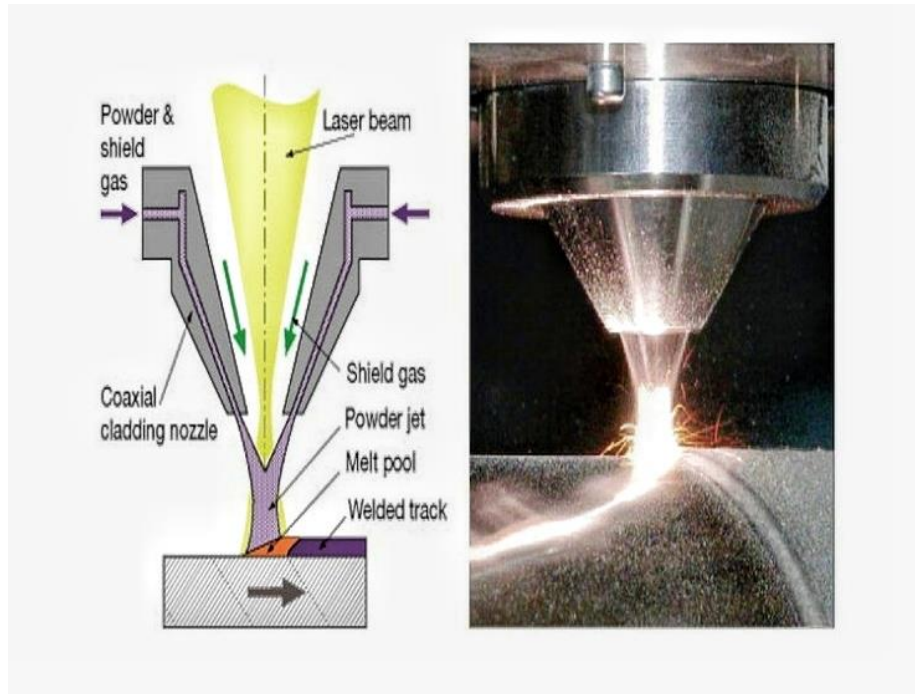


Fig 1.9 Laser Cladding

### Energy Absorption

Laser Texturing forms suitable patterns in a material surface. These surface textured materials can be used in any light energy trapping situation say a solar cell panel where owing to the rough (textured) surface of the material the incident light ray paths get shortened and fail to escape hence most of the energy get absorbed thereby increasing the efficiency of the panel. This method acts as light trapping technique and is also called anti reflection coating.

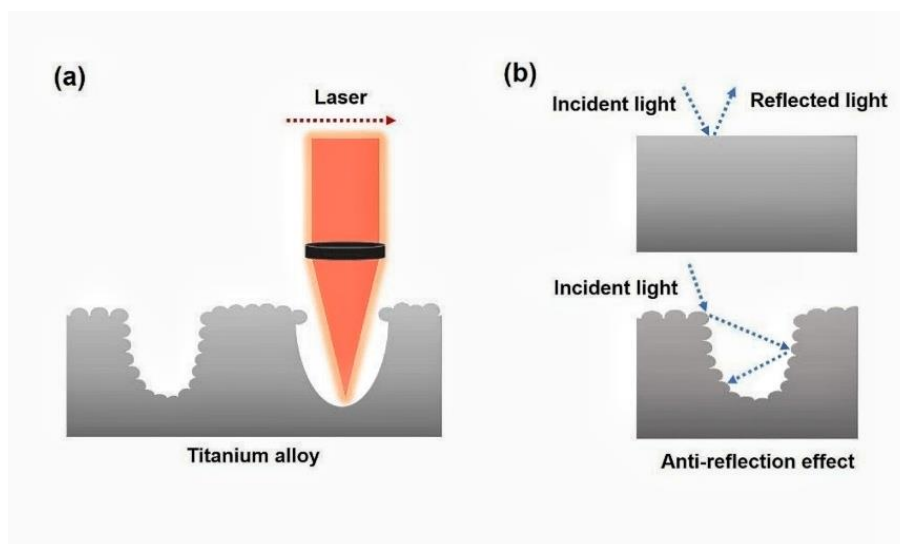


Fig 1.10 Laser Texturing inducing energy absorption

## Thermal Spray Coating

Laser Texturing improves the surface roughness of a material which in return increases the wettability of the material and hence enhances splat spreading, thereby forming stronger bonds between coating and the material surface. It also checks the optimal values of the coating's density and porosity. Treating soft metals like aluminum and magnesium with grit blasting or chemical etching will hamper their surface causing major cracks but however Laser texturing does not allow such thing to happen but the textures block the propagation of cracks to happen. Laser Texturing is efficient in spraying techniques like plasma and cols spraying.

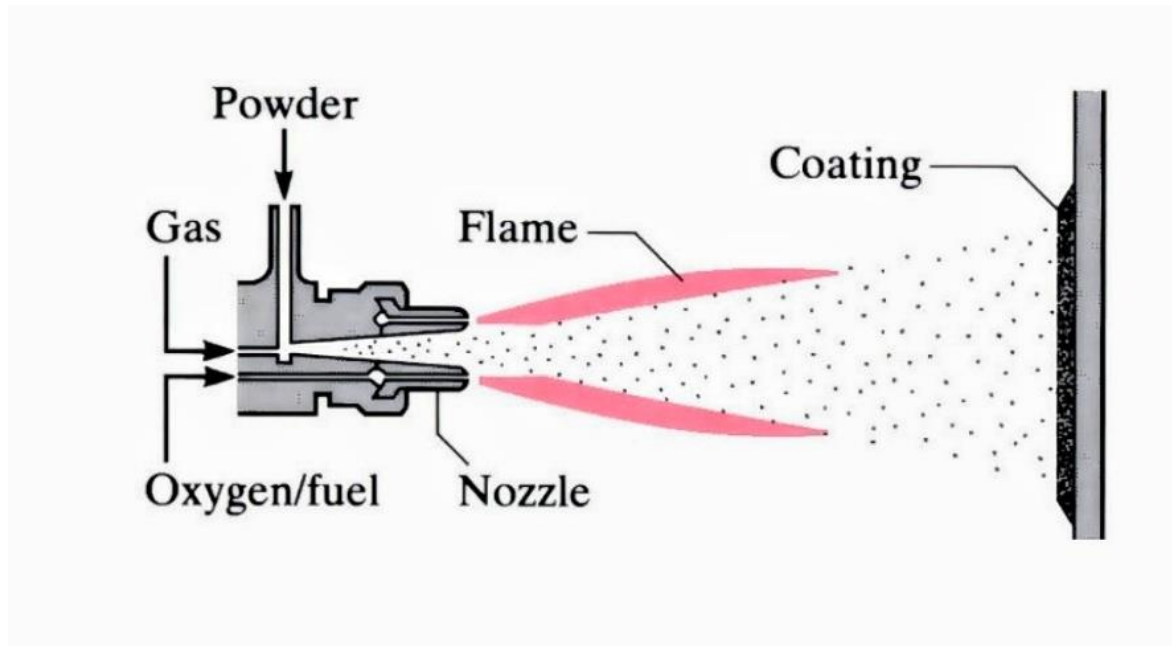


Fig 1.11 Laser Induced Thermal Spraying

## 1.5 Literature Survey

Campbell [1] in his paper shows research that are vividly used to enhance absorption of in thin semiconducting devices such as solar cells. This enhancement is achieved due to internal light being scattered into directions that are totally internally reflected, permitting absorption to enhance. This paper first compares the path length enhancing properties of scatter, whatever the incident angle. Under isotropic incidence at band gap wavelengths absorption enhancement from a randomizing texture can be equaled by many other textures. However, at more strongly absorbed wavelengths, Path length enhancement cannot be used as a performance indicator. One texture has been estimated at normal incidence to enhance absorption of the solar spectrum by 1.8-3% more than a randomizing texture over substrate thicknesses of 280-50 m by developing a higher ratio of trapped-to-escaping modes during early stages of scatter.

Wonga et al [2] studied on improvement of adhesive bonding in aluminum alloys using a laser surface texturing process. Study was done for the laser surface modification of aluminum alloys for the betterment of their adhesive joints. In the process two factor were noticed, one being the concentric circle formation on the alloy surface and the other one being micro cracks which affects the long-term mechanical performance of the metal substrate. Melt pools were observed on the alloy surface covering about 3% of the total surface area distributed randomly all over. Cracks appear to within the melt pool, and did not propagated beyond the pool periphery. Micro cracks tend to appear mostly with increasing intensity of the laser. Cracking phenomenon is mostly material dependent. By pulse shaping technique, both concentric rings and micro cracks could be tailored, to a certain extent, so as to suit better the needs for improving the adhesive bonding of aluminum alloys after the surface texturing.

Damborenea [3] in his paper performed a study on two laser surface modification methods namely Laser Alloying and Laser Cladding. In laser alloying different methods are used to deposit the alloy layer onto the substrate: preplacing the alloying layer by electroplating, vapor deposition, ion implantation, thermal spraying or mechanical procedures; binding the alloying element(s) by an organic resin or by powder/gas feeding. Whereas in Laser Cladding powder used to form the coating intercepts the laser beam and the surface simultaneously. A new coatings obtained on the base surface with minimal dilution with the substrate. This is a versatile process adaptable to automation. The process is always carried out under gas stream (argon, for instance) to avoid oxidation of the coating and to protect the laser optics.

Ozdemir et al [4] have shown an impactful research on owing to advancement of laser surface modification how laser plays an important role in food packaging of polymer materials like treatment of metal cans, glass jars etc. It also increases the lifetime by 3 times thereby reducing maintenance and other costs. For surface modification of polymers few criteria of laser parameters are also necessary like laser power as all materials don't work at same power, then laser pulse number, pulse wavelengths etc. Laser treatment also increases the surface adhesion

and it is essential to minimize leakage, reduce the chances of contamination, and assure food safety, particularly in the case of semi-rigid food.

Etsion [5] in his paper performed a study on Laser Surface Texturing both theoretically and practically to produce the micro-dimples. Each micro-dimple can serve either as a micro-hydrodynamic bearing or as a micro reservoir for lubricant. Theoretical models were developed, and laboratory tests were performed to check the potential of Laser Surface Texturing in tribological components like mechanical seals, piston rings and thrust bearings. In the entire laboratory tests, friction was substantially reduced with Laser Surface Texturing compared to the non-textured components. Both laboratory and field tests show substantial friction reduction and up to threefold increase in seal life. This success is wholly based on the theoretical modeling of Laser Surface Texturing. About 30% reduction in friction was noticed in Laser Surface Textured then non textured ones under full lubrication conditions.

Ajayia et al [6] in his paper shows the impact of LST in lubricated sliding regions. Two lubricants of different viscosity 54.8 and 124.7 cSt at 40 degree C were used. Tests were conducted for both lubricants with lower and higher viscosity only to be found that in both cases the friction coefficient was lower in Laser Surface Texturing by about 30 to 40%. In ground disc, the friction shows transition from a high friction coefficient at the lowest speed to lower values as the speed. A similar result was obtained with the polished disc, but with a lower magnitude of friction coefficient. Advantageous effects of Laser Surface Texturing were more evident at higher speeds and loads and with higher viscosity of oil

Tian et al [7] studied in his paper about Titanium which serves as an important material in chemical, marine and other industries but its high friction coefficient and wear rates limits its properties. His paper suggest different methods of laser treatment for surface modification to overcome these drawbacks of Ti such as laser surface remelting, laser surface alloying and laser cladding. In Laser surface remelting a high power laser beam melts the surface of sample to be treated and the melt pool solidifying rapidly after laser beam movement which have excellent wear and corrosion resistance. In Laser surface alloying the preplaced powders/gases fed into the melt zone with a feeder/nozzle dissolve into the laser-generated melt pool and chemical reactions take place between the additives and the melted substrate. With the laser generated melt pool solidifying, an alloyed layer of 0.5–1.0 mm thickness is thus produced on the surface of the substrate improving wear rates. And in Laser cladding high deposition rates, low dilution of the substrate, high cooling rates, and low distortion is noticed. As a surface coating technique, laser cladding has being developed for improving wear, corrosion and fatigue properties of machine parts.

Etsion [8] in his study showed that the three dimensions that characterize the Laser Surface Texturing are the dimples diameter, depth, and area density. It was found that the actual shape of the micro-dimple does not play a imp role and the most significant parameter for optimum load capacity is the ratio of the dimple depth over diameter. On conducting the experiment on face

seals it was found up to 65% reduction in friction torque and face temp. The LST advantages are not limited to liquid lubrication only, and dry gas seals can benefit from LST as well. The main difference is the dimple depth to diameter ratio, which in gas application is much smaller than in liquid application. Also it was seen that It was found that optimum LST is beneficial under starvation as well, where the dimples serve as micro-reservoirs for lubricant. The escape of oxide wear debris into the LST micro-dimples resulted in up to 84% reduction in the electrical contact resistance of the textured fretting surfaces compared to the case with non-textured surfaces.

Park et al [9] in his paper has done studies about Ultrafast laser ablation of indium tin oxide thin films for organic light-emitting diode application. It was experimented on an ITO coated laser substrate using an ultrafast laser irradiation to see that the ITO coating can be successfully removed through ablation without causing any damage to the glass. This was also possible because the ablation threshold of the thin filmed ITO is much higher than that of a normal glass. Then these etched ITO glass were fabricated in organic light emitting diodes (OLED) to enhance their applicability. The depth and width of the trenches produced on the ITO coated glass surface can be varied by changing the laser fluence and the number of pulses irradiated. It was also observed that keeping the laser fluence fixed if the number of pulses is increased then the depth of the ablation also increases. The width also increases with increase in number of laser pulses. These patterned ITO coated glass were able to enhance the performance of the OLED.

Ryk et al [10] in his paper performed a study between partially textured surface of a piston ring and fully textured surface is done. Friction in the internal combustion of the engine is mainly due to piston-cylinder system. The set up was like for Fully Textured Surface, piston face in contact to cylinder was fully textured and for partially one only a part of the surface in contact was textured. It was observed for fully textured surface Reduction in friction obtained by 30% with respect to un-textured surface. And for partially textured a 25% reduced friction was observed in comparison to fully textured. Additionally it was seen if both piston and cylinder surface textured no such effect in friction reduction obtained. For higher dimple density higher friction obtained and for lower dimple density reduced friction obtained

Xu et al [11] in his paper researched about the etching of an ITO coated glass using a free electron laser. The experiment it was observed that partial to almost fine removal of the ITO layer can be removed. The ITO was seen to almost behave like a metal due to its strong absorption at this wavelength and a high thermal conductivity. By applying a low fluence at multiple pulses and a very reduced scanning speed, smooth and crack free micro channels were observed at a single scan. Not only that the unaffected part of ITO coatings remained intact showing their previous values of electrical conductivity, chemical composition and transparency.

Raciukaitis et al [12] in his paper showed researches about patterning of an ITO coated glass at different wavelengths and then check the results of ablation. Very clean removal of the thin ITO coating was observed at 260nm wavelength and very little fluence of 0.20 J/cm<sup>2</sup> , at 355 nm wavelength well defined trenches were formed but more residues and dust were created at the side

of the trenches. At a greater wavelength like 532nm the trenches and their adjacent sides were seen to be thermally affected. For areas with fluence above 1.55 J/cm<sup>2</sup> substantial damages were noticed. A rapid increase in the absorption rate was observed at a wavelength lesser than 350 nm. Thus the processing parameters needed to be very carefully selected.

Dobrzan et al [13] studied in his research about silicon which is very much efficient in comparison to photovoltaic cells and solar cells and hence Laser Surface Texturing on Multi-crystalline silicon was done to observe that more light gets absorbed. After Laser Surface Texturing an etching process was carried on the silicon surface which made the grooves look more interlocked and hence creating obtuse angles. It was seen that LST reduced effective reflectance more than four times compared to raw and un-textured surface. Then chemical etching was done to remove the top layer of distorted silicon to remove ablation slag caused due to Laser Surface Texturing.

Vincent et al [14] in his paper studied the Laser Surface Texturing of a heterogeneous material (lamellar cast iron) and it was chosen for good friction properties. The surface grooves are of different shapes like triangular, semicircular etc and the dimples are cylindrical. 3 techniques of control are adopted i.e roughness, profilometry, SEM and non- contacting optical measurement to see which method gives better surface quality images. It was observed that profilometry, SEM and non- contacting optical measurement to see which method gives better surface quality images. SEM though is contactless but only gives qualitative results. And for Optical Confocal Microscopy both contactless and quantitative and hence most effective. From 2D images proper 3D image can be captured through suitable algorithm. For the tilted surfaces proper imaging of the surface profile gets difficult hence a Galvanometer Scanner adjusted to get that properly.

Yi et al [15] in his paper showed the use of Nd YAG laser on a T8 steel to produce micro pores. A disc (rotating) and a ring (fixed) used to check friction properties. Laser Surface Texturing was done on disc surface. Speed and Load were varied to check how friction works on Laser Surface Textured and un-textured surfaces. The ring was placed on vertical holder, disc surface was textured then smeared in oil and made to rotate to remove excess oil. After experimentation it was observed that when speed inc, friction on textured surface becomes more than polished one, when load increase, drastic decrease in friction in textured than un-textured. After the load and speed exceed certain critical value the friction coefficient increases.

Etsion et al [16] in his research shows that studies were done to see the effect of LST piston ring on the fuel consumption and exhaust gas composition under wide range of engine speeds under near-half-load conditions. Then non textured and partially textured rings were compared. 4 near-half- load working conditions engine speeds were chosen: 1500, 1800, 2000, and 2200 rev/min. partial Laser Surface Texturing treated piston rings exhibited up to 4% lower fuel consumption at 1800 rev/min, which correspond to the maximum torque of the engine. However the Laser Surface Texturing did not produce a significant change in the composition of exhaust gas. at both axial ends of cylindrical face rings. Laser Surface Texturing was done on the rings with a 5 kHz



pulsating Nd:YAG laser with a power of 11kW and a pulse of 30ns duration. Effect of Laser Surface Texturing was negligible for very high and very low engine loads.

Gualtieri et al [17] studied in his paper that steels are used for mechanical applications because of their high strength, toughness, good machinability and low cost. A study was done on modifications induced by laser beam during the texturing process on the mechanical properties of a nitride steel. The discs were 26mm in diameter and 8mm thick. The discs were first lapped to obtain a surface roughness (Ra) of 0.05 mm, then textured by Laser Surface Texturing. The laser beam was of wavelength 1.06 mm Pulse duration 30ns Laser beam energy 4mJ. Tribological tests performed in “full lubrication” configuration which showed an improvement in friction. Friction coefficients in textured surfaces were seen to be reduced 2 times in comparison to textured surfaces.

Krishna et al [18] shows studies on stainless Steel and its many properties but its stiffness is its most important feature but it is prone to wear and corrosion. Laser surface treatment leads to variation in its Martensitic properties and austenitic one thereby making it safer to corrosion and increasing hardness. Stainless steel sheet with 20\*10\*3 mm dimensions were used. They were heated for 45min at 965C followed by water quenching before laser treatment. The melt depth and width of laser-melted specimens increased with increase in the laser power and decrease in the scanning speed. The amount of retained austenite decreased with increase in the laser power but increased with laser scan speed. Laser surface melting of AISI 410 martensitic stainless steel considerably increased the surface hardness by reducing the retained austenite

Vilhena et al. [19] in his paper have shown researches that Nd YAG Laser (1064nm) was used on a steel sample to produce micro pores which also act as lubrication reservoirs and then various laser parameters like pulse energy, pulse no. and modes (single and multi) can be varied to study the relation between laser parameters and micro pores. He also observed that for multimode operating lasers as pulse energy increase the pore diameter also increase but up to a saturated value and also results in reduced pore depth. As no. of pulses increase no effect on diameter but the pore depth increase. But in single mode however with increase in pulse energy less impact on diameter observed. With increase in pulse no. the depth increase but with further increase in no. of pulses the depth reduce and the side heights increase.

Basu et al [20] in his research work focus on the enhancement of transmittance of Indium Tin Oxide (ITO) coated glass plates. ITO acts as one of the finest coating layers of glass substrates that can be used as conducting plates in the solar panel cells. However the transmittance of the coated glass can be enhanced by layering it with SiO<sub>2</sub> without causing any effect to the conductance of the material. Initially when the glass was coated with only ITO it had a certain transmittance intensity sat T<sub>1</sub>, but after deposition of SiO<sub>2</sub> coating on the surface the transmittance intensity changes to T<sub>2</sub>. It was observed that T<sub>1</sub><T<sub>2</sub>. Thus after the deposition of SiO<sub>2</sub> layer on the ITO coated glass an enhancement in transmission was observed of about 2-

10% over the visible region. The variation in wavelengths in the SiO<sub>2</sub> coated along with ITO is somewhat lesser than when only coated with ITO.

Lamraoui et al [21] in his research work shows that thermal spraying is one of the efficient surface treatment techniques that provide well defined structures. This surface treatment requires good coating/substrate interfacial adhesion. Amongst other methods the LST serves the best. This paper aims to study variation in number of shots per hole and the power of the laser in order to get the best adhesion of the coating on the substrate. Laser radiation removes contaminants on the surface, produce changes in the morphology of the substance by creating cavities, and chemically modify the outer layer of the metal substrate. This increases the adhesion between the material surface and the coating thereby enhancing coating textures.

Wang et al [22] shows studies on Optical absorption enhancement in nano pore textured-silicon thin film for photovoltaic application. The surface is textured using a laser with different parameters being varied to check which parameter gives the maximum absorption. The parameters considered for variation are array periodicity  $P$ , the nano pore depth  $H$ , and the nano pore diameter  $D$ . It is seen that the light absorption due to the Si nano pore array is enhanced in high-energy range. Absorption shifts towards low value as  $D$  increases. At low  $P$  (100 to 300 nm), the light-absorption increases in the high-energy region 2.6 eV). However, with further increasing  $P$ , the light absorption enhancement in the low-energy range becomes more prominent. The light absorption is maximized when  $H$ ,  $P$ , and  $D$  v/s  $P$  ratio are set at 2000 nm, 700 nm, and 87.5%, respectively. The corresponding ultimate efficiency is 35%.

Sher et al [23] in his study shows pulsed laser hyper doping and surface texturing for photo voltaics. An increase in absorption of photovoltaic by two main methods is observed. Firstly pulsed laser hyper doping introduces dopants in semiconductors which creates an intermediate band in the band gap of the material and modifies the absorption coefficient. Secondly pulsed laser texturing can enhance geometric light trapping by increasing surface roughness. Geometric light trapping from micrometer sized silicon spikes decreases reflection and enhances length of optical path. After Laser Surface Texturing the height, spacing, and subtended angle determine the extent of geometric light trapping. In the spikes an average cone angle of 45 degrees is noticed which results in less than 5% of light reflection and an enhancement in absorption of about 40%. This leads to energy converting efficiency >63%.

Chikarakara et al [24] shows studies in his paper about Ti-6Al-4V being the most frequently and successfully used titanium alloy in bio medics due to its favorable properties but has poor surface properties leading to wear and corrosion. Laser surface modification of improve mechanical and tribological properties of titanium and its alloys. The sample was grit blasted before laser treatment so remove surface impurities. After Laser surface treatment certain changes were noticed like surface roughness found to decrease with increase of irradiance and residence time. As the irradiance increased, a more homogeneous melt pool depth with fewer

discontinuities was observed. And the laser treated region showed hardness increase of up to 67% compared to the as received alloy.

Meskamp et al [25] shows that surface structures like periodic gratings and surface patterns can increase the optical optimization of a material and can enhance power storing efficiency by increasing the path lengths of the incident light creating light trapping feature. In this paper direct laser interference patterning (DLIP) is used where two or more coherent laser beams are made to interfere with each other on a substrate creating different patterns and a study is made on these patterns to see which one gives best results of efficiency increase of power. In order to form hexagonal grid structures, two successive exposures of the PET substrate was done, with a rotation of 60° between steps of irradiation at a spatial period of 0.7 μm and a laser fluence of 100 mJ/cm<sup>2</sup> PET substrates were patterned directly with a pulsed UV laser using energy densities (laser fluences) from 20 to 400 mJ/cm<sup>2</sup> for periodic line structures.

Riveiro et al [26] in his paper describes how Laser Surface Texturing can change the properties of biomedical polymers and enhance their biological properties. The techniques include deformation, removal or controlled addition of material to the surface to increase the roughness, and by modifying its surface chemistry. He conducted the experiment in two ways. First with a stationary laser beam that and second with a relative motion of the laser beam with respect to the work piece. And the 3 processes that he adopted were thermal process, photochemical process and photophysical process.

Bian et al [27] in his paper performed a study on Femtosecond laser patterning on a thin ITO coated glass which later can be fabricated on thin solar cells to enhance their performance. The ITO coated films were judged based on 2 experimental ways, the first one being the threshold of damage on the ITO film at a single laser pulse with varying pulse duration. It was observed that at single laser pulse with increase in pulse duration the damage threshold gradually increases. The second experimentation was based on how the laser fluence, laser pulse duration and scanning speed affect the groove geometry and the surface profile. It was seen that the material can get damaged if the laser fluence is too high. Now if the fluence is kept fixed and the pulse duration is varied it can be seen with increase in pulse duration, the laser intensity decreases and so does the groove width and depth. The scanning speed plays an important role in the surface profile of the material, as the scanning speed decrease the groove depth increases. Thus there parameters can optimize the quality of grooves in an ITO coated glass which later can be fabricated on solar cells.

Bathe et al [28] performed a study on Laser Surface Texturing on a Gray cast iron (comprising of C, Mn, Si, Mo, P, Fe) using 3 different laser pulse durations. Milli-s, Nano-s and Femto-s pulse durations. These lasers were irradiated on the iron surface to study the friction coefficient variations. The samples were 10\*10 mm<sup>2</sup> square shaped with 5 mm thickness. Sample was mechanically polished to an average roughness of about 0.1 μm. Prior to laser irradiation, they were cleaned with acetone. The lasers employed for irradiation were ms pulsed Nd:YAG laser,

ns pulsed Nd:YVO4 laser and fs pulsed Ti:Sapphire laser. It was keenly observed that For ns pulse the friction coefficient was about 0.31 and there was a substantial decomposition of molten material around the groove increasing the surface roughness. For ns pulse the friction coefficient was 0.02 and slight re-solidification of molten substance around periphery of dimple. For fs pulse the friction coefficient was 0.01 and there was almost same level of re solidification of material as the surface thereby making it almost smooth only.

Braun et al [29] This paper focuses on the effect of the LST at the friction coefficient when certain lubricant parameters are varied like temperature, viscosity whereas keeping the laser textured surface parameter like dimple depth to diameter ratio constant at 0.1 and dimple density on surface at 10% Polyalphaolefin (PAO) was used as the lubricant. A constant dimple density of 10% was maintained. The polished surface and the surface with 800 micro m dimple diameter showed the highest coefficient of friction where the transition is between 500 to 1000 mm/s. The surface with 40 mm dimples generates the lowest friction coefficients in the mixed lubrication regime at sliding speeds between 1000 and 40 mm/s. Keeping both the depth-to-diameter ratio and the total area of the dimples constant at 0.1 a decrease in friction can be realized by LST Decreasing the oil temperature from 100 to 50 degree C increases the viscosity almost 3 times. The friction coefficient is found to be lower in mixed lubrication

Calvani et al [30] shows studies on CVD (chemically vapor deposited) diamond is a material for high energy detection. Its wide band gap (5.47 eV), makes it transparent in the visible and infrared (IR) ranges. In this paper the laser-induced periodic surface structures (LIPSS), formed by single-beam fs laser under certain condition aims at enhancing the absorption properties of CVD by means of a surface laser treatment. Micro-Raman spectroscopy was performed at room temperature. It was seen the laser treatment enhances light trapping, so that absorbance strongly increases in the entire investigated wavelength range, especially in visible and IR, up to more than 80 %. In the UV range, close to diamond band gap of 5.47 eV, corresponding to a wavelength of approximately 226 nm, absorbance reaches values of 95 %. Absorbance increases by 2 times in the entire visible range and up to more than 2.5 in the IR. The sample absorbance (A), transmittance (T) and reflectance (R) satisfy the relation  $A + T + R = 1$ , absorbance can be derived from the measurement of T and R.

Dunna et al [31] showed in his paper the use of a pulsed, ns fiber laser to texture grade 316 stainless steel and a 'low alloy' carbon steel in order to generate contacts with high static friction coefficients. High friction contacts reduce the tightening force required in joints. It also easily secures precision fittings, for larger components when other methods are difficult and expensive. The effect of laser pulse separation and normal pressure was studied in high static friction tests in which both surfaces in the contact LST. High static friction coefficients  $\mu_s > 1.25$  were consistently achieved when using normal pressures of 50 MPa and 100 MPa with pulse separation of less than 60 micro m, an increase of 346% over un-textured samples at 100 MPa.

Li et al [32] in his paper analyzes surface morphology, crystal structure and photoelectric properties of Ni/FTO films with different thicknesses of Ni layer to find which thickness of the layer shows best photoelectric effect and how surface modification can increase the conductance. FTO being a conducting oxide shows good properties of surface conduction and it can be enhanced by layer deposition of other materials along with it (Ni in this paper). Magnetic field free laser irradiation of the Ni10/FTO film was also carried out for comparison. It was found that magnetic field assisted laser irradiation using a fluence of 1.0 J/cm<sup>2</sup> was more effective for simultaneously achieving texturing and annealing, that results in the formation of ideal grating textures and subsequent increased grain size. The corresponding film showed the highest conductance of 22.8\*10<sup>-3</sup> ohm inv compared to 13.1\*10<sup>-3</sup> ohm inv of the FTO glass and 1.4\*10<sup>-3</sup> ohm inv of the Ni10/FTO film, the Ni/FTO film with a 10-nm-thick Ni layer over FTO had the best overall photoelectric property.

Nattapat et al [33] in his paper mainly focuses on the study of removal of the topmost layer of Carbon Fiber Reinforced Composites (CFRC) without causing an damage to the surface by using an extremely low powered carbon laser. 60W CO<sub>2</sub> marker laser along with a high speed galvanometer mirror used CFRC sheets were of 3mm thickness and 50\*50 mm dimensions. CFRP composite was held stationary on an open frame fixture throughout the scanning operation. The experiment was carried out at 3 power value 8W, 14W and 20W. The resin surface divided into 3 zones. Zone A which decreases in power with increase in speed with no resin layer removal. Zone B which has an Optimal range of power and speed and results in complete removal of top layer of resin, without any damage to material. And in Zone C increase in laser power and decrease in speed and damage of the top resin layer was observed

Drygała et al [34] in his studies have shown that the optical properties of any surface (polycrystalline silicone for his paper) can be enhanced by reducing the reflectance of the surface. In order to do so LST followed by Al<sub>2</sub>O<sub>3</sub> antireflection coating (ARC). In usual cases about 8% of the light incident is lost due to reflection. But after Laser Surface Texturing and antireflection coating i.e layers of Al<sub>2</sub>O<sub>3</sub> deposition on the surface of p type polycrystalline silicon it was observed that the reflectance gets reduced by 2-3%. The reflectance of silicon was 30% which gets reduced to 20% over the entire range. Though the material thickness was of 300 micro m but about 11 micro m of the thickness was etched off owing to damage.

Triana et al [35] shows in his studies the effect of wet etching process on the morphology and transmittance of fluorine doped tin oxide (FTO). Dye sensitized solar cell (DSSC) hold many advantages over silicon-based solar cells like high purity and low cost but its major problems are lower efficiency and stability. The efficiency of DSSC can be enhanced by light trapping method. It is basically surface texturing at the transparent electrode surface of solar cell. Some of lights on the surface of solar cell will reflect, others will absorb or transmit. FTO surface is relatively uniform. After etching with HCl solution the surface modification was observed. The root mean square roughness was 18nm for T32, 13nm for T49 and 12nm for T55, but after the wet etching a decrease in the roughness values observed. Also it is observed with patterning of

surface reflectance can be minimized and transmittance can be enhanced. The FTO etching process is more complicated since FTO cannot be reduced to the metal by using hydrogen ions in strong acid solution. It needs a catalyst such as zinc particles (Zn). Hence the surface was masked using a Zinc powder paste.

Wahab et al [36] shows studies in his paper that Laser Surface Texturing is one of the most improved methods for improving material surface properties. It finds its use in forming anti-reflection, anti-corrosion, anti-fouling surfaces. In comparison to other methods Laser Surface Texturing has advantages, such as rapid fabrication without causing pollution and control of the shape and size of texture formed. A study on different sized textures were performed and it was found out that 20micrometer textured surface produces greater results in tribological properties in arrange of 50 to 20 micrometer sized dimples. Laser Surface Texturing is also used to change wettability of material, which is influenced by surface roughness. In Laser Surface Texturing, circular dimples are the most used textured pattern because of their convenience for simulation and isotropic characteristic. But the circular dimples are not as effective as the crossed channel in friction reduction.

Riveiroa et al [37] in his paper shows study on the surface characteristics of Polyether-ether-ketone (PEEK) under surface modification for three laser wavelengths (1064, 532, and 355 nm) with the aim to see which processing condition increases the roughness and wettability. It was measured by surface profiler at treated areas that Roughness value  $Ra \geq 1$  were obtained for 1064 and 532 nm laser wavelengths. These values are adequate for initiating cell adhesion. UV laser radiation 355 nm does not help much in modifying surface roughness. Contact angle measurement was done by sessile drop technique Minimization of contact angle improves wettability. Contact angle gets reduced when the spot diameter is large and scanning speed is slow. Finally, processing by means of UV laser radiation (355 nm) shows improved wettability results.

Singh et al [38] in his paper deals with the variation in contact angle (CA) and coefficient of friction (CoF) in a textured and un-textured surface of different kind of materials. In hydrophobicity CA is more than  $90^\circ$  and in hydrophilic less than  $90^\circ$ . In super hydrophobic its greater than  $150^\circ$ . Also how the micro dimple densities vary the CA and CoF is seen. 3 Areal densities of surface textured grooves chosen ( 44, 24, and 13%). 44% makes the CoF most as it deposits surface debris. But in 24% amongst the 3, the CoF is observed to be least. However CoF is most in un-textured surface materials. It was noticed Contact Angle increases ( $110^\circ$  to  $160^\circ$ ) for water. These surfaces become nearly super hydrophobic. The more be the contact angle the less be the wettability of the material. It was also observed that When a water drop comes in contact with high areal density micro-dimple array surface, air pockets developed enhance the contact angle and make the surface hydrophobic in nature.

Kim et al [39] in his research shows studies on surface texturing on solar cells for their enhancement in efficiency. The largest drawback of solar cell is low energy conversion

efficiency due to optical loss. Application of surface texturing methods utilizing micro/Nano scale structure on the surfaces of solar cells are useful. These texturized surfaces with unique optical properties can be implemented as anti-reflective or light-trapping interfaces to reduce optical loss and thus enhance the efficiency of solar cells. Optical loss of solar cells can be reduced by adjusting the design parameters of patterns, including the size, shape, and materials. In general, two typical strategies, enhancement of the transmittance by an anti-reflection structure and enhancement of optical path length by light trapping, are used.

Yuan et al [40] in his paper used a 6061 steel surface for Laser Surface Texturing and its surface parameters were varied with respect to change in temperature was observed like its influence on the formation of micro-features, evolution of oxidation reactions, surface morphology, re solidification characteristics and other surface components. 4 temperatures were chosen 25°C 100°C, 200°C and 300°C. It was observed that the ablation efficiency can be enhanced with increase in temperature due to enhanced coupling reactivity between the laser and material and Surface microstructures, re solidification and oxidation characteristics can be enhanced due to higher temperature and slow cooling process. Reflectivity of the material also decreases making it more absorptive due to the increase in debris deposition along the grooves. Darkening effect on the sample surface with a temperature of 300°C is approx. four times faster than that with room temperature 25°C. A preheating of the material helps in decrease of micro cracks while processing the material

Tsai et al [41] in his paper studies about the variation in surface wettability and electrical resistance analysis of water droplets on an ITO coated glass after laser radiation. The wettability and electrical performance was varied using various electrode voltages. The method of laser surface modification was adopted to control the contact angle of the droplet by varying certain parameters like pitch width, depth and scanning speed. This enables the surface of better transmission and higher electrical conductivity. It was observed that the contact angle and the spherical shape of the droplets can be maintained by reducing surface which again can be reduced by lowering the scanning speed. Also by decreasing the line pitch and width hydrophilic surface can be converted to hydrophobic or neutral one.

## 1.7 Objective of Present Research

From review of past literature of Laser Surface Texturing it is evident that a lot of research work has been carried out in this field. Most of the research studies are focused on removal of the conductive layer of coating by setting different parametric conditions without causing any harm to the glass substrate. Achieving results on FTO coated glass is a challenging task and very few research works so far has been reported.. But from the few papers it can be seen that laser surface modification of FTO coated glass can be done.. In our present research work we have used certain parameters which have not been worked with previously and performed laser texturing on FTO coated glass.

In view of the above requirements the objective of the present research work has been framed as follows:

- FTO coated glass being a very fragile material out 1<sup>st</sup> objective was to see if laser texturing can be done on the material surface.
- A range of parametric values need to be fixed after a set of trial experimentation upon which further experiment can be done.
- Study of light absorption at FTO coated glass surface without any Laser Surface Texturing
- Study of light absorption at FTO coated glass surface after Laser Surface Texturing for the range of feasible wavelength
- Study of light absorption at FTO coated glass surface after Laser Surface Texturing by varying certain laser parameters and base materials.
- Compare the results of each output to check which combination gives the best absorption result for the greater wavelength range.
- Study the results of the different parameter setting to check the surface roughness
- Check which parameter gives the maximum roughness so as to allow most of the light rays to get absorbed.



## **Chapter - 2**

### **Experimental Setup, Procedure and Materials**

## **2.1 Experimental Setup and Measuring Equipment**

### **2.1.1 Fiber Laser Cutting Machine**

The fiber laser belongs to MEHTA Fiber Laser Cutting machine with a power of 500W. The machine is equipped with a console that is being installed on the side walls of the cutting machine. It is controlled basically by a computer controlled laser Cypcut System. The fiber cutting laser machine along with it consists of a chiller unit which is basically used for cooling purposes. This chiller unit is installed at the back of the main cabinet of the machines. The assist gas is supplied to the laser by a gas cylinder. There also equipped with the laser machine is a stabilizer that well controls the optimum voltage level needed for the machine to function properly. It is a Q switched laser source which also consists of a clipping equipment in order to hold the work pieces at their fixed position. Thus the main components that built up the Fiber cutting machine as one are the laser itself, supporting console, computer controlled operator, chiller unit, assist gas, a clipping equipment and a voltage stabilizer.

Before switching the Laser machine, the voltage stabilizer and the chiller unit was switched on. Then the gas cylinder was opened upto the optimum value of required gas, this was followed up by starting the laser monitor and the machine along with. The Laser machine was then puffed in order to remove the excess amount of gases present. Then with the help of the Cypcut Software the parameters were set and the frame was adjusted. The shutter was closed and laser machining of the material was initiated.

The Laser Cutting machine consists of the following sub systems

- a. Fiber Laser System
- b. Console Monitor for the Laser
- c. Chiller Unit of the Laser
- d. Assist Gas Cylinder
- e. Voltage Stabilizer of the Laser
- f. Clipping Unit of the equipment



Fig 2.1 Fiber Laser Cutting Machine



Fig 2.1 b) Console Monitor for the Laser



Fig 2.1 a) Fiber Laser System

**Table 2.1 Specifications of the Fiber Laser Cutting Machine**

Sl No.	Parameter	Value
1.	Maximum Output Power	500 W
2.	Switching and mode of operation	Q switched continuous operation
3.	Assist Gas	Nitrogen
4.	Nozzle Distance Range	10 cm to 25 cm
5.	Wavelength	1064 nm
6.	Laser Spot Diameter	50 micro m at focus



**Fig 2.1 c) Chiller Unit of the Laser**



Fig 2.1 d) Assist Gas Cylinder



Fig 2.1 e) Voltage Stabilizer of the Laser

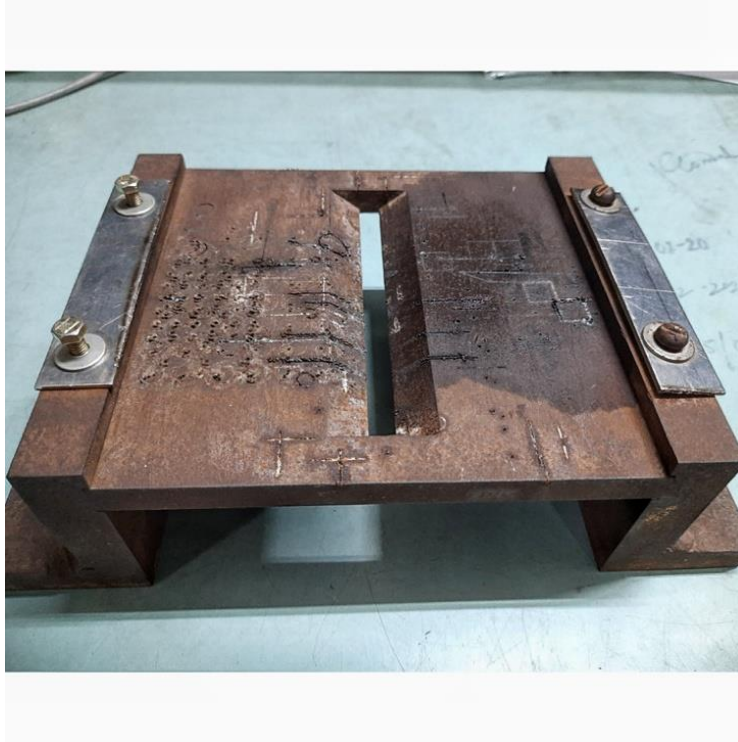


Fig 2.1 f) Clipping Unit of the Equipment

### **Cypcut Laser Machine Software**

Cypcut Software System is software system that is being designed to plane laser cutting. Most of its functions include graphics processing, parameter settings, custom cutting process editing, layout designing, path planning simulation and cutting process control.

The figure at the black background consists of the Drawing interface where the desired layout is being drawn while the white display signifies the machine breadth and usually highlighted with grids. Above the interface from top to bottom are Title Bar, Menu Bar and Tool Bar. There also is a “Quick Access Bar” at the left of the title bar which is used for simultaneous creating, opening and saving a file. At the left of the interface is present the “Drawing toolbar” which provides with basic drawing functions. At the right of the drawing area is the “Process Toolbar” which functions in order to set and vary the process parameters.



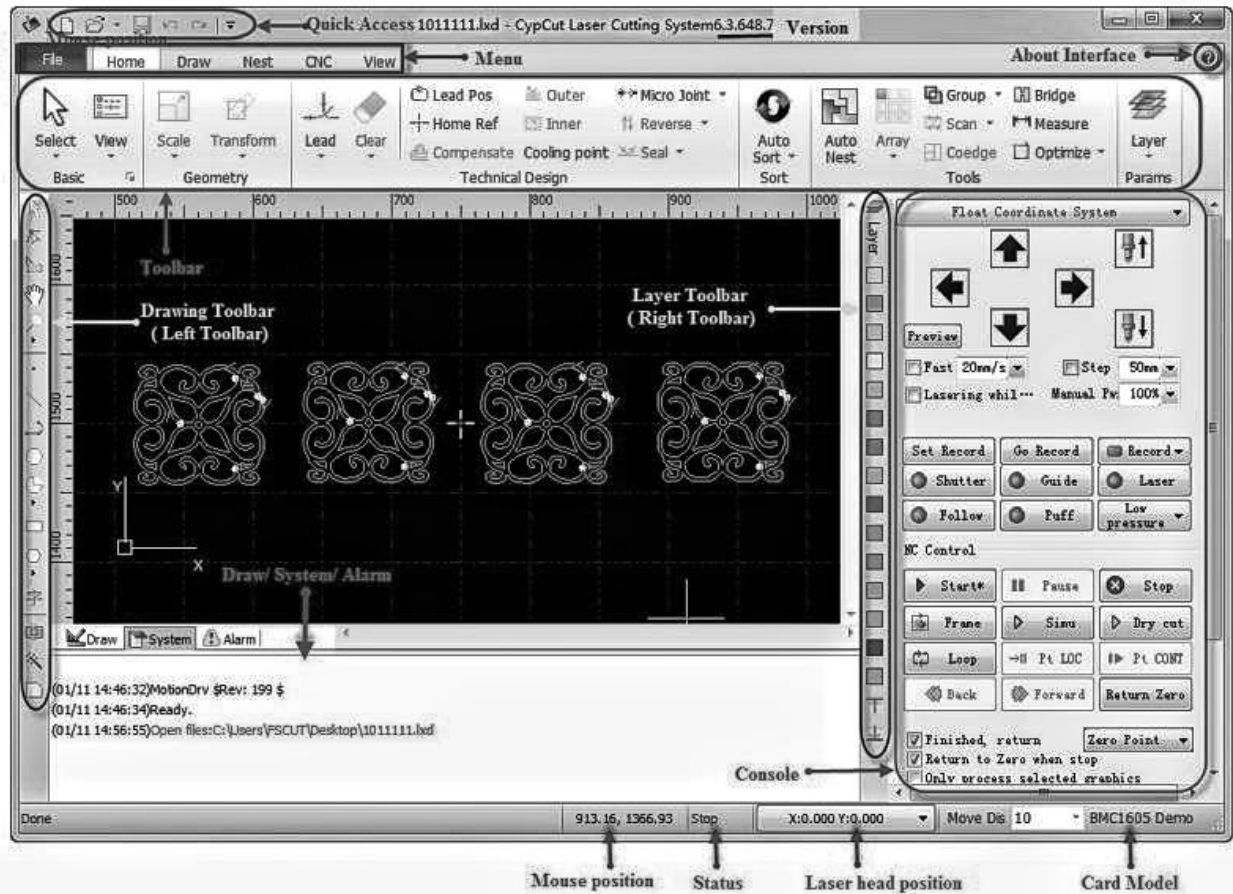


Fig 2.2 Cypcut Laser Cutting Software Screen Display

## 2.1.2 Measuring Equipment

### 2.1.2.1 Optical Microscope

The optical microscope belonged to ZEISS of Stemi 508. It was used to minutely record the values of all the output responses. The data was collected from ScopeImage9.0 software installed in the laptop. It consist of two lenses which either can be operated together which no image formed on screen i.e. only for précised viewing operation or operated with one laser at a time which proper imaging on the screen i.e. for précised viewing as well as measurement.

After the machining of the material their characteristics were checked in the microscope by adjusting the focusing power. The Microscope was first connected to the main power supply and then switched on. After switching on the microscope the optical lights automatically fall on the positioned place where later on the sample is being placed for measurement. There are two sets of focusing arrangements. The first one is adjusted for a better view of the product at the optimal

focusing value and simultaneously this value is adjusted with the value in software. The 2<sup>nd</sup> one is used for clarity at the most focused point. It basically adjusts the microscope head.

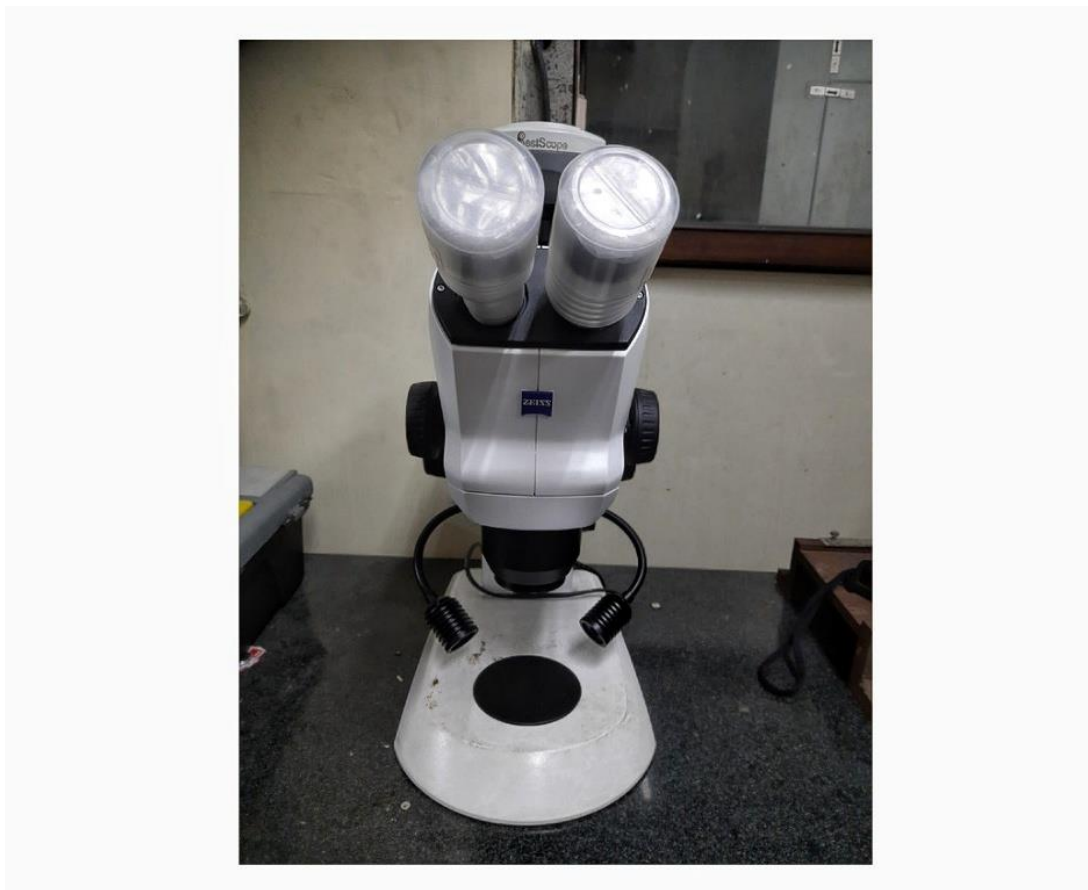


Fig 2.3 Optical Microscope

#### **2.1.2.2 UV-Vis Spectrophotometer**

The UV-Vis Spectrophotometer belongs to BIOBASE of BK-D580. This instrument is used for measuring the absorbance and transmittance of any optically transparent material. It is a single beam system with a wavelength range of 190nm to 1100nm and the spectral bandwidth ranges from 2 nm to 4 nm. The detector is a Silicon Photodiode. It consists of two holders where the sample can be placed and radiation is passed along the material to get the desired response. This response is recorded in the computer aided software.

The machine consists of a holder with an open pore through which the light passes. In the holder the material is placed. It is a work of precision as the holder space is not only narrow but the aperture is very small as well. So the material needs to be kept at its position with very care and sensitivity. Then the lid of the machine is closed and air base line is generated with the spectrophotometer software. Thereafter the measuring of absorption of the machine is being started.





Fig 2.4 UV-Vis Spectrophotometer

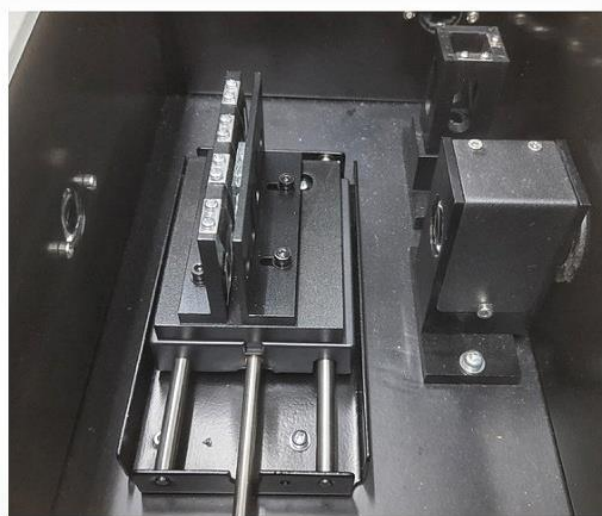


Fig 2.5 Inside view of UV-Vis Spectrophotometer

## UV-Vis Spectrophotometer BIOBASE Software

The UV-Vis Spectrophotometer BIOBASE Software gives complete instrument control along with data acquisition and an entire set of mathematical tools for interpretation and analysis of output results. It provides with spectral analysis, quantitative analysis, kinetic analysis and photometric analysis.

The spectrum workspace is used to scan across a user defined range of spectrum that allows to measure the absorbance and transmission. At the very beginning of the experiment a baseline needs to be created so that the value can be later deleted from the actual absorbance or transmittance value obtained. In this experiment the baseline is created with respect to air. However the “Peak Pick” tool is to determine the wavelength at this the peaks or the valleys have occurred in the given spectral range.

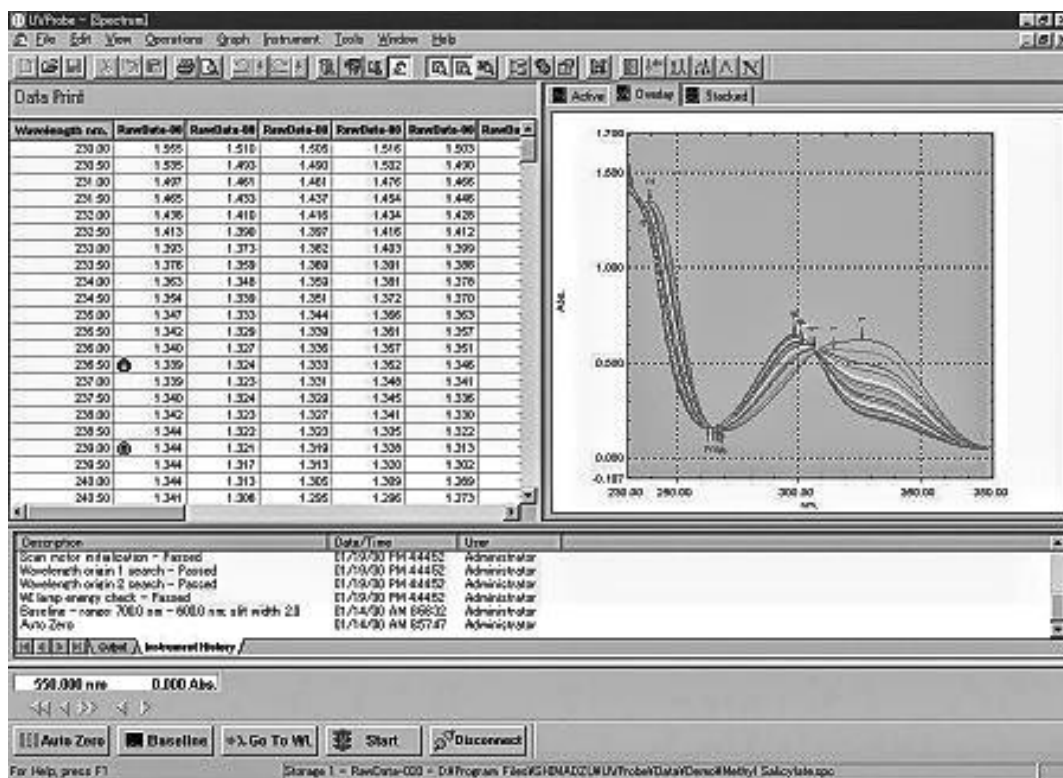


Fig 2.6 UV-Vis Spectrophotometer Software Screen Display

### 2.1.2.3 Surftest - Surface Roughness Tester

The machine belongs to Category SJ-410 (Standard: ISO1997) of Mitutoyo for surface roughness testing. The tester is contact type roughness measuring instrument which basically consists of a probe that runs along the reassigned length of the machining region and measures the roughness. The roughness is basically measured in 3 forms namely, Ra which is the

arithmetic mean deviation of roughness,  $R_q$  which is the mean square of roughness and finally the  $R_z$  which is the difference between the maximum peak and valley.



Fig 2.7 Surface Roughness Tester

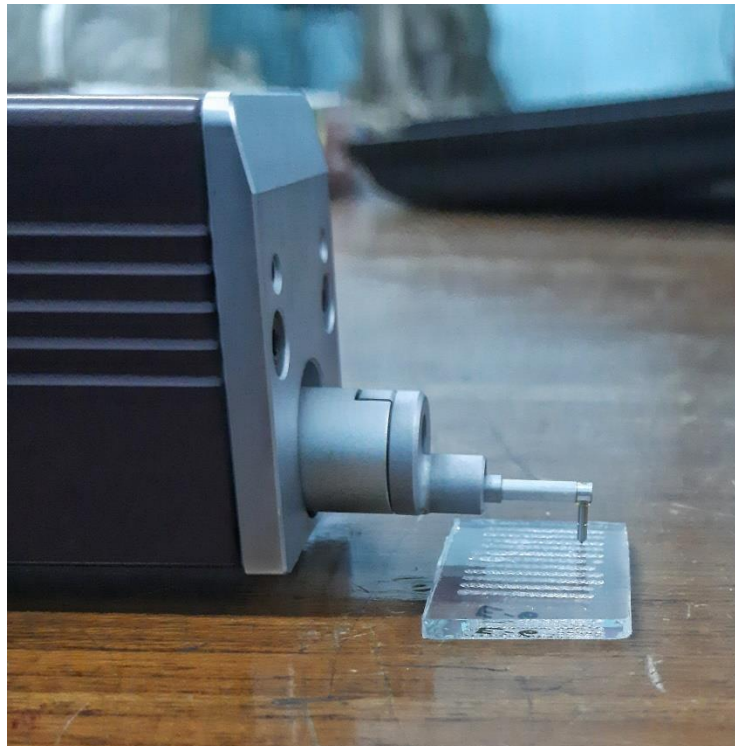


Fig 2.8 Close view of a probe testing a FTO sample

**Table 2.2 Specifications of the Surface Roughness Tester**

Sl No.	Parameter	Value
1.	Cut off length	0.8 micro meter
2.	No. of samplings	10
3.	Speed of probe	0.5mm/s
4.	Length covered	8.8mm
5.	Radius of tip of probe	5 micro meter
6.	Measuring force	4nN

## **2.2 Materials Investigated**

The experiment is carried out on a FTO (Fluorine doped Tin Oxide) coated glass substrate and ITO (Indium Tin Oxide) coated glass. And for base material basically 3 metals have been used namely Stainless Steel, Copper and Aluminum.

### **2.2.1 FTO coated glass**

Transparent Conducting Films (TCO) is thin films of materials that are transparent as well as electrically conductive. FTO is a type of Transparent Conducting Film which is coated with Fluorine Doped Tin Oxide. It finds its usage in making Solar Cell and Display Technologies. FTO coated glass substrates are highly temperature resistant in comparison to other metal oxide's layers. FTO coated glass can be used in the fabrication of transparent electrodes for photo voltaics with thin film.

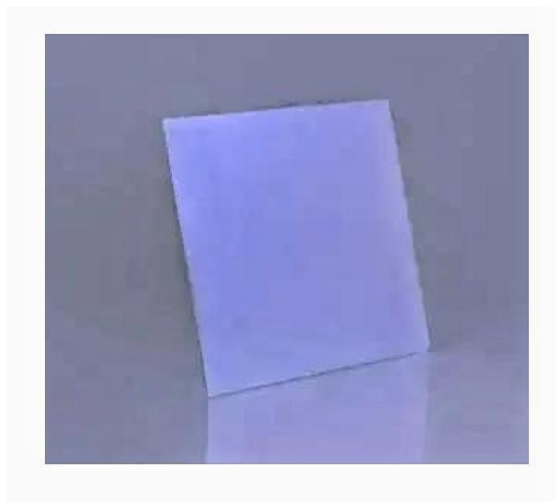
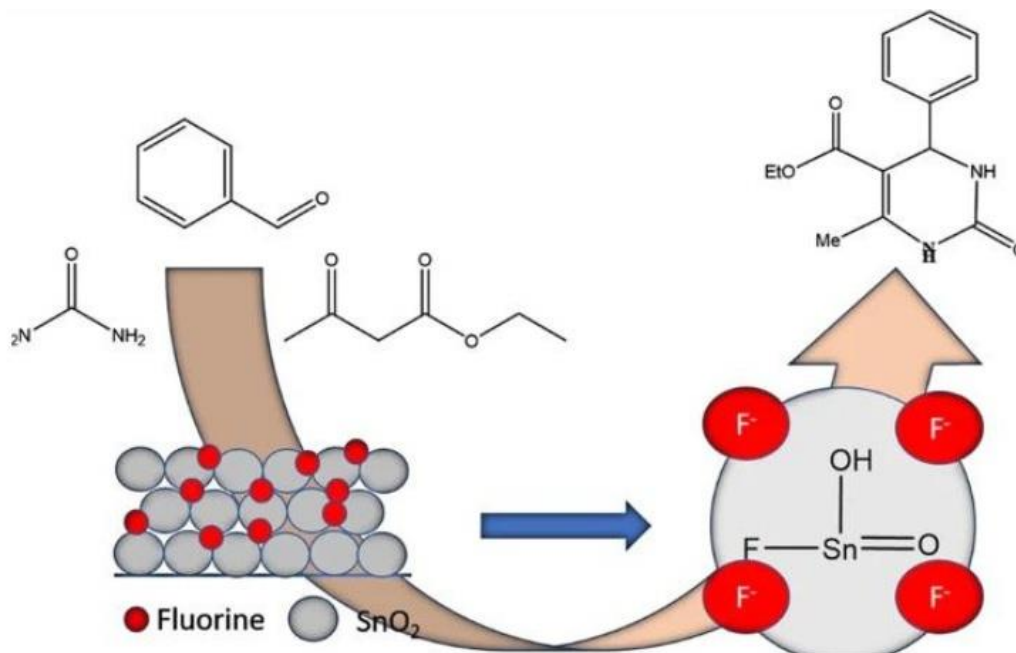


**Fig 2.9 FTO Coated Glass**

Fluorine doped tin oxide (FTO) thin films are prepared by using Ammonium Fluoride ( $\text{NH}_4\text{F}$ ) and DBTDA. These two solutions are mixed and the final output is Fluorine doped with tin oxide ( $\text{SnO}_2/\text{F}$ ). This work is focused on producing high transparency materials above 85% which allows more sunlight absorption by the inner part of solar cell. The FTO atoms basically replace the oxygen atoms present in the lattice structure and donate free electrons in order to enhance the electrical conductivity of the FTO Samples.



## FTO used in Solar Cells

In the making of the solar cell a transparent electrode is necessary so that it can help the incident light to reach the photoactive layer. Certain transparent conducting oxide films like ITO (Indium Tin Oxide) and FTO (Fluorine doped tin oxide) play this role due to their nature of transparency and conductivity.

Before using the FTO coated glass substrates for the experiment they need to be preprocessed or cleaned properly. They need to undergo ultrasonic cleaning where the FTO coated glass is put



under ethyl alcohol and ultrapure water, each for about 15 minutes. Then they are left for drying and again cleaned with ethyl alcohol and then proceeded with experimentation

**Table 2.3 Comparison between ITO and FTO**

Sl No.	Point of comparison	FTO	ITO
1.	Conductivity	Better conductivity than ITO	Lesser Conductivity than FTO
2	Price	Moderately pricy	Expensive
3	Stability	Electrical properties remain unaffected at high temperature	Electrical properties can get degraded in presence of oxygen at high temperature

### 2.2.2 Copper

In our experimentation of laser surface texturing FTO coated glass one of the base materials that was taken into consideration was copper. Copper didn't have any direct contact with laser beam but was kept as support material along with FTO Coated glass. It was used as one of the parameters to see how the properties of copper affect the texturing of FTO glass and helps in variation of the absorption.

**Table 2.4 Characteristics of Copper**

1.	Name	Copper (Cuprum)
2.	Symbol	Cu
3.	Atomic Number	29
4.	Atomic Mass	63.546 u
5.	Melting Point	1085 degree C
6.	Boiling Point	2563 degree C
7	Properties	Malleable, Ductile and Conductive.

### Important Facts about Copper

- It had a reddish Metallic color that is unique amongst all other elements.
- Copper readily forms alloys with other metals such as brass (copper and zinc) and bronze (copper and tin).
- It is malleable, ductile and a very good conductor of electricity.
- It gets oxidized to a green color when comes in contact with oxygen. There are two oxidation states of Copper. One that produced a blue flame and the other a green flame.
- In terms of Industrial use Copper ranks the 3<sup>rd</sup> after iron and aluminum.
- Copper easily forms binary compounds (compounds with only two elements) like copper chloride, copper oxide etc.
- It finds its usage in making of utensils, copper wires etc.

### Copper in presence of Laser

In this paper Copper has been used as a base material i.e FTO coated glass is the main material that undergoes laser irradiations and comes in direct contact with laser beam. Copper however has no direct intervention with Laser. But copper when comes in prolonged contact with laser beam it gets oxidized to form one of its stoichiometric forms,  $\text{Cu}_2\text{O}$  or  $\text{CuO}$ . Also when Copper is irradiated with laser fluence their wetting response through static contact angle measurements can be checked only to find that progressive increase of the contact angle forming highly hydrophobic copper samples with contact angles reaching values around  $160^\circ$ [42].

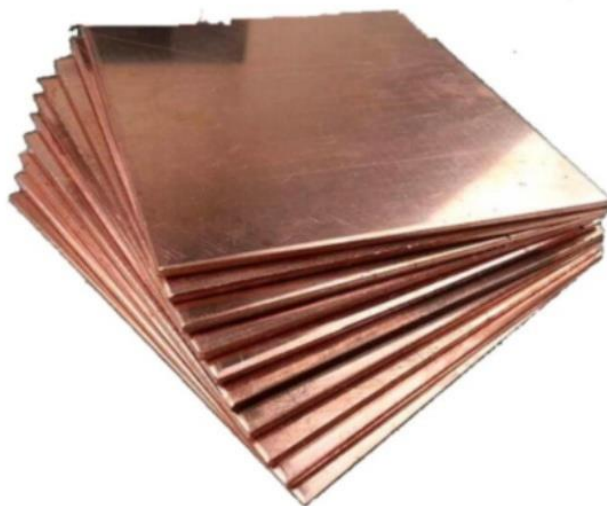


Fig 2.11 Copper Plates (Base Material)

### 2.2.3 Aluminum

In our experimentation of laser surface texturing FTO coated glass one of the base materials apart from Copper that was taken into consideration was Aluminum. Aluminum didn't have any direct contact with laser beam but was kept as support material along with FTO Coated glass. It was used as one of the parameters to see how the properties of copper affect the texturing of FTO glass and helps in variation of the absorption.

**Table 2.5 Characteristics of Aluminum**

1.	Name	Aluminum
2.	Symbol	Al
3.	Atomic Number	13
4.	Atomic Mass	26.981539 u
5.	Melting Point	660.3 degree C
6.	Valence	3
7.	Properties	Light weight, soft and malleable

#### **Important Facts about Aluminum**

- It is a silvery white light weight metal.
- It is the 2<sup>nd</sup> most malleable metals and 6<sup>th</sup> most ductile
- It is often used as an alloy as Aluminum itself is not a very strong metal.
- They are good conductors of electricity and are often used in electrical transmission lines.
- It is the most abundant material available on the earth's crust.
- Due to its light weight it finds its usage in aircraft manufacturing, foils etc.

#### **Aluminum in presence of Laser**

In this paper Aluminum has been used as a base material i.e FTO coated glass is the main material that undergoes laser irradiations and comes in direct contact with laser beam. Aluminum however has no direct intervention with Laser. However treating Aluminum alloys under Laser possesses major constraints of lower melting point of aluminum and the poor absorption of



electromagnetic radiation (7%) due to high density of free electrons present, which strongly relate to surface conditions [43]. Absorptivity also gets affected to high impulse electron radiation to the surface of the alloy.



Fig 2.12 Aluminum Sheets (Base Material)

#### **2.2.4 Stainless Steel**

In our experimentation of laser surface texturing FTO coated glass one of the base materials apart from Copper and Aluminum that was taken into consideration was Stainless Steel. Stainless Steel didn't have any direct contact with laser beam but was kept as support material along with FTO Coated glass. It was used as one of the parameters to see how the properties of copper affect the texturing of FTO glass and helps in variation of the absorption.

Stainless Steel is an alloy of Steel family which is mainly composed of 10 to 30 % of Chromium which helps in resisting corrosion of the alloy. The other elements like Nickel, Molybdenum, Titanium, Aluminum, Copper, Niobium, Nitrogen, Phosphorous or Selenium can also be added in order to reduce the corrosion.

There are more than 100 grades of Stainless Steel. The majority of which is classified into 5 major categories namely Austenitic, Ferritic, Martensitic, Duplex and Precipitation hardening. Amongst this the Austenitic is the most corrosion resistive and are non-magnetic in nature.

The biological cleaning ability of Stainless Steel is more than both Aluminum and Copper and they are ductile in nature and thus can be easily rolled into wires and plates.

**Table 2.6 Characteristics of Stainless Steel**

1.	Name	Stainless Steel
2.	Type	Alloy with around 11% Chromium
3.	Properties	Ductile, non-magnetic (mostly), heat resistant, anti-corrosive.
4.	Types	Austenitic, Ferritic, Martensitic, Duplex and Precipitation hardening

### **Stainless Steel in Presence of Laser**

In this paper Stainless Steel has been used as a base material i.e. FTO coated glass is the main material that undergoes laser irradiations and comes in direct contact with laser beam. Stainless Steel however has no direct intervention with Laser. However laser surface texturing had a marked potential for modulating friction and wear properties [44] of stainless steel if treated under laser radiation.



**Fig 2.13 Stainless Steel Sheets (Base Material)**

## 2.3 Analysis of Results

Minitab is basically a software that is being used for data analysis. It gives the most effective, and quick analysis of the given data in the most précised manner.

Taguchi designs also known as orthogonal array is the process of Optimization method that is based on a few steps of planning, conducting and evaluation of results. The first step of Taguchi Analysis includes the “trial and error” approach which helps to decide which parameter needs to be varied and that to up to which certain range. This follows up with the step of “Design of Experiments”. In this step all the pre obtained parameters are varied to a certain range and this gives a much better approach towards obtaining a systematic data. The third step that comes to existence is the “Taguchi method” based on orthogonal array which gives a reduced variance with controlled parameters. Dr. Taguchi’s Signal to Noise (S/N) Ratio serves the objective of giving desired output with optimization and to help in data analysis and prediction of Optimum Results.

Taguchi Method treats the problems for optimization in two categories, namely Static Problems and Dynamic Problems. The problem that helps in determining the best control factor levels so that the output is the target value is termed as “Static Problem”. In this problem noise remains present in the process which however has no significant effect on the output

There are basically 3 Signal to Noise ratios used in Static Problem optimization.

### a. Smaller the Better

$$n = -10 \log_{10} (\text{mean of sum of squares of measured data})$$

This is the chosen S/N Ration for all the undesirable characteristics’ present in the output like defects and noise for which the ideal value is zero.

### b. Larger the Better

$$n = -10 \log_{10} (\text{mean of sum squares of reciprocal of measured data})$$

This case has been converted to Smaller the betterby taking the reciprocals of measured data and then taking the S/N ratio as in the smaller the better case scenario.

### c. Nominal the Best

$$n = 10 \log_{10} (\text{Square of mean / variance})$$

This scenario arises when the most desired output is needed i.e. neither smaller the best or larger the best.

Dynamic Problems are the ones that we come across when the output signal is supposed to follow input signal in a pre-determined manner. In the Dynamic method a liner relationship between input and output is expected generally.

My experimentation is basically based on the optimization of Static problem with Larger the Better Signal to Noise Ratios.

The 8 steps of Taguchi Analysis are shown in the flowchart diagram.

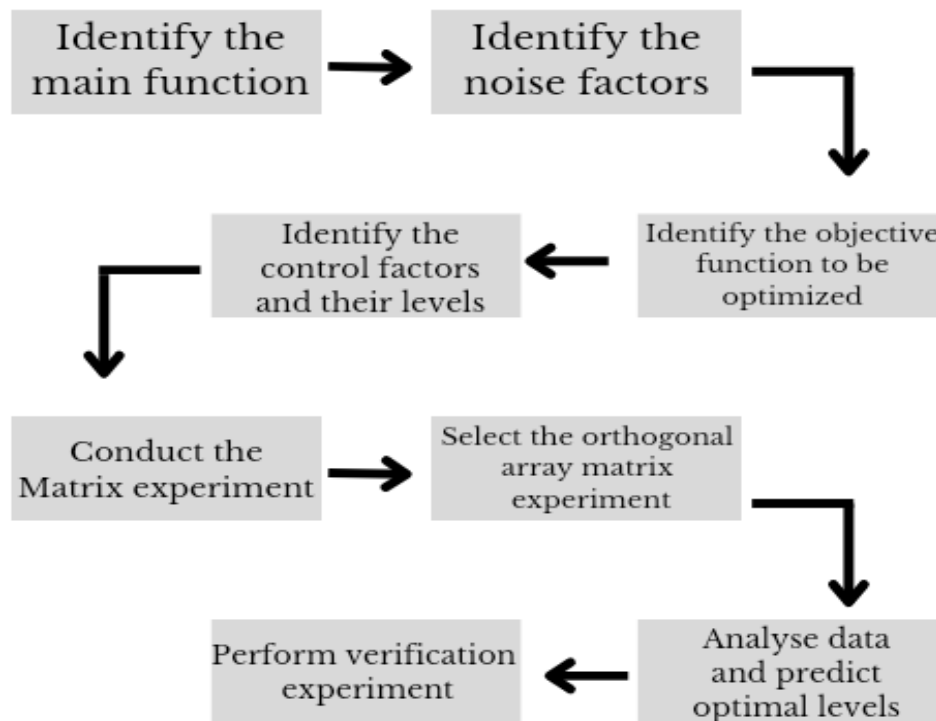


Fig 2.14 8 step Flowchart Diagram for Taguchi Analysis

## **Chapter – 3**

### **Experimental Investigation and Analysis**

### **3.1 Experimental Plan**

A Q-switched Fiber Laser with 1064 nm wavelength was used to surface texture FTO Coated glass material substrate experimented under different parametric conditions each of whose dimensions were taken as 30mm x 20mm x 2mm. Then one by one they were placed under the FTO coated material as the base material. The Laser machine was started and framing was done. Then shutter was closed and experimentation was initiated. Responses were notes down for each base material.

In this experiment three parameters were varied to get the responses at the output. The parameters that were varied are Power (Watts), Nozzle Distance (mm), and the base material. The maximum power of the laser machine was 500Watts and we have certain percentages of the value to calculate our result. The power was varied within the range of 50% to 70% and the nozzle distance was kept within the limits of 10mm to 20mm.

Certain parameters were kept at a fix namely Frequency, the step size (distance between each etching on the material surface), delay time and wavelength.

After the experimental machineries were set up a series of trails and errors were done whose results can be summarized in the following table.

**Table 3.1 Trial and Errors for Experimentation**

Sl No .	Power (Watts )	Nozzle Distance (mm)	Base Material	Peak Absorbance	Peak Transmittance	Wavelength of peak absorbance (nm)	Patterns formed
1.	150	25	Copper	-	-	-	Cracks formed
2.	150	20	Copper	2.046	62%	281	Overlapped patterns formed
3.	300	20	Stainless Steel	2.783	34%	264	Less overlapping patterns formed.
4	300	10	Copper	2.912	12.67%	265	A bit précised patterns formed
5.	25	25	Stainless Steel	-	-	-	Cracks formed.
6.	400	10	Stainless Steel	-	-	-	Light cracks formed
7.	400	10	Aluminum	-	-	-	Light cracks formed
8.	300	15	Aluminum	1.940	81%	277	Overlapping but clear patterns formed.

It was seen that irrespective of material or the power whenever the Nozzle Distance was 25mm then cracks were formed on the material surface. So the range of nozzle distance was fixed from 10mm to 20mm of distance. The lower limit was set to 10mm because that the maximum distance of the nozzle that can be moved towards the material. So Nozzle distances were chosen as 10mm, 15mm and 20mm.

Irrespective of the material or the nozzle distance when the Power was increased upto the value of 400 Watts then lights cracks were seen to be formed on the material surface and thus power values below it was taken. A good result of absorption was seen at 300Watts so keeping it the middle value 250Watts to 350 Watts was taken as the power value range.

Copper, Aluminum and Stainless Steel were the chosen base materials for the experimentation.

### 3.1.1 Setting Parameter Levels

**Table 3.2 Parameter Levels**

Sl No.	Parameters	Units	Limits		
			-1	0	+1
1.	Power	Watts	250	300	350
2.	Nozzle Distance	mm	10	15	20
3.	Base Material	-	Aluminum	Copper	Stainless Steel

After the selection of levels of parameters certain trials and errors were performed in order to decide the range of the experiment to be performed and Design of Experimentation was performed with the help of Taguchi Method.

### 3.1.2 Plan of Experiment

In the present research work 3 base materials were chosen namely Copper, Aluminum and Stainless Steel. From the methodology of trial and error the power values chosen were 250 Watts, 300 Watts and 350 Watts. The Nozzle distance was set at 10mm, 15mm and 20mm. This values were used. The following results were used to design the plan of experiment in Taguchi L9 method.



**Table 3.3 Plan of Experiment**

SL No.	Power (Watts)	Nozzle Distance (mm)	Material
1.	250	10	Copper
2.	250	15	Stainless Steel
3.	250	20	Aluminum
4.	300	10	Stainless Steel
5.	300	15	Aluminum
6.	300	20	Copper
7.	350	10	Aluminum
8.	350	15	Copper
9.	350	20	Stainless Steel

After the set of experiments being performed they were collected and taken to the Spectrophotometer for getting the values of wavelength at which absorption changes.

### **3.1.3 Sample Preparation**

For the experiment three samples of Aluminum, Stainless Steel and Copper were taken each of dimensions 100mm x 75mm x 1mm. They are well cleaned in solution of Acetone in order to remove surface dirt and impurities. This was followed by cleaning then up with cloth material and drying them for a few minutes before the experiment to get performed.

The FTO coated glass samples were of dimension 30mm x 20mm x 2mm. Before the experiment the total area of surface to be textured was outlined using a CD Marker. Then after that laser surface texturing was performed and before using the same materials for UV-Vis testing their

surface was well cleaned using an Acetone solution. Then kept to rest for a few minutes and again cleaned with acetone. Surface was then rubbed with cloth and left to dry for some time before finally conducting the experiment to detect the absorption.

### **3.2 Experimental Procedure**

The experiments were done in MEHTA Fiber Laser Cutting machine of wavelength 1064 nm and Power of 500 W. After the selection of the parameters and their proper combinations to work upon the sample were one by one fixed or held properly to clipping equipment also termed as a fixture. Before initiating with the experiment all the precautionary measures were taken and the requirements were checked upon. The assist gas pressure, proper functioning of the chiller unit, the optimum level of the voltage stabilizer and proper positioning of the fixture were all taken care of.

After that the Laser Machine was turned with the help of the Cypcut Laser Cutting Software which was pre-installed in the console machine and well adjusted for the experiment to start. In the software all the values were being given one by one as per the Design of Experiment. Then the desired path of the Laser was chosen. It was a single laser pulse at the pre-determined point in this case of experimentation. Framing of the point within the limits were done. The shutter of the machine was closed and then the laser was started and proper functioning of the laser took place to provide us with the desired output.

The responses were recorded and well checked with the help of the Optical microscope. The output images were being taken at 16x zooming of the focusing lenses of the Optical Microscope.

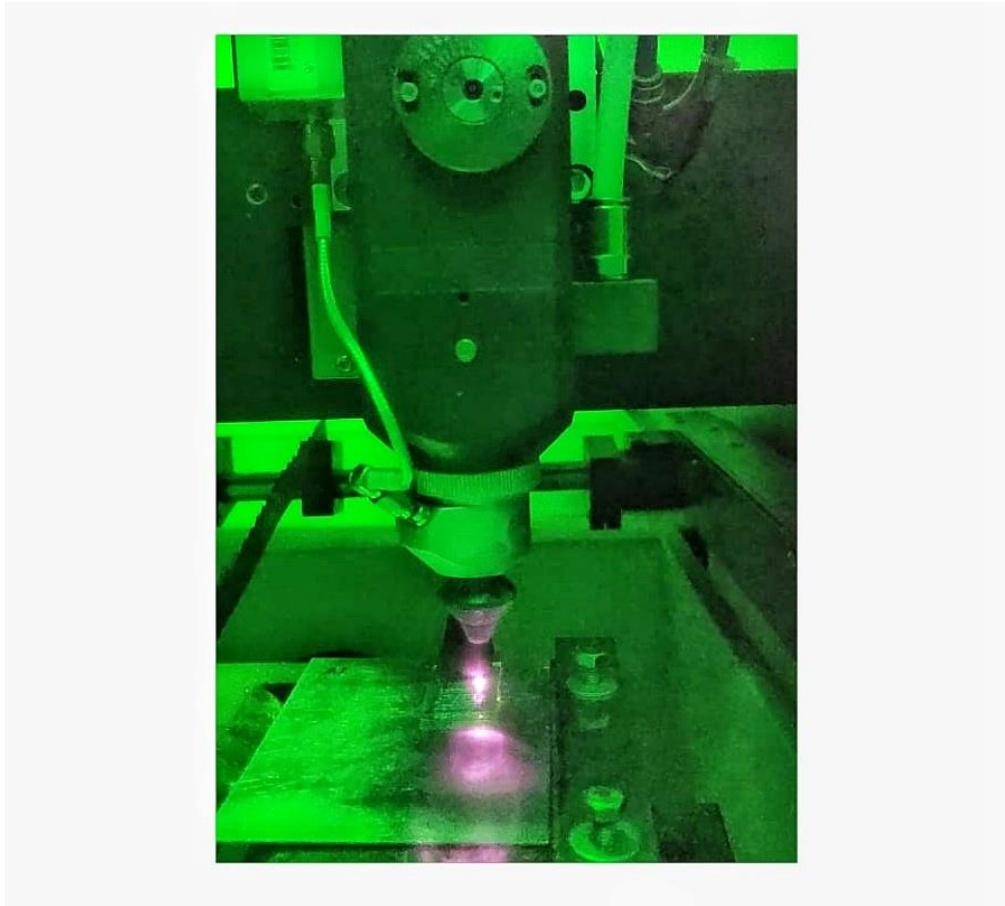


Fig 3.1 Texturing of Laser on FTO Coated Glass

After the experimentation performed at the Laser the textured samples were taken to the UV-Vis Spectrophotometer to get the desired output. The materials were preprocessed and with the help of tongs they were safely placed at the slide chamber in the Spectrophotometer. The results were performed by taking air as the reference, Then the UV-Vis software was started I the monitor and at very first as air baseline was generated. This was done only once at the very beginning of the experiment. It was done in order to subtract the values of the air absorption if any from the desired responses that we will be getting.



Fig 3.2 Experimentation of Textured FTO Coated Glass in Spectrophotometer.

### 3.3 Analysis of the Effect of Variable Parameters on Wavelength

**Table 3.4 Response on Wavelength at variable parameters**

SL No.	Power (Watts)	Nozzle Distance (mm)	Material	Wavelength (nm)
1.	250	10	Copper	291
2.	250	15	Stainless Steel	289
3.	250	20	Aluminum	287
4.	300	10	Stainless Steel	269
5.	300	15	Aluminum	281
6.	300	20	Copper	284
7.	350	10	Aluminum	268
8.	350	15	Copper	272
9.	350	20	Stainless Steel	262

In the above table we can see that the parameters of Power was varied in the values of 250 W, 300 W and 350 W. The Nozzle distance was varied in the values of 10mm, 15mm and 20mm. Also the base material was simultaneously altered between Copper, Aluminum and Stainless Steel. By varying these parameters the output wavelength is obtained. This wavelength is the value where the absorption curve reaches its maximum peak i.e. the values of wavelength obtained are the particular wavelength values at which the Absorption reaches their maximum value. In our experimentation it will be a better effect if the absorption peak is attained at a greater wavelength value i.e. away from the UV Radiation wavelength so that at greater wavelength value the incident light can be easily absorbed at its peak value and thus more energy can be converted to as and when required.

We will discuss about the various graphs obtained from the Output Table after the parameters were varied as per Taguchi analysis along with the normal results of a FTO Coated glass when no surface texturing or etching was done. Then we will compare the results of the normal glass substrate and then how the value varies after being Laser Surface Textured after varying the parameters.

### 3.3.1 Results for Un-textured FTO Coated Glass

At the beginning of experimentation with Laser Surface Texturing on FTO coated glass, a normal sample of the coated glass was taken and the UV Vis experiment was done on it in order to check its Absorption. This experiment was done with the sole motive of seeing the absorption of the glass material un-textured and to compare the value with textured glass sample. .

Table 3.5 Absorbance on un-textured FTO Coated Glass

Sl No.	Wavelength	Absorbance	% Transmittance
1.	262.0	0.035	92.2
2.	261.0	0.077	83.7
3.	260.0	0.092	80.8
4.	259.0	0.073	84.5
5.	258.0	0.061	86.9

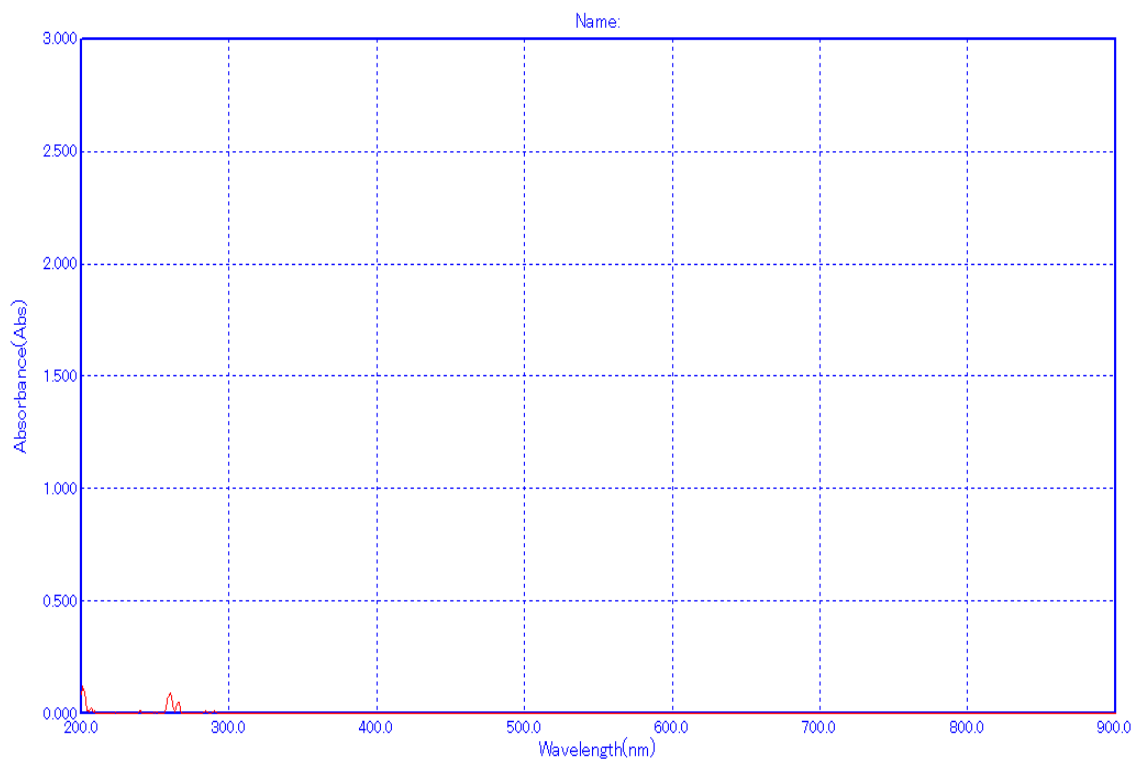


Fig 3.3 Graph of absorbance for un-textured FTO Coated Glass

### 3.3.2 Results Obtained for Textured FTO Coated Glass

#### Experimentation 1

The first set of experiment was carried at a Power of 250 Watt at a Nozzle distance of 10mm with Copper as the base material. The scanning wavelength was kept within the range of 200 nm to 900 nm. The result obtained is shown in the graph below with the tabulation of experimental data.

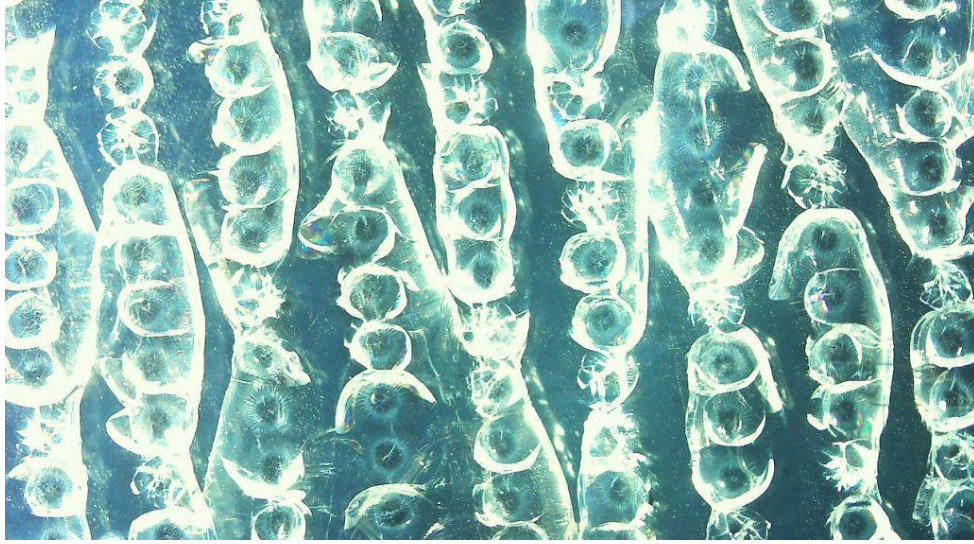


Fig 3.4 FTO Coated Glass after Experimentation 1

Table 3.5 Response for absorbance in terms of wavelength after Experimentation 1

Sl No.	Wavelength	Absorbance	% Transmittance
1.	294	2.800	0.2
2.	293	2.901	0.1
3.	292	2.948	0.1
4.	291	3.000	0.1
5.	290	3.000	0.1

It was seen that the absorption peak was maximum from the wavelength range of 291nm to 293nm.



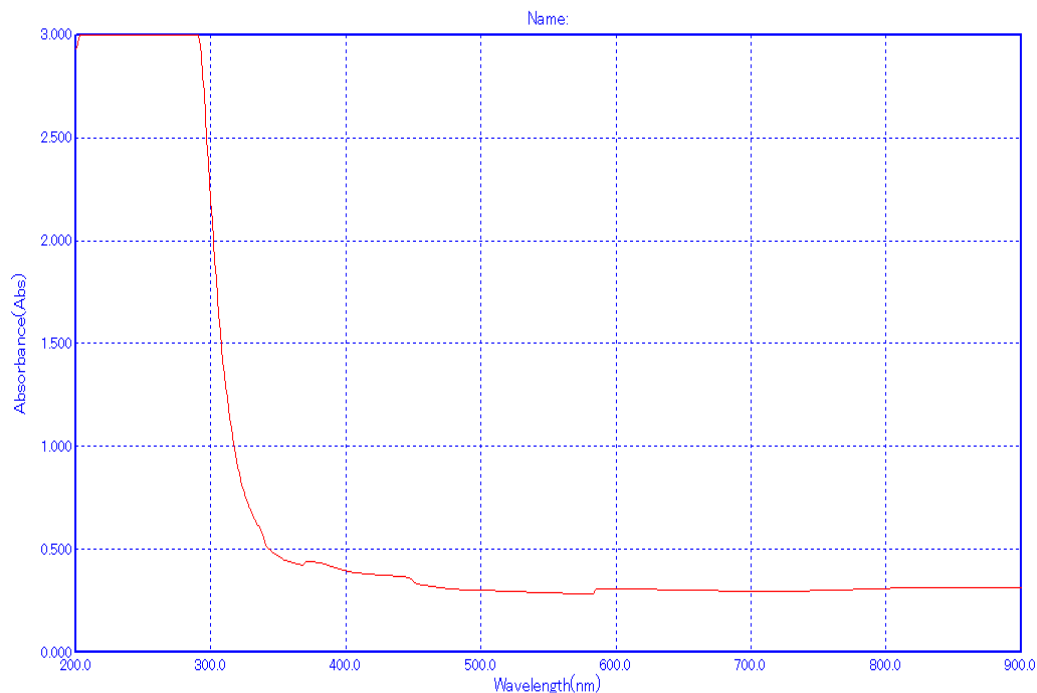


Fig 3.5 Graph for absorbance after Experimentation 1

## Experimentation 2

The second set of experiment was carried at a Power of 250 Watt at a Nozzle distance of 15mm with Stainless Steel as the base material. The scanning wavelength was kept within the range of 200 nm to 900 nm. The result obtained is shown in the graph below with the tabulation of experimental data.

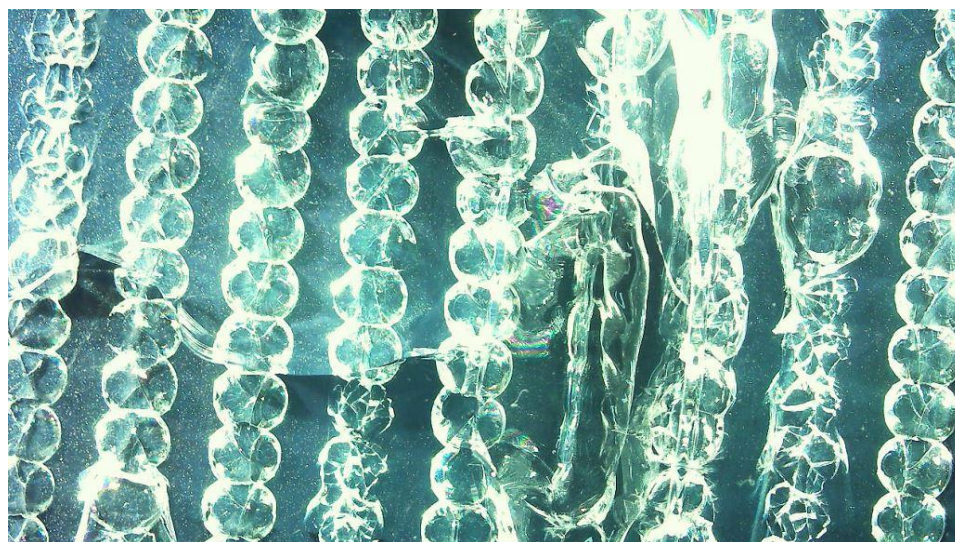


Fig 3.6 FTO Coated Glass after Experimentation 2



Table 3.6 Response for absorbance in terms of wavelength after Experimentation 2

SI No.	Wavelength	Absorbance	% Transmittance
1.	292.0	2.914	0.1
2.	291.0	2.982	0.1
3.	290.0	2.980	0.1
4.	289.0	3.000	0.1
5.	288.0	3.000	0.1

It was seen that the absorption peak was maximum from the wavelength range of 289nm to 205nm.

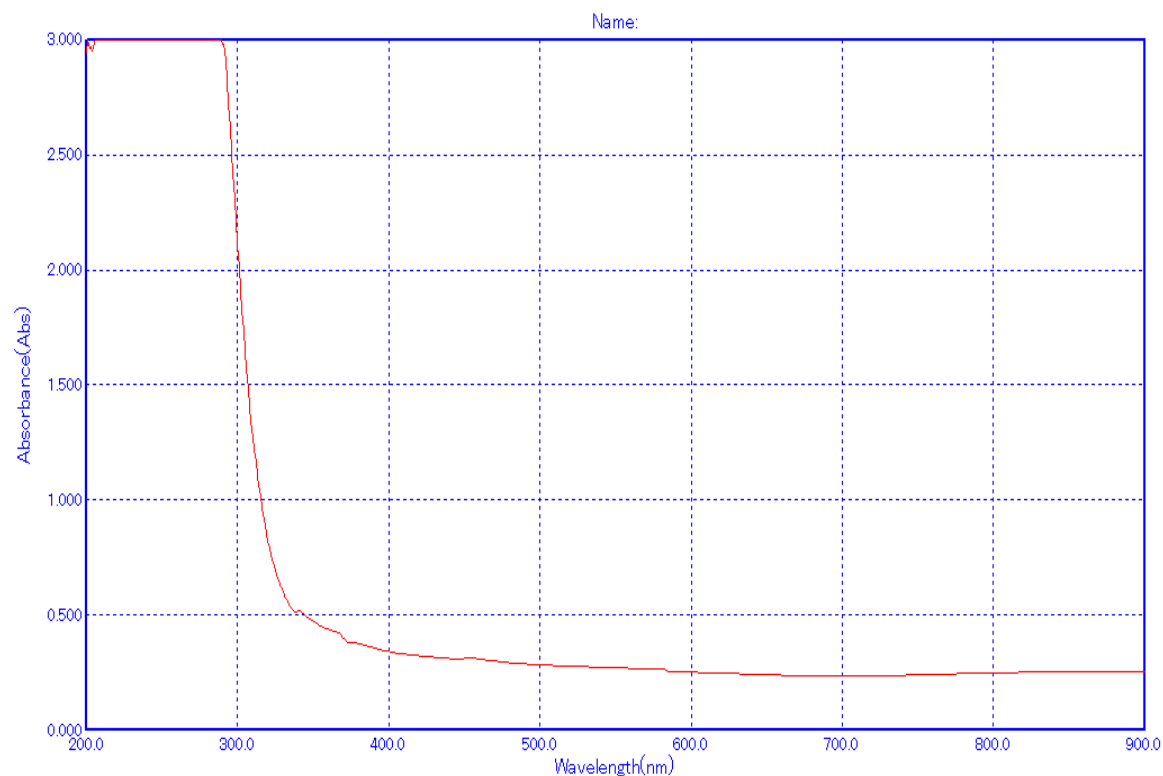


Fig 3.7 Graph for absorbance after Experimentation 2

### Experimentation 3

The third set of experiment was carried at a Power of 250 Watt at a Nozzle distance of 20mm with Aluminum as the base material. The scanning wavelength was kept within the range of 200 nm to 900 nm. The result obtained is shown in the graph below with the tabulation of experimental data.

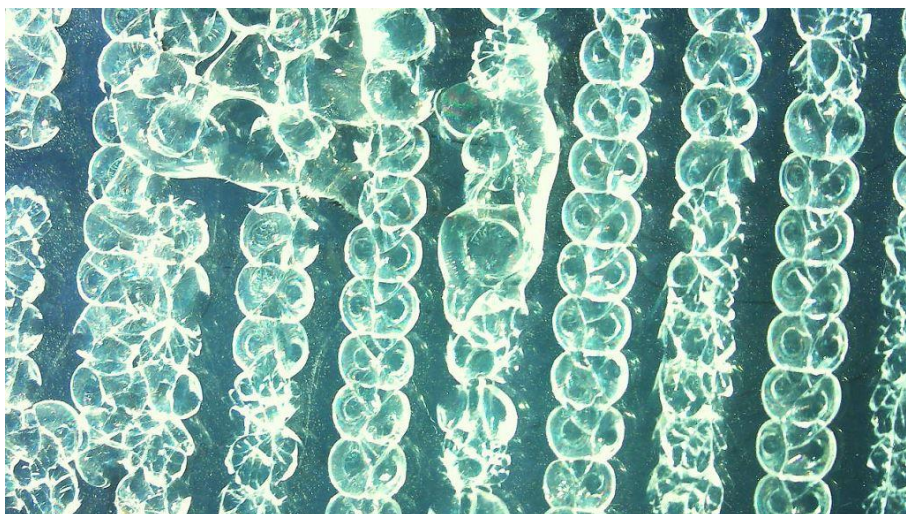


Fig 3.8 FTO Coated Glass after Experimentation 3

Table 3.7 Response for absorbance in terms of wavelength after Experimentation 3

SI No.	Wavelength	Absorbance	% Transmittance
1.	290.0	2.931	0.1
2.	289.0	2.961	0.1
3.	288.0	2.986	0.1
4.	287.0	3.000	0.1
5.	286.0	3.000	0.1

It was seen that the absorption peak was maximum from the wavelength range of 287nm to 229nm.

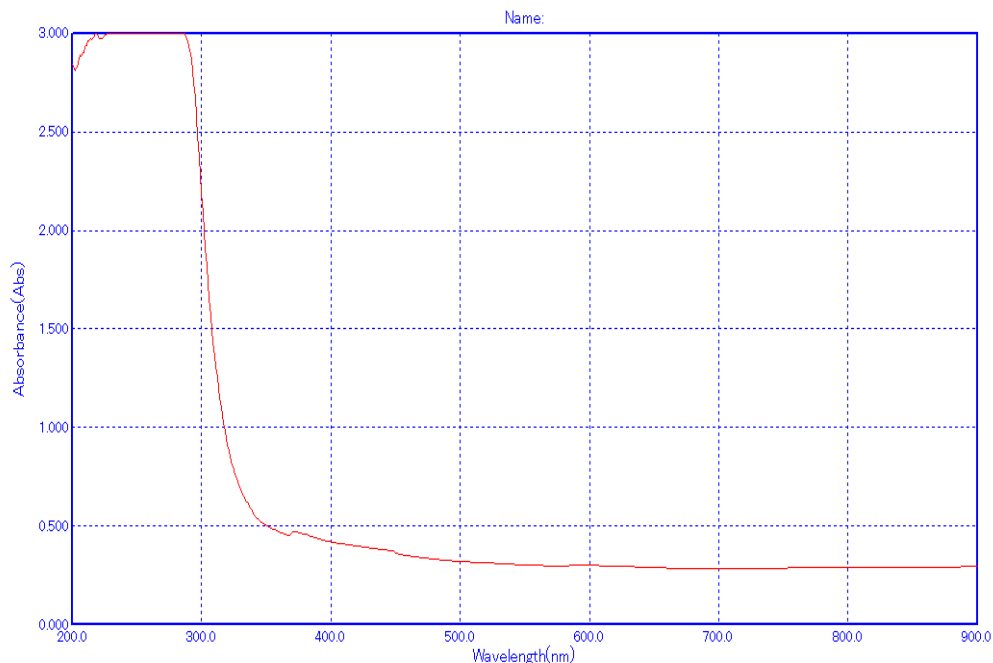


Fig 3.9 Graph for absorbance after Experimentation 3

#### Experimentation 4

The fourth set of experiment was carried at a Power of 300 Watt at a Nozzle distance of 10mm with Stainless Steel as the base material. The scanning wavelength was kept within the range of 200 nm to 900 nm. The result obtained is shown in the graph below with the tabulation of experimental data.

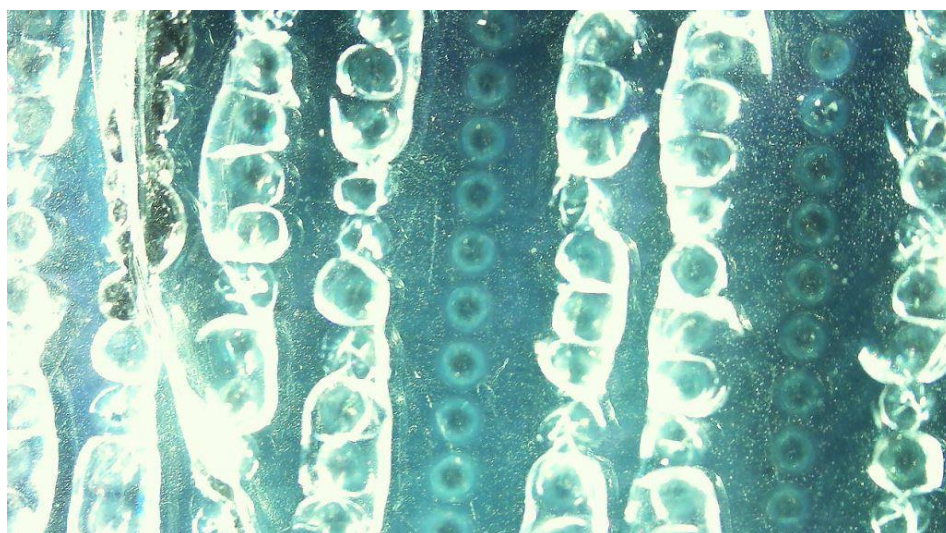


Fig 3.10 FTO Coated Glass after Experimentation 4

Table 3.8 Response for absorbance in terms of wavelength after Experimentation 4

SI No.	Wavelength	Absorbance	% Transmittance
1.	272.0	2.984	0.1
2.	271.0	2.988	0.1
3.	270.0	2.981	0.1
4.	269.0	3.000	0.1
5.	268.0	3.000	0.1

It was seen that the absorption peak was maximum from the wavelength range of 269nm to 211nm.

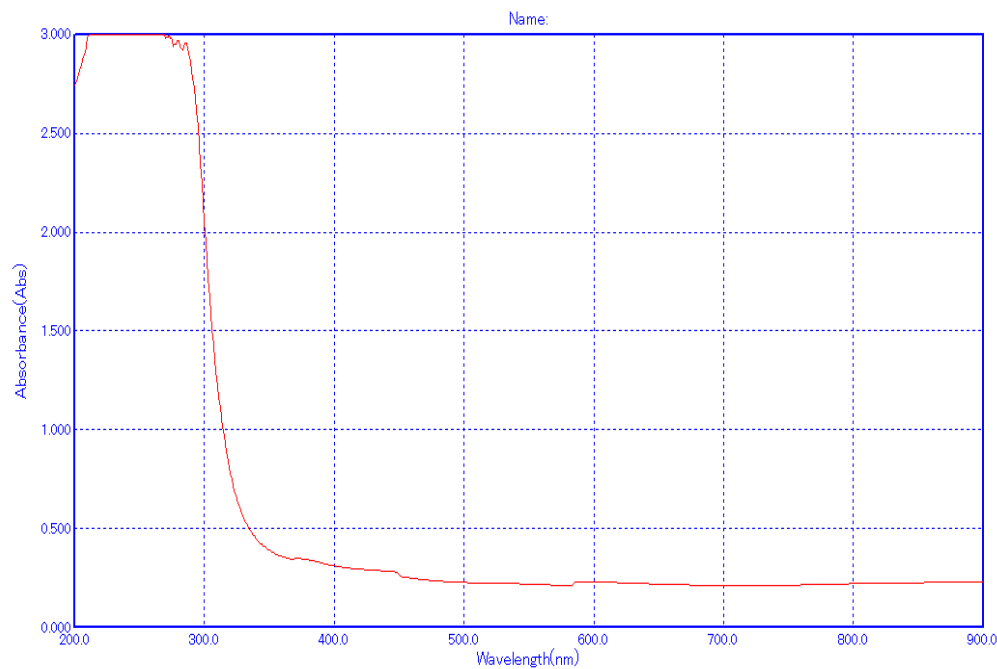


Fig 3.11 Graph for absorbance after Experimentation 4

### Experimentation 5

The fifth set of experiment was carried at a Power of 300 Watt at a Nozzle distance of 15mm with Aluminum as the base material. The scanning wavelength was kept within the range of 200 nm to 900 nm. The result obtained is shown in the graph below with the tabulation of experimental data.

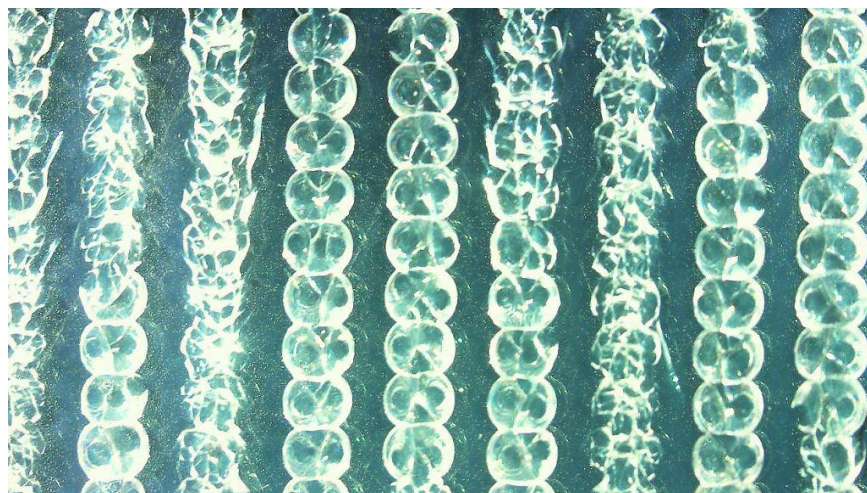


Fig 3.12 FTO Coated Glass after Experimentation 5

Table 3.9 Response for absorbance in terms of wavelength after Experimentation 5

SI No.	Wavelength	Absorbance	% Transmittance
1.	284.0	2.992	0.1
2.	283.0	2.974	0.1
3.	282.0	2.986	0.1
4.	281.0	3.000	0.1
5.	280.0	3.000	0.1

It was seen that the absorption peak was maximum from the wavelength range of 281nm to 210nm.



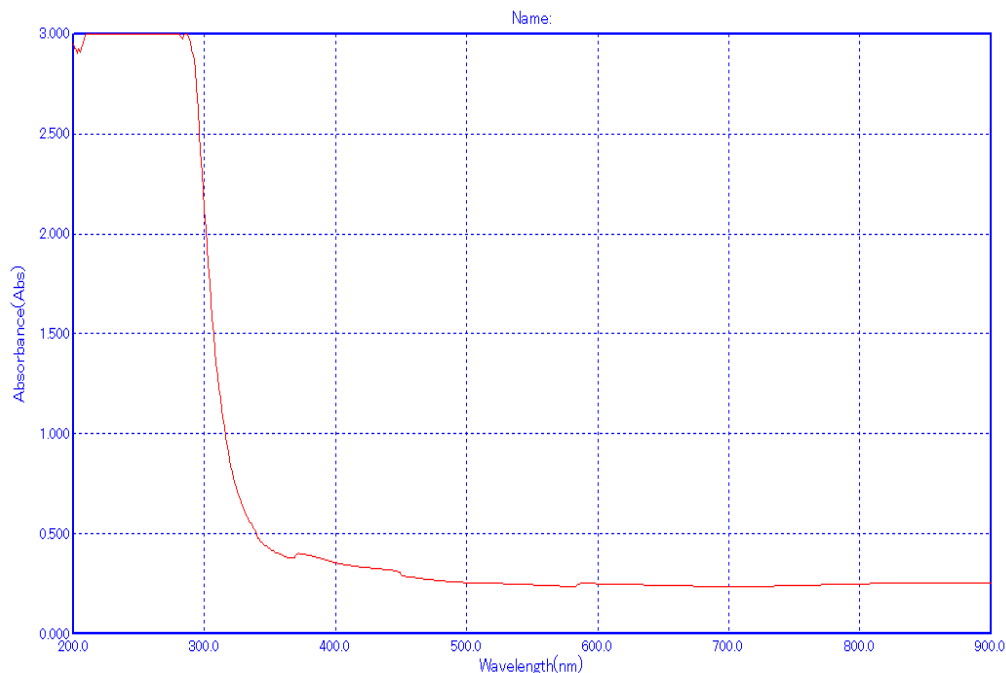


Fig 3.13 Graph for absorbance after Experimentation 5

### Experimentation 6

The sixth set of experiment was carried at a Power of 300 Watt at a Nozzle distance of 20mm with Copper as the base material. The scanning wavelength was kept within the range of 200 nm to 900 nm. The result obtained is shown in the graph below with the tabulation of experimental data.

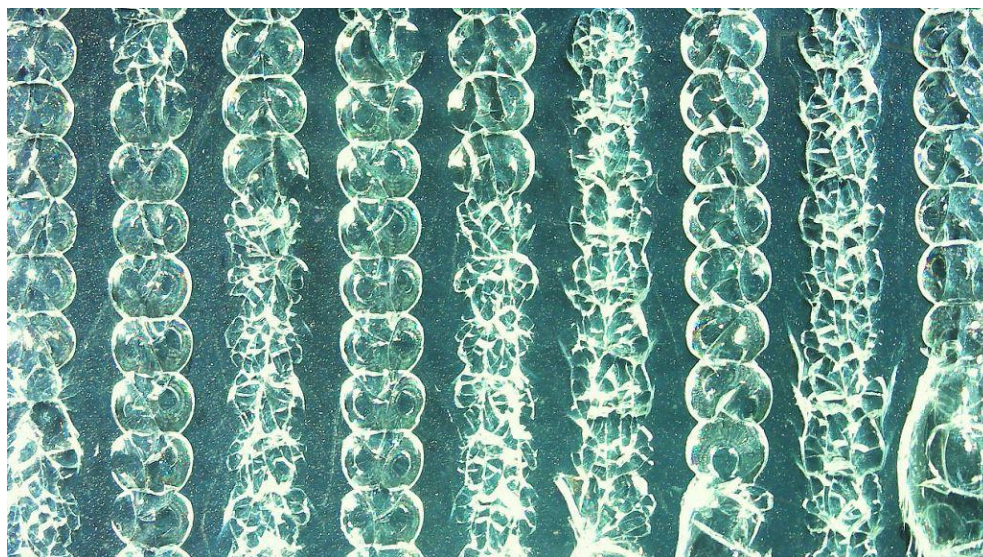


Fig 3.14 FTO Coated Glass after Experimentation 6

Table 3.10 Response for absorbance in terms of wavelength after Experimentation 6

SI No.	Wavelength	Absorbance	% Transmittance
1.	287.0	2.971	0.1
2.	286.0	2.981	0.1
3.	285.0	2.992	0.1
4.	284.0	3.000	0.1
5.	283.0	3.000	0.1

It was seen that the absorption peak was maximum from the wavelength range of 284nm to 208nm.

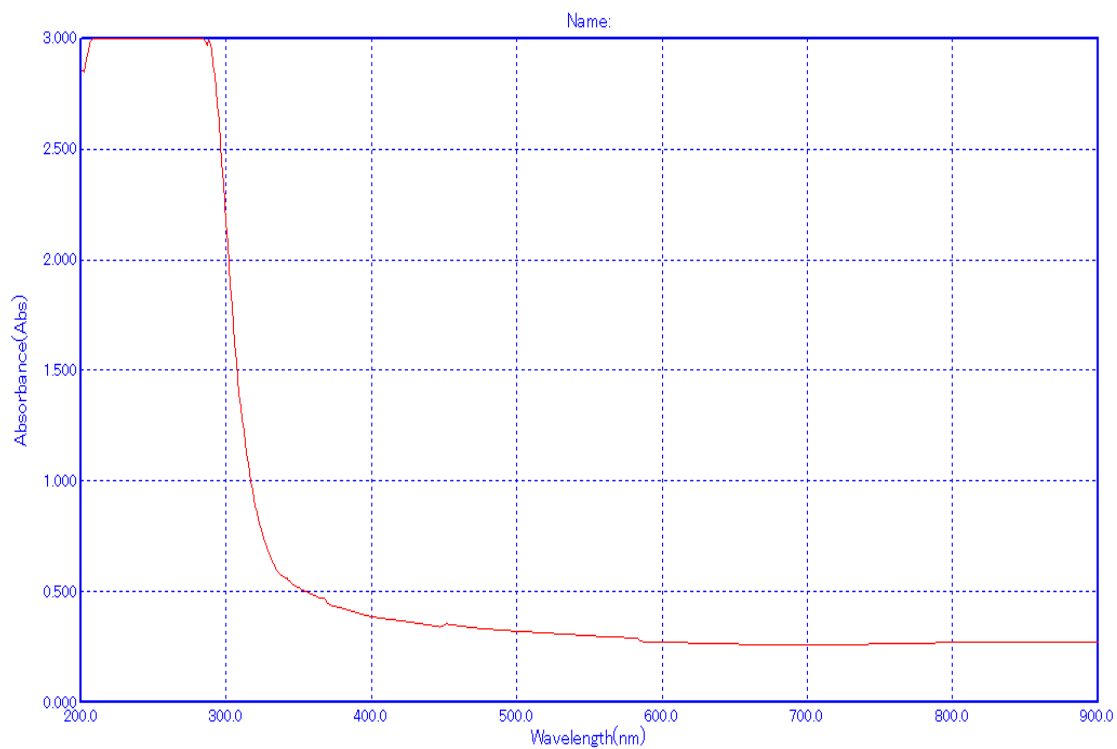


Fig 3.15 Graph for absorbance after Experimentation 6

### Experimentation 7

The seventh set of experiment was carried at a Power of 350 Watt at a Nozzle distance of 10mm with Aluminum as the base material. The scanning wavelength was kept within the range of 200 nm to 900 nm. The result obtained is shown in the graph below with the tabulation of experimental data.

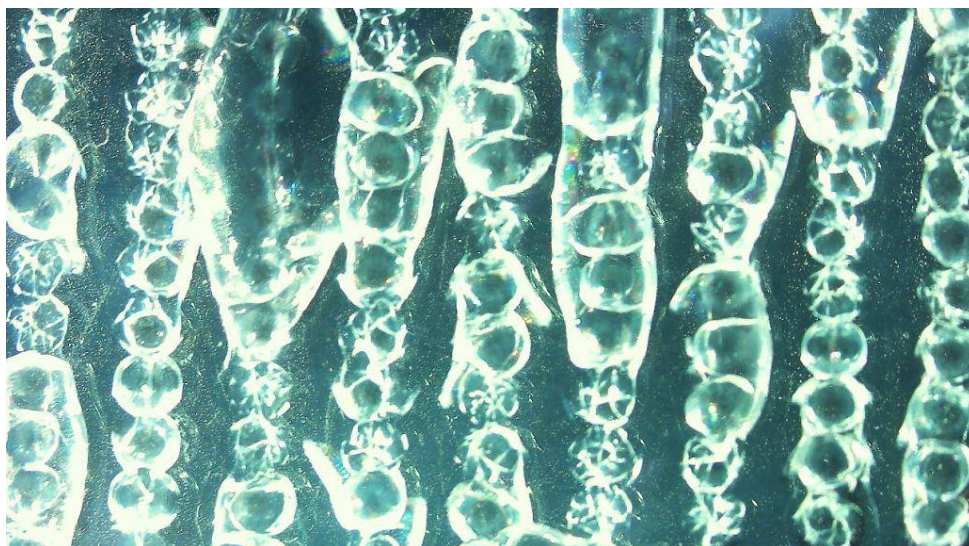


Fig 3.16 FTO Coated Glass after Experimentation 7

Table 3.11 Response for absorbance in terms of wavelength after Experimentation 7

SI No.	Wavelength	Absorbance	% Transmittance
1.	271.0	2.964	0.1
2.	270.0	2.978	0.1
3.	269.0	2.999	0.1
4.	268.0	3.000	0.1
5.	267.0	3.000	0.1

It was seen that the absorption peak was maximum from the wavelength range of 268nm to 234nm.



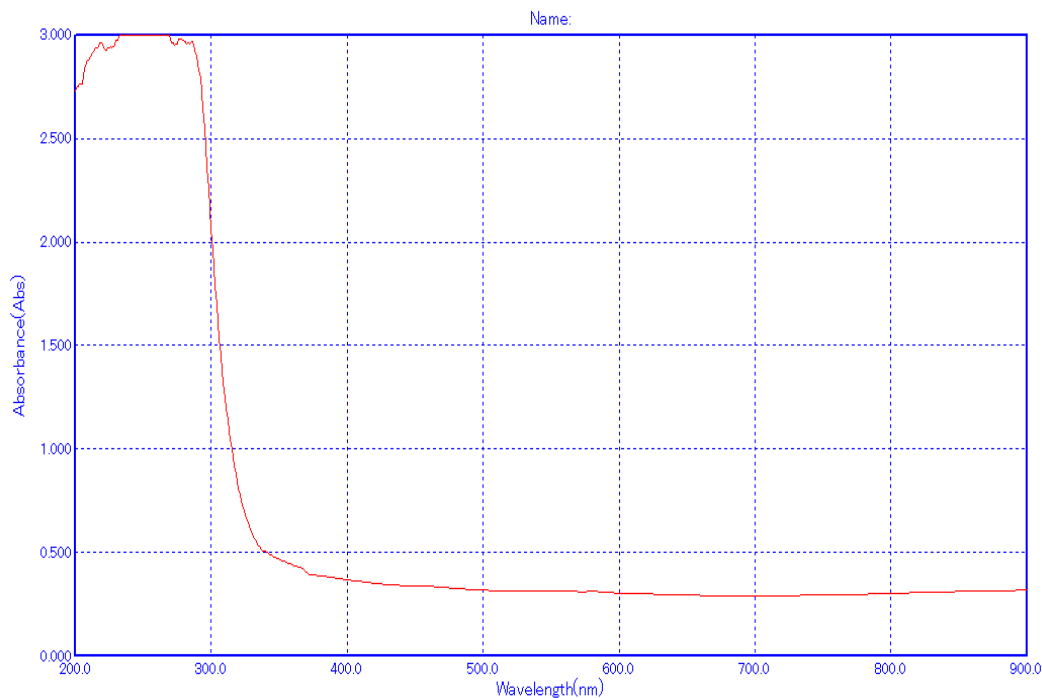


Fig 3.17 Graph for absorbance after Experimentation 7

### Experimentation 8

The eighth set of experiment was carried at a Power of 350 Watt at a Nozzle distance of 15mm with Copper as the base material. The scanning wavelength was kept within the range of 200 nm to 900 nm. The result obtained is shown in the graph below with the tabulation of experimental data.

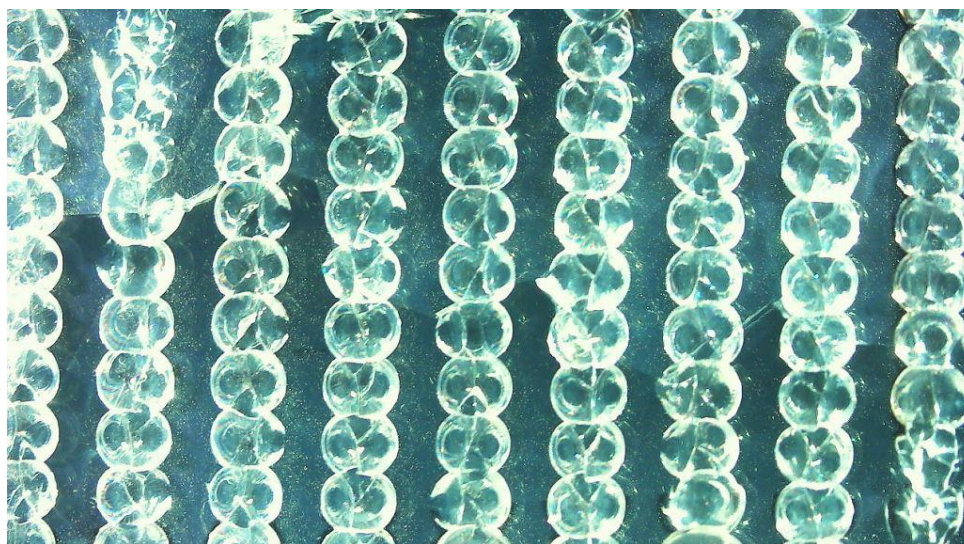


Fig 3.18 FTO Coated Glass after Experimentation 8

Table 3.12 Response for absorbance in terms of wavelength after Experimentation 8

SI No.	Wavelength	Absorbance	% Transmittance
1.	275.0	2.958	0.1
2.	274.0	2.969	0.1
3.	273.0	2.988	0.1
4.	272.0	3.000	0.1
5.	271.0	3.000	0.1

It was seen that the absorption peak was maximum from the wavelength range of 272nm to 210nm.

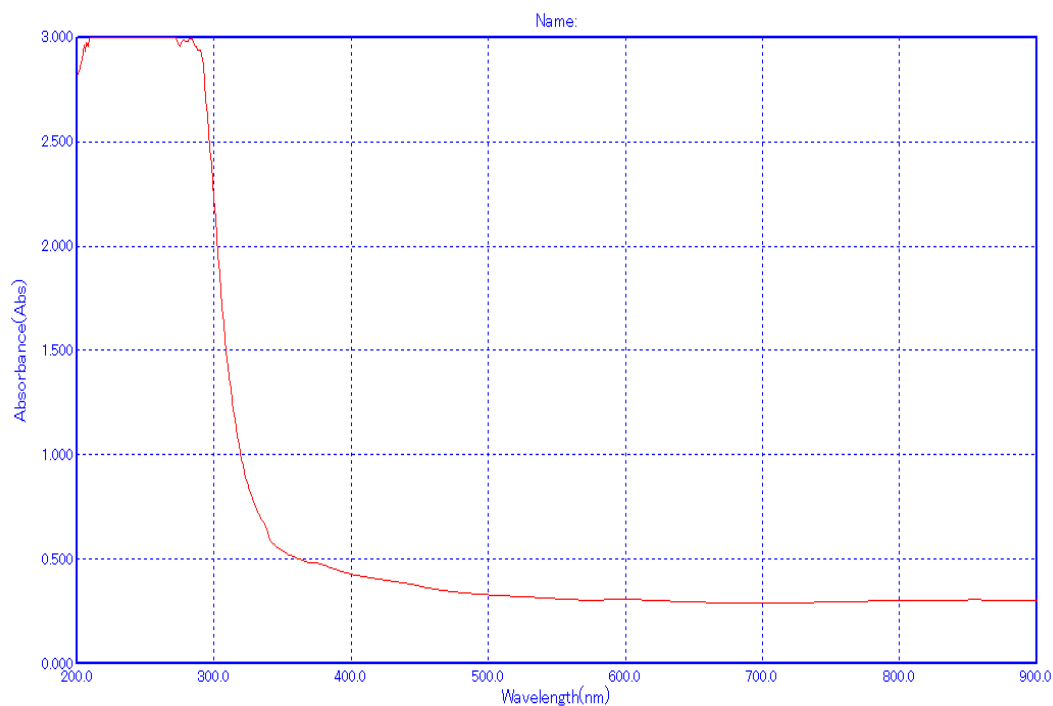


Fig 3.19 Graph for absorbance after Experimentation 8

### Experimentation 9

The ninth set of experiment was carried at a Power of 350 Watt at a Nozzle distance of 20mm with Stainless Steel as the base material. The scanning wavelength was kept within the range of 200 nm to 900 nm. The result obtained is shown in the graph below with the tabulation of experimental data.

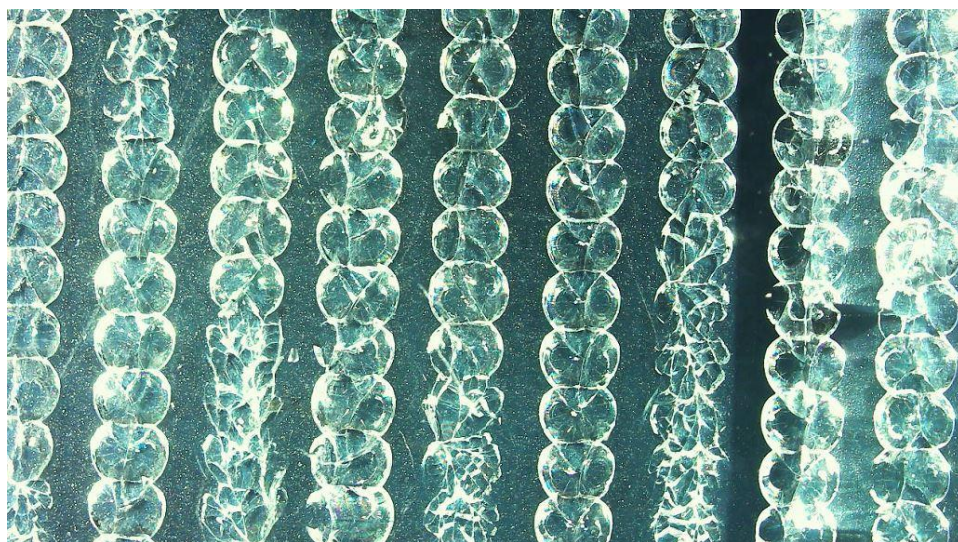


Fig 3.20 FTO Coated Glass after Experimentation 9

Table 3.13 Response for absorbance in terms of wavelength after Experimentation 9

SI No.	Wavelength	Absorbance	% Transmittance
1.	265.0	2.975	0.1
2.	264.0	2.971	0.1
3.	263.0	2.985	0.1
4.	262.0	3.000	0.1
5.	261.0	3.000	0.1

It was seen that the absorption peak was maximum from the wavelength range of 262nm to 235nm.

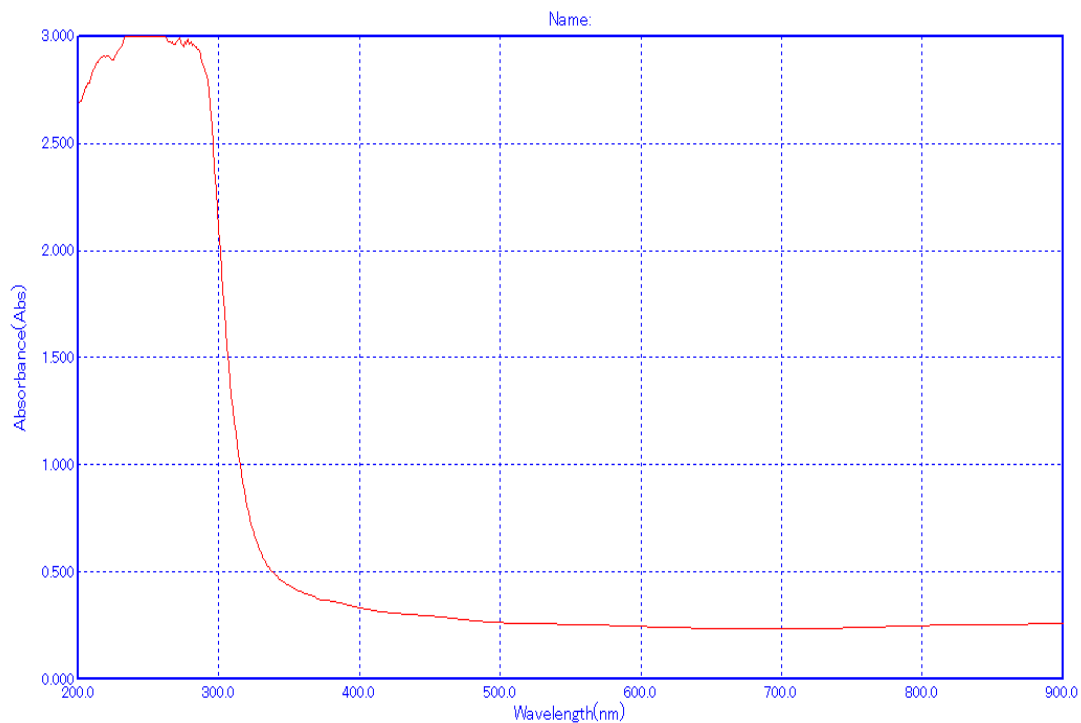


Fig 3.20 Graph for absorbance after Experimentation 9

### 3.3.3 Analysis of S/N Ratio plots for Wavelength

Table 3.14 Analysis of Variable in terms of Wavelength

Sl. No.	P	ND	Material	Wavelength
1	250	10	1	291
2	250	15	2	289
3	250	20	3	287
4	300	10	2	269
5	300	15	3	281
6	300	20	1	284
7	350	10	3	268
8	350	15	1	272
9	350	20	2	262

**Taguchi Analysis: Wavelength versus P, ND, Material**  
**Linear Model Analysis: SN ratios versus P, ND, Material**

**Table 3.15 Estimated Model Coefficients for SN ratios**

Term	Coef	SE Coef	T	P
Constant	48.8788	0.03890	1256.682	0.000
P 250	0.3390	0.05501	6.164	0.025
P 300	-0.0003	0.05501	-0.005	0.996
ND 10	-0.0669	0.05501	-1.217	0.348
ND 15	0.0824	0.05501	1.497	0.273
Material 1	0.1331	0.05501	2.419	0.137
Material 2	-0.1524	0.05501	-2.771	0.109

**Table 3.16 Model Summary**

S	R-Sq	R-Sq(adj)
0.1167	96.89%	87.55%

**Table 3.17 Analysis of Variance for SN ratios**

Source	DF	Seq SS	Adj SS	Adj MS	F	P
P	2	0.68909	0.68909	0.34454	25.31	0.038
ND	2	0.03450	0.03450	0.01725	1.27	0.441
Material	2	0.12397	0.12397	0.06199	4.55	0.180
Residual Error	2	0.02723	0.02723	0.01362		
Total	8	0.87480				

We have taken P value for the analysis of the results in the ANOVA table. The value of P needs to be equal to or less than 0.05 in order to be a suitable output. We can see that for Power the value is less than 0.05 i.e. 0.039 so power has the most effect on the output of wavelength to increase

**Linear Model Analysis: Means versus P, ND, Material****Table 3.18 Estimated Model Coefficients for Means**

Term	Coef	SE Coef	T	P
Constant	278.111	1.252	222.105	0.000
P 250	10.889	1.771	6.149	0.025
P 300	-0.111	1.771	-0.063	0.956
ND 10	-2.111	1.771	-1.192	0.355
ND 15	2.556	1.771	1.443	0.286
Material 1	4.222	1.771	2.384	0.140
Material 2	-4.778	1.771	-2.698	0.114

**Table 3.19 Model Summary**

S	R-Sq	R-Sq(adj)
3.7565	96.83%	87.30%

**Table 3.20 Analysis of Variance for Means**

Source	DF	Seq SS	Adj SS	Adj MS	F	P
P	2	704.22	704.22	352.11	24.95	0.039
ND	2	33.56	33.56	16.78	1.19	0.457
Material	2	122.89	122.89	61.44	4.35	0.187
Residual Error	2	28.22	28.22	14.11		
Total	8	888.89				

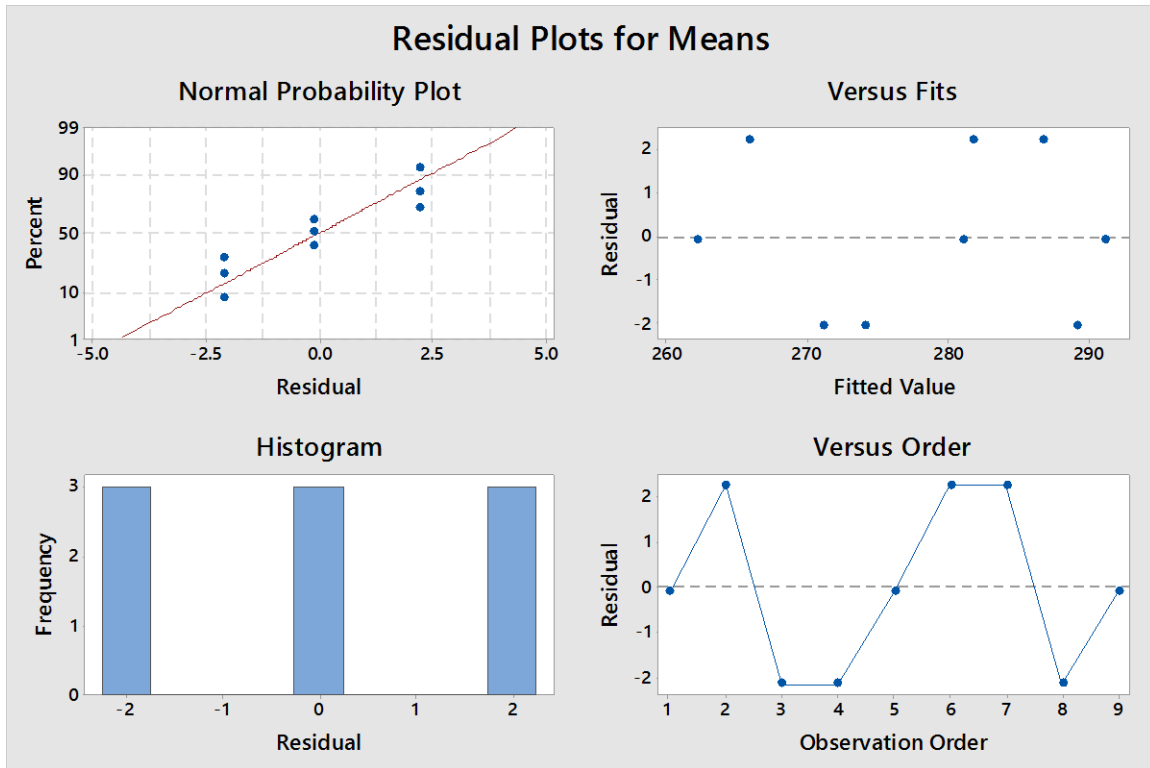


Fig 3.21 Residual Plot for Means

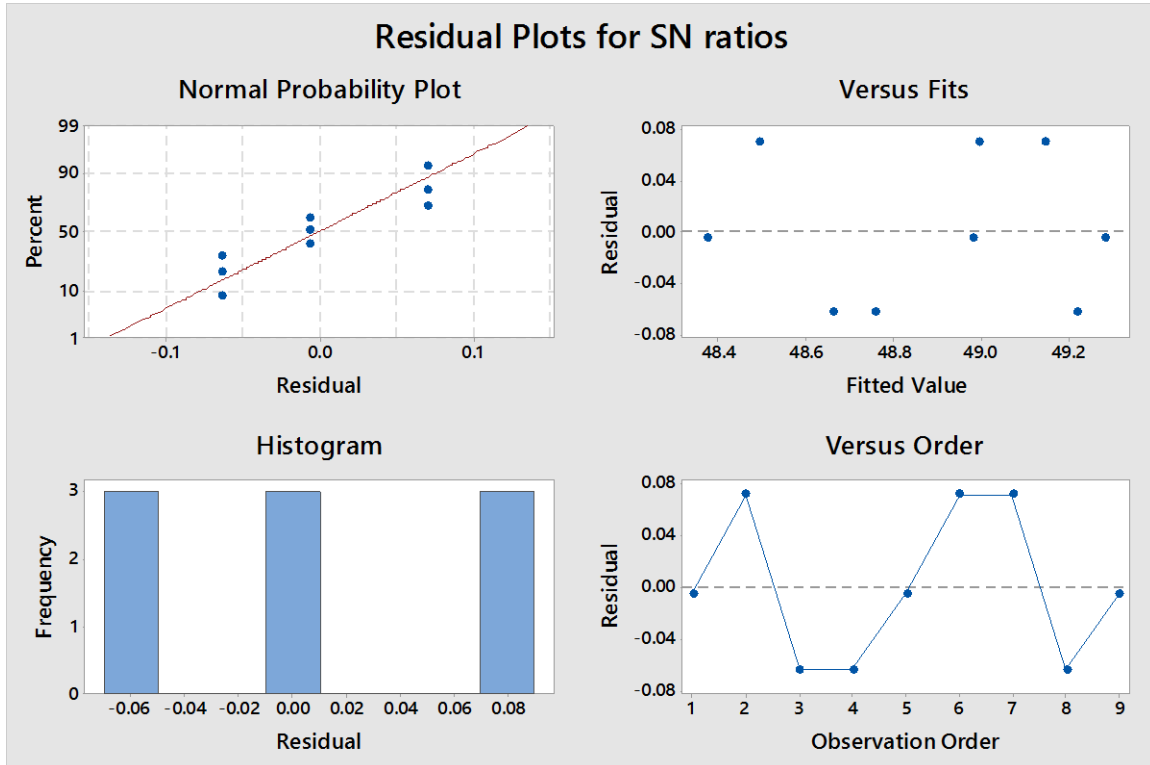


Fig 3.22 Residual Plots for SN Ratios

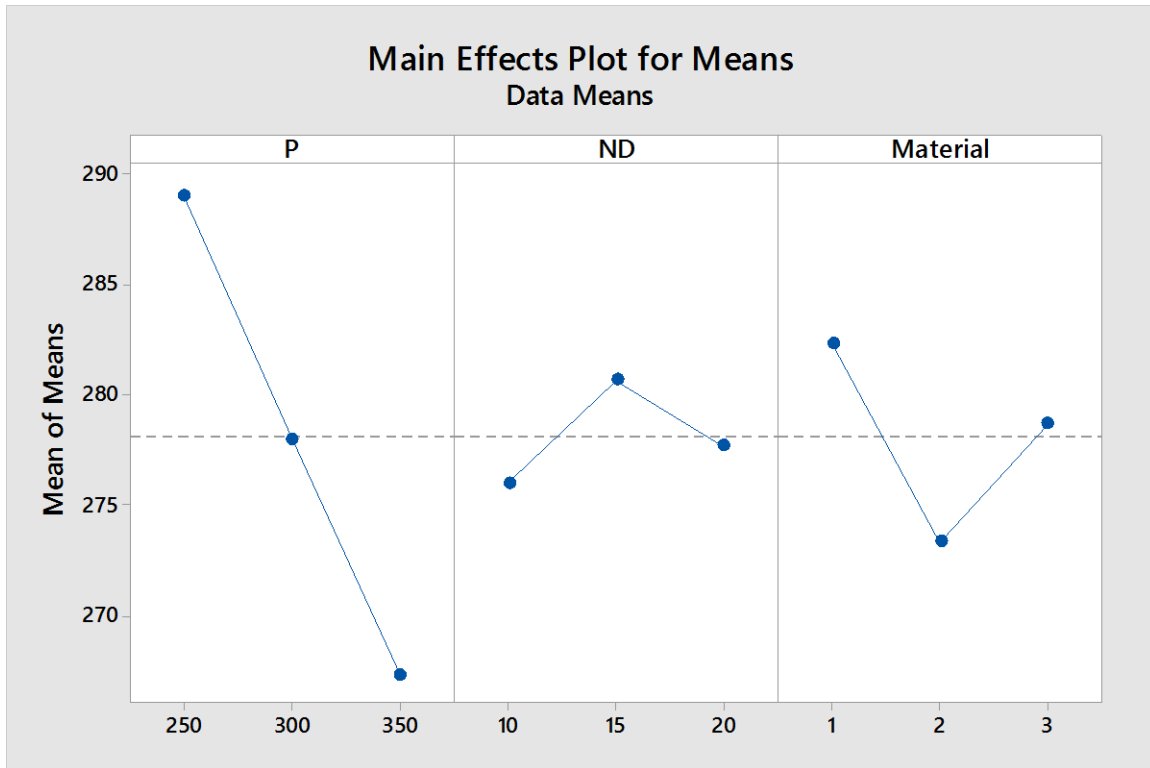


Fig 3.23 Main Effects Plots for Means

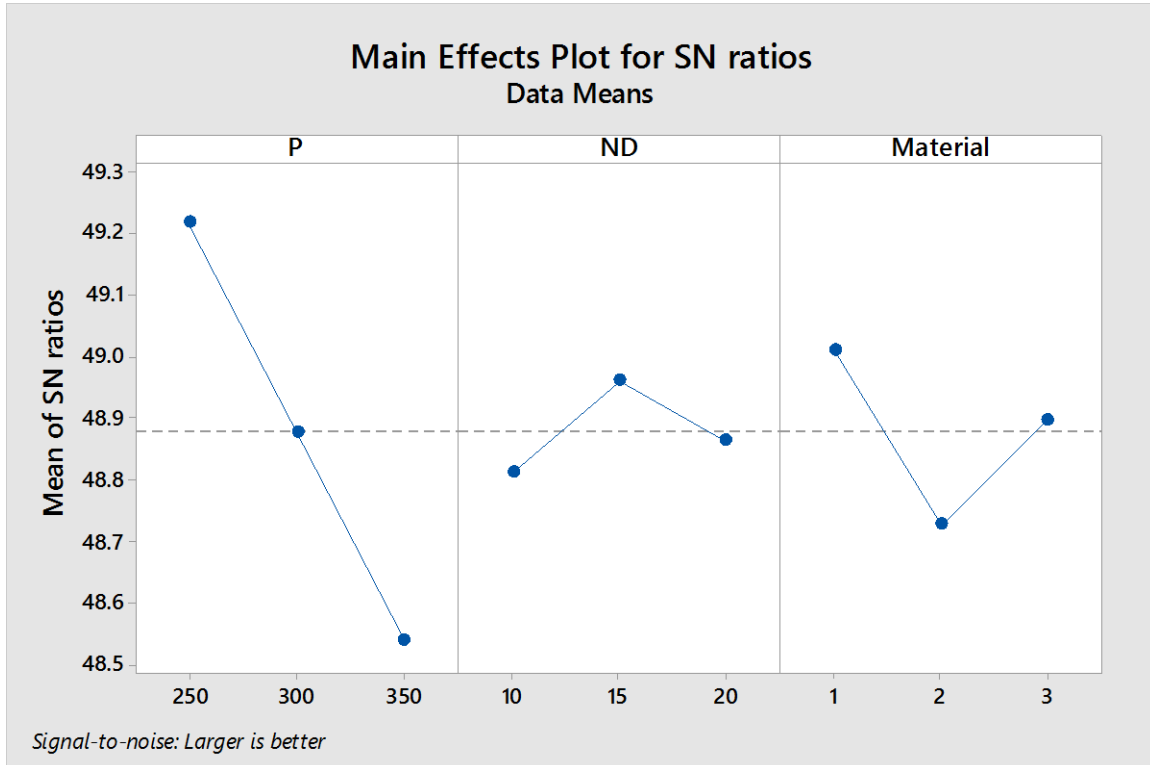


Fig 3.24 Main Effects Plot for SN Ratios



From the above S/N ratio it can be seen that the best results of roughness can be obtained from the combination where the Power is 250 Watt, the Nozzle distance is 15mm and the base material is Copper

In the above experiment it can be seen that the wavelength at which absorption reaches the maximum value or the range of wavelengths where the absorption stays at its peak value for the textured material varies for the variation of the different parameters. Earlier when the material was not textured or any kind of patterning was not done then the material was seen to absorb no or very little amount of light radiation. After the texturing of the material is done it is seen to absorb a higher amount of light emission and a substantial decrease in the amount of transmission is noticed. If the range of wavelength at which the absorption stays at its peak is greater, then the amount of light radiation that gets absorbed is more in comparison. Now if the value of the wavelength increases at which the absorption reaches its peak then it means that the material has absorbed more amount of radiation. We can see from the various graphs that are being plotted of absorbance against wavelength that for the base material copper, nozzle distances of 10mm and Power 250Watts the absorbance stays at peak value for a greater range of wavelength.

From the Main Effect Plots of Means it can be seen that the wavelength value is maximum for a Power value of 250Watt and it gradually decreases with increase in the power value. This is because as the power of the laser increases then more area of the material gets energized (affected) and hence more area gets thermally affected causing a bit of cracks or non-uniformities in the material as it being a glass, i.e. a very fragile and sensitive material and so owing to the defects and irregularities most of the light rays pass through it instead of getting absorbed due to texturing and hence the value of wavelength at which the absorption reaches maximum value also gets affected and reduces in value. It can also be seen from the Main Effect Plots of Means that the wavelength of peak absorption is maximum at 15mm and gradually reduces at 10mm and 20mm nozzle distance. When the nozzle distance is maximum then the focus is not proper and the spot diameter is too large to texture a particular area with precision and hence the peak wavelength for absorption decreases, again as the nozzle distance decreases to a value of 10mm the laser gets too focused at the point and the spot diameter is very small thereby affecting a very small area and a very minute etching of the place takes place. This thus have very low effect on the absorption and so the peak wavelength has comparatively lower value. But for a nozzle distance of 15mm a proper positioning of the focus with an optimal spot diameter is achieved. This allows the light radiation to be properly absorbed and hence increases the wavelength and the range of wavelengths at which the absorption reaches and stays at the peak. Lastly from the Main Effect Plots of Means it can be seen that for Copper the wavelength value is maximum followed by Aluminum and Stainless Steel. Amongst the remaining two base materials the reflectivity of Copper is the minimum, which means it has a greater absorbance in comparison to the other two materials. Thus at the point of contact of the material when laser radiation is passed very less is reflected back and most is absorbed thereby heating up the surface

and the point of contact as well. The material also gets heated up and a précised texturing of the point takes place and thsu the absorbance peak is reached at a greater value of wavelength.

In our present experiment it is seen that set of combinations where Power is 250 Watts, Nozzle distance is 15mm and the base material is copper then the absorption reaches the maximum value at a greater wavelength.

Amongst the different set of parametric values it is seen that the absorption stays at its peak value or maximum amount of absorption is noticed at in the 1<sup>st</sup> set of experiment where the power is 250 Watts, nozzle distance is 10mm and the base material is copper.

### 3.4 Analysis of the effect of variable parameters on Surface Roughness

**Table 3.21 Analysis of Variable in terms of Surface Roughness**

SL No.	Power (Watts)	Nozzle Distance (mm)	Material	Surface Roughness (micro meter)
1.	250	10	Copper	1.100
2.	250	15	Stainless Steel	1.000
3.	250	20	Aluminum	0.915
4.	300	10	Stainless Steel	1.110
5.	300	15	Aluminum	0.995
6.	300	20	Copper	1.010
7.	350	10	Aluminum	1.090
8.	350	15	Copper	1.102
9.	350	20	Stainless Steel	1.004

We will discuss about the surface roughness value obtained from experimentation as mentioned in from the Output Table after the parameters were varied as per Taguchi analysis along with the normal results of a FTO Coated glass when no surface texturing or etching was done. Then we will compare the results of the normal glass substrate and then how the value varies after being Laser Surface Textured after varying the parameters.

### 3.4.1 Results obtained for an un-textured FTO coated glass

**Table 3.22 Surface Roughness for un-textured FTO Glass**

Sl No.	Material type	Surface Roughness (micro meter)
1.	Un-textured FTO coated glass	0.031

### 3.4.2 Results obtained for textured FTO coated glass

**Table 3.23 Surface Roughness for textured FTO Glass at different input parameters**

SL No.	Power (Watts)	Nozzle Distance (mm)	Material	Surface Roughness (micro meter)
1.	250	10	Copper	1.100
2.	250	15	Stainless Steel	1.000
3.	250	20	Aluminum	0.915
4.	300	10	Stainless Steel	1.110
5.	300	15	Aluminum	0.995
6.	300	20	Copper	1.010
7.	350	10	Aluminum	1.090
8.	350	15	Copper	1.102
9.	350	20	Stainless Steel	1.004

### 3.4.3 Analysis of S/N Ratio plots for Surface Roughness

**Table 3.24 Analysis of Surface Roughness (Ra)**

Sl. No.	P (Watt)	ND (mm)	Material	Surface Roughness (micro meter) Ra
1	250	10	Copper	1.100
2	250	15	Stainless Steel	1.000
3	250	20	Aluminum	0.915
4	300	10	Stainless Steel	1.110
5	300	15	Aluminum	0.995
6	300	20	Copper	1.010
7	350	10	Aluminum	1.090
8	350	15	Copper	1.102
9	350	20	Stainless Steel	1.004

#### Taguchi Analysis: Output versus P, ND, Material

#### Linear Model Analysis: SN ratios versus P, ND, Material

**Table 3.25 Estimated Model Coefficients for SN ratios**

Term	Coef	SE Coef	T	P
Constant	0.29250	0.01691	17.300	0.003
P 250	-0.27374	0.02391	-11.448	0.008
P 300	0.02395	0.02391	1.002	0.422
ND 10	0.53512	0.02391	22.379	0.002
ND 15	-0.02580	0.02391	-1.079	0.393
Material 1	0.29348	0.02391	12.274	0.007
Material 2	0.02122	0.02391	0.887	0.469

**Table 3.26 Model Summary**

S	R-Sq	R-Sq(adj)
0.0507	99.80%	99.21%

**Table 3.27 Analysis of Variance for SN ratios**

Source	DF	Seq SS	Adj SS	Adj MS	F	P
P	2	0.41369	0.41369	0.206846	80.40	0.012
ND	2	1.63928	1.63928	0.819638	318.57	0.003
Material	2	0.55683	0.55683	0.278413	108.21	0.009
Residual Error	2	0.00515	0.00515	0.002573		
Total	8	2.61494				

We have taken P value for the analysis of the results in the ANOVA table. The value of P needs to be equal to or less than 0.05 in order to be a suitable output. We can see that for all 3 input parameters Power, base Materials and Nozzle Distance the value is less than 0.05. But for Nozzle distance it is the smallest i.e. 0.003 making it the most significant input parameters upon which surface roughness depends, followed by Base material and power.

### Linear Model Analysis: Means versus P, ND, Material

**Table 3.28 Estimated Model Coefficients for Means**

Term	Coef	SE Coef	T	P
Constant	1.03622	0.003057	338.959	0.000
P 250	-0.03122	0.004323	-7.222	0.019
P 300	0.00211	0.004323	0.488	0.674
ND 10	0.06378	0.004323	14.752	0.005
ND 15	-0.00389	0.004323	-0.900	0.463
Material 1	0.03444	0.004323	7.967	0.015
Material 2	0.00178	0.004323	0.411	0.721

**Table 3.29 Model Summary**

S	R-Sq	R-Sq(adj)
0.0092	99.53%	98.14%

**Table 3.30 Analysis of Variance for Means**

Source	DF	Seq SS	Adj SS	Adj MS	F	P
P	2	0.005480	0.005480	0.002740	32.58	0.030
ND	2	0.023008	0.023008	0.011504	136.77	0.007
Material	2	0.007505	0.007505	0.003752	44.61	0.022

Residual Error	2	0.000168	0.000168	0.000084
Total	8	0.036162		

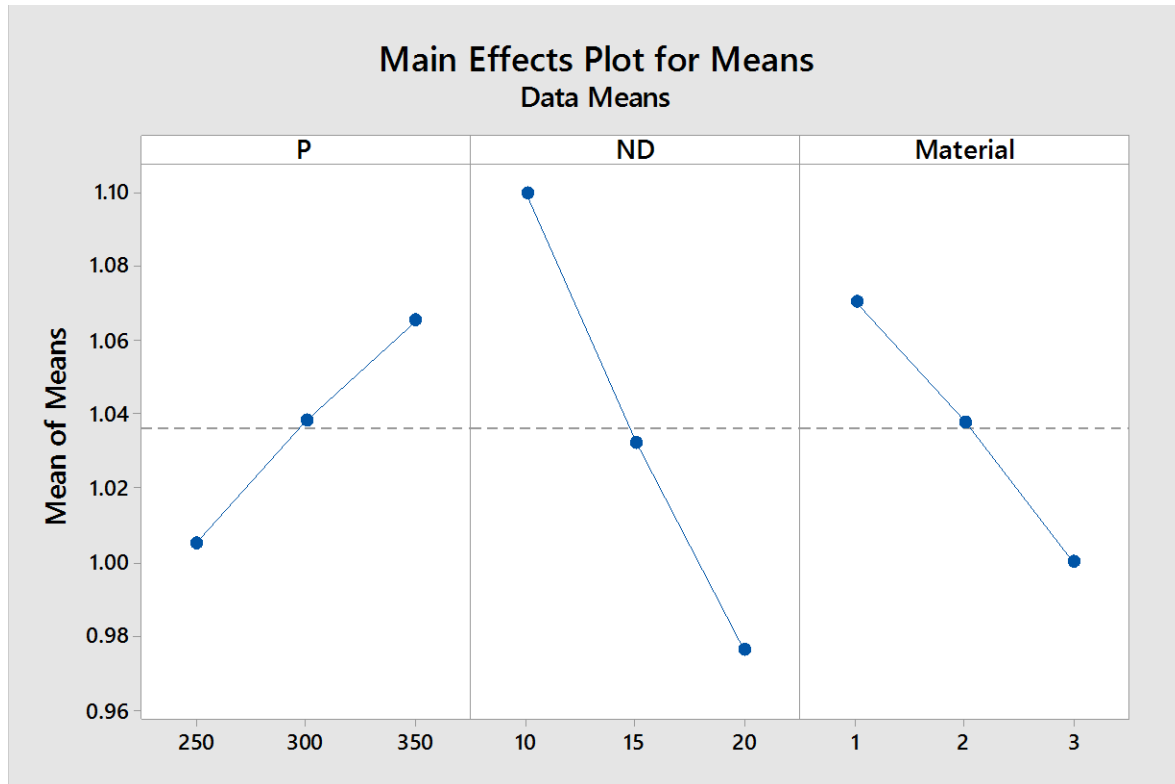


Fig 3.25 Main Effects Plots for Means

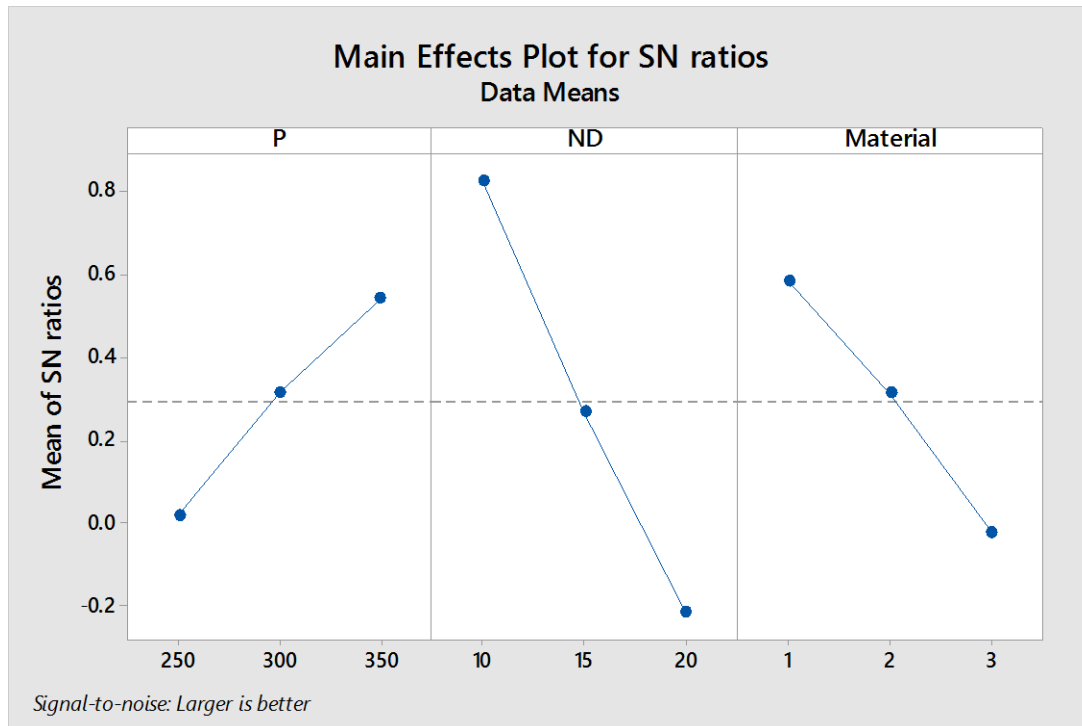


Fig 3.26 Main Effects Plot for SN Ratios

**Note: 1 stands for Copper, 2 stands for Stainless Steel, 3 stands for Aluminum**

From the above S/N ratio it can be seen that the best results of roughness can be obtained from the combination where the Power is 350 Watt, the Nozzle distance is 10mm and the base material is Copper.

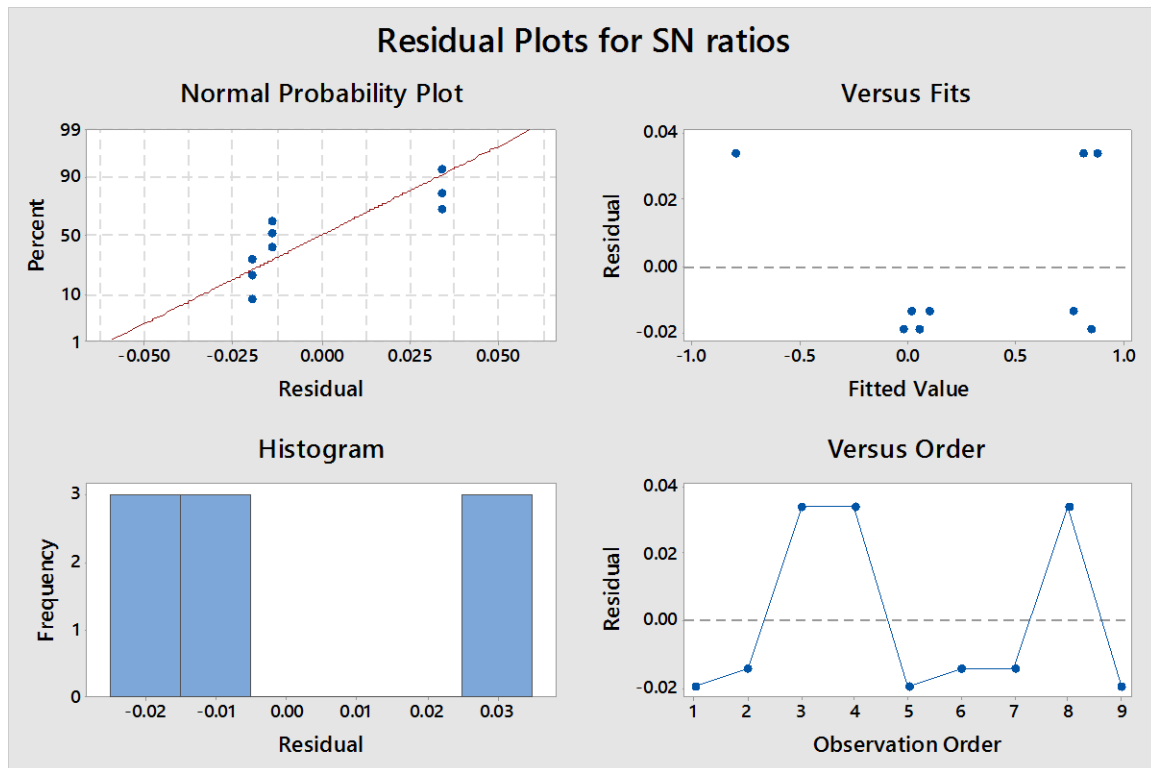


Fig 3.27 Residual Plots for SN Ratios

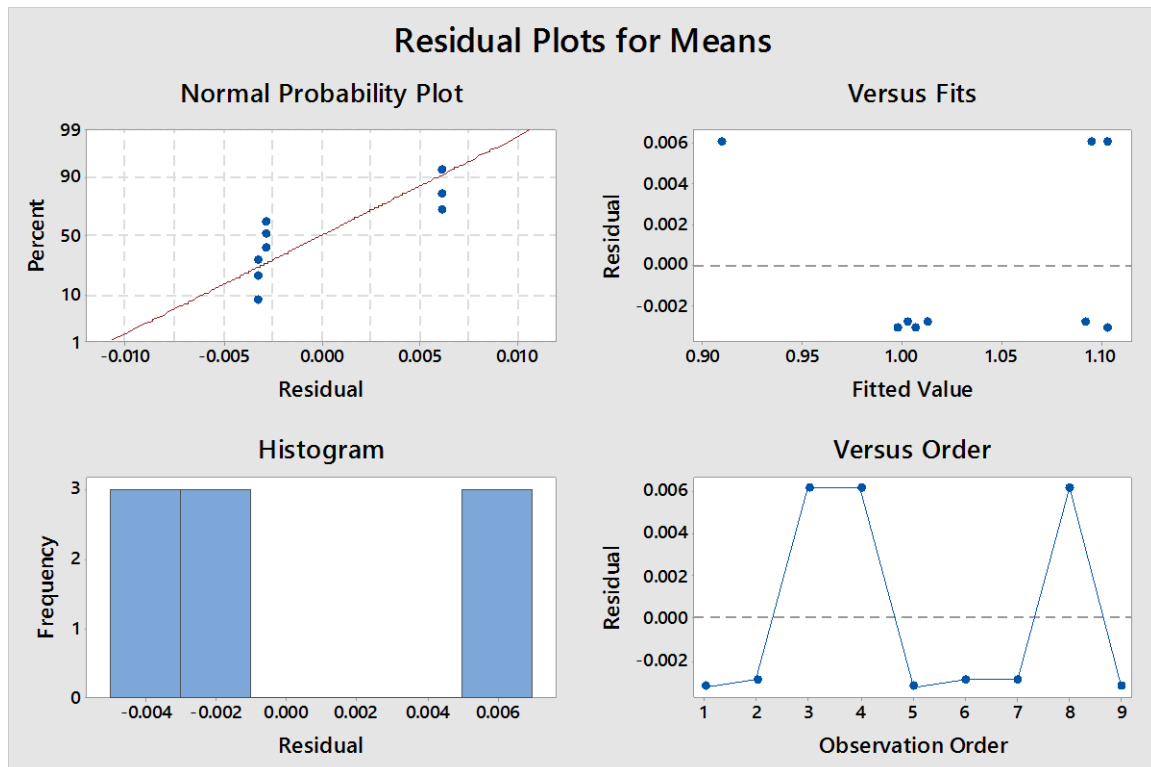


Fig 3.28 Residual Plots for Means.



In the above experiment it can be seen that the roughness of the textured material varies for the variation of the different parameters. The roughness is an important aspect of a surface characteristic when it comes to absorption of the material. If for a transparent material the surface roughness is almost none then any kind of radiation will pass through it and nothing will get absorbed. But if the surface roughness of the material is increased then the light rays entering the material will get trapped due to many internal reflections which will gradually result in more absorption and less reflection. For a sample this equation can be satisfied as  $A+T+R=1$  i.e. the absorbance, transmittance and reflectance adds to be 1. Thus theoretically it can be explained that if the transmittance or reflectance of the material decreases eventually its absorbance will increase.

In the Analysis of Variance of SN Ratio the P Value for all the parameters are less than 0.05 i.e. for 95% confidence level all the parameters are significant. Nozzle Distance has a P value of 0.003, followed by the base material having a P value of 0.009 and the Power of 0.012. This makes the Nozzle distance the most significant parameter which will affect the Surface Roughness followed by base material and power.

From the Main Effect Plots of Means we can see that as the Power of the laser increases the surface roughness increases as well. This is because the as the power increases, the energy deposition also increases on the material thereby making the material more affected and increasing its roughness. Again it can also be seen that if the nozzle distance of the laser increases the surface roughness decreases. This is because as the nozzle distance of the material decreases the focusing point becomes more appropriate as the spot diameter decreases and energy accumulation at a particular area becomes denser. This will in return increase the surface roughness. Finally it can be seen that for Copper the surface roughness is maximum followed up with Stainless Steel and minimum in Aluminum. It is known that the reflectivity of Aluminum is the largest, and then comes stainless steel and finally that of copper is the lowest. So what happens is that at the contact point of the FTO coated glass and the base material assembling of energy takes place after laser radiation. The most of energy accumulation occurs for Copper due to its low reflectivity in comparison to the other base materials and so the FTO material being at the contact to Copper also get affected and the roughness of the material becomes the most in

case of Copper as base material. For the same reason the surface roughness is the least observed in case of Aluminum.

Thus here in our present research work we can see from the main effect plot for the SN ratio that the combination of Power at 350 Watts, Nozzle distance at 10mm and base material copper gives the best results of increased roughness thereby allowing the material to absorb more radiation.

## **Chapter – 4**

### **General Conclusion and Future Scope of Research**

## 4.1 General Conclusion

In the present research work an experimental investigation on Laser Surface Texturing on FTO coated Glass is successfully carried out. Based on the availability of resources and limitation of time the following conclusions can be drawn:

- i) The surface texture of FTO coated glass can be altered according to requirement by suitable laser radiation.
- ii) A set of trial experiments were carried out to select the range of input parameters.
- iii) Based on survey of past literature a set of parameters were selected for each experiment using Taguchi methodology
- iv) The absorbance and roughness of the textured surface were chosen as the output criteria whereas Power, Nozzle distance and base material as the input variables.
- v) Implementing the L9 orthogonal array of Taguchi analysis a set of parametric combinations for laser texturing were selected. Then each sample was placed in UV-Vis Spectrophotometer for measurement of absorbance.
- vi) The absorbance value between un-textured and textured FTO samples was compared. At the different parametric value which set of combinations allows the absorption peak to stay at maximum value i.e. absorb most energy for a longer period of wavelength range is being calculated.
- vii) The absorbance graphs for each set of combinations and their values of absorbance against each wavelength for a range of 200nm to 900 nm were noted down in a tabular manner
- viii) The textured FTO Coated samples used for measurement of Surface Roughness. And for each experiment 3 sets of data were taken. The average value was taken as the roughness of each textured sample.
- ix) Comparison between the roughnesses of each textured samples was done in accordance to their effect on the absorption of the material.
- x) If the roughness of a sample increases then the surface irregularities trap the light rays entering the surface and increase the absorbance of the material. The textured samples with the highest roughness are possible to trap the most light and hence show results of maximum absorption.
- xi) The optimum parametric setting for absorbance and surface roughness were founds as a) Power 250 Watts, Nozzle Distance 15mm, Base Material Copper and b) Power 350 Watts, Nozzle Distance 10mm, Base Material Copper respectively.
- xii) It can be concluded that for different parametric set of combinations Laser Surface Texturing increases the surface absorption of an FTO Coated Glass.

## 4.2 Future Scopes

There are several aspects of texturing of FTO Coated Glass to investigate further. The following are some of the areas where the research work can be carried further:

In our present research work we have come to the conclusive part where laser surface texturing increases the absorption of the material in comparison to an un-textured one. Now Perovskites Solar Cells (PVSCs) have made a great progress in the recent days. Researches are going on for the enhancement of the absorption of these solar cells. FTO coated glasses being conducting plates are used as electrodes in these PVSCs [45]. Texturing them and using then along with the solar cells can increase the light trapping effect of the PVSCs and add on to their benefits. Experiments are still in process which shows use of etched FTO coated glass increases their absorption by 13.2% in comparison to an un etched one. Thus further improvements in the quality of the etching process or design of specific patterns or variation in more parametric set of combinations may improve the value of absorbance in the material.

FTO Coated glass are transparent, electrically conductive substrates so laser surface texturing can form anti-reflective coating on the surface and help in trapping of light radiation which can later be suitably converted to energy. In the optical point of view anti-reflective coating will help in increasing the energy conversion efficiency of the material which later can be used in places of need. Our experimentation was based on three parameters i.e. Power, Nozzle Distance and Base Material, other parametric conditions like density of texturing, frequency of the laser radiation and variation of laser wavelength can also be checked upon to see the variation of absorption for textured surface.

## Reference

- [1] Campbell, P. (1993). Enhancement of light absorption from randomizing and geometric textures. *JOSA B*, 10(12), 2410-2415.
- [2] Wong, R. C. P., Hoult, A. P., Kim, J. K., & Yu, T. X. (1997). Improvement of adhesive bonding in aluminium alloys using a laser surface texturing process. *Journal of materials processing technology*, 63(1-3), 579-584.
- [3] De Damborenea, J. (1998). Surface modification of metals by high power lasers. *Surface and Coatings Technology*, 100, 377-382.
- [4] Ozdemir, M., & Sadikoglu, H. (1998). A new and emerging technology: Laser-induced surface modification of polymers. *Trends in Food Science & Technology*, 9(4), 159-167.
- [5] Etsion, I. (2004). Improving tribological performance of mechanical components by laser surface texturing. *Tribology letters*, 17(4), 733-737.
- [6] Kovalchenko, A., Ajayi, O., Erdemir, A., Fenske, G., & Etsion, I. (2005). The effect of laser surface texturing on transitions in lubrication regimes during unidirectional sliding contact. *Tribology International*, 38(3), 219-225.
- [7] Tian, Y. S., Chen, C. Z., Li, S. T., & Huo, Q. H. (2005). Research progress on laser surface modification of titanium alloys. *Applied surface science*, 242(1-2), 177-184.
- [8] Etsion, I. (2005). State of the art in laser surface texturing. *J. Trib.*, 127(1), 248-253.
- [9] Park, M., Chon, B. H., Kim, H. S., Jeoung, S. C., Kim, D., Lee, J. I., ... & Kim, H. R. (2006). Ultrafast laser ablation of indium tin oxide thin films for organic light-emitting diode application. *Optics and Lasers in Engineering*, 44(2), 138-146.
- [10] Ryk, G., & Etsion, I. (2006). Testing piston rings with partial laser surface texturing for friction reduction. *Wear*, 261(7-8), 792-796.
- [11] Xu, M. Y., Li, J., Lilge, L. D., & Herman, P. R. (2006). F2-laser patterning of indium tin oxide (ITO) thin film on glass substrate. *Applied Physics A*, 85(1), 7-10.
- [12] Račiukaitis, G., Brikas, M., Gedvilas, M., & Darčianovas, G. (2007). Patterning of ITO layer on glass with high repetition rate picosecond lasers. *Journal of Laser Micro/Nanoengineering*, 2(1), 1-6.
- [13] Dobrzański, L. A., Drygała, A., Gołombek, K., Panek, P., Bielańska, E., & Zięba, P. (2008). Laser surface treatment of multicrystalline silicon for enhancing optical properties. *Journal of Materials Processing Technology*, 201(1-3), 291-296.

- [14] Vincent, C., Monteil, G., Barriere, T., & Gelin, J. C. (2008). Control of the quality of laser surface texturing. *Microsystem technologies*, 14(9), 1553-1557.
- [15] Wan, Y., & Xiong, D. S. (2008). The effect of laser surface texturing on frictional performance of face seal. *Journal of materials processing technology*, 197(1-3), 96-100.
- [16] Etsion, I., & Sher, E. (2009). Improving fuel efficiency with laser surface textured piston rings. *Tribology International*, 42(4), 542-547.
- [17] Gualtieri, E., Borghi, A., Calabri, L., Pugno, N., & Valeri, S. (2009). Increasing nanohardness and reducing friction of nitride steel by laser surface texturing. *Tribology International*, 42(5), 699-705.
- [18] Krishna, B. V., & Bandyopadhyay, A. (2009). Surface modification of AISI 410 stainless steel using laser engineered net shaping (LENSTM). *Materials & Design*, 30(5), 1490-1496.
- [19] Vilhena, L. M., Sedlaček, M. M. B. J., Podgornik, B., Vižintin, J., Babnik, A., & Možina, J. (2009). Surface texturing by pulsed Nd: YAG laser. *Tribology International*, 42(10), 1496-1504.
- [20] Basu, A., Naqvi, M. M., & Chakraborty, T. K. (2010). Enhancement of transmittance of indium tin oxide coated glass plates.
- [21] Lamraoui, A., Costil, S., Langlade, C., & Coddet, C. (2010). Laser surface texturing (LST) treatment before thermal spraying: A new process to improve the substrate-coating adherence. *Surface and Coatings Technology*, 205, S164-S167.
- [22] Wang, F., Yu, H., Li, J., Sun, X., Wang, X., & Zheng, H. (2010). Optical absorption enhancement in nanopore textured-silicon thin film for photovoltaic application. *Optics letters*, 35(1), 40-42.
- [23] Sher, M. J., Winkler, M. T., & Mazur, E. (2011). Pulsed-laser hyperdoping and surface texturing for photovoltaics. *MRS bulletin*, 36(6), 439-445.
- [24] Chikarakara, E., Naher, S., & Brabazon, D. (2012). High speed laser surface modification of Ti-6Al-4V. *Surface and Coatings Technology*, 206(14), 3223-3229.
- [25] Müller-Meskamp, L., Kim, Y. H., Roch, T., Hofmann, S., Scholz, R., Eckardt, S., ... & Lasagni, A. F. (2012). Efficiency enhancement of organic solar cells by fabricating periodic surface textures using direct laser interference patterning. *Advanced Materials*, 24(7), 906-910.
- [26] Riveiro, A., Soto, R., Comesaña, R., Boutinguiza, M. D., Del Val, J., Quintero, F., ... & Pou, J. (2012). Laser surface modification of PEEK. *Applied Surface Science*, 258(23), 9437-9442.

- [27] Bian, Q., Yu, X., Zhao, B., Chang, Z., & Lei, S. (2013). Femtosecond laser ablation of indium tin-oxide narrow grooves for thin film solar cells. *Optics & laser technology*, 45, 395-401.
- [28] Bathe, R., Sai Krishna, V., Nikumb, S. K., & Padmanabham, G. J. A. P. A. (2014). Laser surface texturing of gray cast iron for improving tribological behavior. *Applied Physics A*, 117(1), 117-123.
- [29] Braun, D., Greiner, C., Schneider, J., & Gumbsch, P. (2014). Efficiency of laser surface texturing in the reduction of friction under mixed lubrication. *Tribology international*, 77, 142-147.
- [30] Calvani, P., Bellucci, A., Girolami, M., Orlando, S., Valentini, V., Lettino, A., & Trucchi, D. M. (2014). Optical properties of femtosecond laser-treated diamond. *Applied Physics A*, 117(1), 25-29.
- [31] Dunn, A., Wlodarczyk, K. L., Carstensen, J. V., Hansen, E. B., Gabzdyl, J., Harrison, P. M., ... & Hand, D. P. (2015). Laser surface texturing for high friction contacts. *Applied Surface Science*, 357, 2313-2319.
- [32] Li, B. J., Huang, L. J., Ren, N. F., Kong, X., Cai, Y. L., & Zhang, J. L. (2015). Two-step preparation of laser-textured Ni/FTO bilayer composite films with high photoelectric properties. *Journal of Alloys and Compounds*, 640, 376-382.
- [33] Nattapat, M., Marimuthu, S., Kamara, A. M., & Esfahani, M. N. (2015). Laser surface modification of carbon fiber reinforced composites. *Materials and Manufacturing Processes*, 30(12), 1450-1456.
- [34] Drygała, A., Dobrzański, L. A., Szindler, M., Szindler, M. M., & Prokopowicz, M. P., & Jonda, E. (2016). Influence of laser texturization surface and atomic layer deposition on optical properties of polycrystalline silicon. *International Journal of Hydrogen Energy*, 41(18), 7563-7567.
- [35] Triana, S. L., & Suryana, R. (2016, November). Effect of wet etching process on the morphology and transmittance of fluorine doped tin oxide (FTO). In *Journal of Physics: Conference Series* (Vol. 776, No. 1, p. 012005). IOP Publishing.
- [36] Wahab, J. A., Ghazali, M. J., Yusoff, W. M. W., & Sajuri, Z. (2016). Enhancing material performance through laser surface texturing: A review. *Transactions of the IMF*, 94(4), 193-198.
- [37] Riveiro, A., Maçon, A. L., del Val, J., Comesaña, R., & Pou, J. (2018). Laser surface texturing of polymers for biomedical applications. *Frontiers in physics*, 6, 16.



- [38] Singh, A., Patel, D. S., Ramkumar, J., & Balani, K. (2019). Single step laser surface texturing for enhancing contact angle and tribological properties. *The International Journal of Advanced Manufacturing Technology*, 100(5), 1253-1267.
- [39] Kim, M. S., Lee, J. H., & Kwak, M. K. (2020). Surface texturing methods for solar cell efficiency enhancement. *International Journal of Precision Engineering and Manufacturing*, 21(7), 1389-1398.
- [40] Yuan, J., Liang, L., & Lin, G. (2020). Study of laser surface texturing of 6061 aluminium with thermal assistance. *Journal of Micromechanics and Microengineering*, 30(3), 035003.
- [41] Tsai, H. Y., Hsu, C. N., Li, C. R., Lin, Y. H., Hsiao, W. T., Huang, K. C., & Yeh, J. A. (2021). Surface wettability and electrical resistance analysis of droplets on indium-tin-oxide glass fabricated using an ultraviolet laser system. *Micromachines*, 12(1), 44.
- [42] Allahyari, E., Nivas, J. J., Oscurato, S. L., Salvatore, M., Ausanio, G., Vecchione, A., ... & Amoroso, S. (2019). Laser surface texturing of copper and variation of the wetting response with the laser pulse fluence. *Applied Surface Science*, 470, 817-824.
- [43] Quazi, M. M., Fazal, M. A., Haseeb, A. S. M. A., Yusof, F., Masjuki, H. H., & Arslan, A. (2016). Laser-based surface modifications of aluminum and its alloys. *Critical Reviews in Solid State and Materials Sciences*, 41(2), 106-131.
- [44] Wang, Z., Zhao, Q., Wang, C., & Zhang, Y. (2015). Modulation of dry tribological property of stainless steel by femtosecond laser surface texturing. *Applied Physics A*, 119(3), 1155-1163.
- [45] Li, J. F., Hao, H. Y., Hao, J. B., Shi, L., Dong, J. J., Liu, H., & Xing, J. (2019, February). Light trapping effect of textured FTO in perovskite solar cells. In *IOP Conference Series: Materials Science and Engineering* (Vol. 479, No. 1, p. 012046). IOP Publishing.

## Appendix

The full set of data of wavelength in accordance to Absorbance and Transmission for experimentation 1

No.	Wavelength(nm)	Abs	Trans(%T)	Energy	Energy(100%T)	Energy(0%T)
1	900.0	0.318	48.1	10024	20862	28
2	899.0	0.318	48.1	10003	20808	28
3	898.0	0.318	48.1	9977	20759	28
4	897.0	0.318	48.1	9947	20699	28
5	896.0	0.318	48.1	9923	20642	28
6	895.0	0.318	48.1	9893	20580	28
7	894.0	0.318	48.1	9864	20517	28
8	893.0	0.318	48.1	9832	20456	28
9	892.0	0.318	48.1	9802	20391	28
10	891.0	0.318	48.1	9770	20328	28
11	890.0	0.318	48.1	9741	20264	28
12	889.0	0.318	48.1	9712	20206	28
13	888.0	0.318	48.1	9685	20147	28
14	887.0	0.318	48.1	9658	20092	28
15	886.0	0.318	48.1	9630	20038	28
16	885.0	0.318	48.1	9604	19980	28
17	884.0	0.318	48.1	19169	39864	70
18	883.0	0.318	48.1	19112	39749	70
19	882.0	0.318	48.1	19057	39619	70
20	881.0	0.318	48.1	18997	39502	70
21	880.0	0.318	48.1	18941	39378	70
22	879.0	0.318	48.1	18883	39259	70
23	878.0	0.318	48.1	18832	39151	70
24	877.0	0.318	48.1	18774	39039	70
25	876.0	0.318	48.1	18727	38924	70
26	875.0	0.318	48.1	18679	38823	70
27	874.0	0.318	48.1	18627	38722	70
28	873.0	0.318	48.1	18580	38611	70
29	872.0	0.318	48.1	18526	38502	70
30	871.0	0.318	48.1	18471	38399	70
31	870.0	0.318	48.1	18430	38295	70
32	869.0	0.318	48.1	18376	38194	70
33	868.0	0.318	48.1	18332	38096	70
34	867.0	0.318	48.1	18293	38005	70
35	866.0	0.318	48.1	18251	37920	70
36	865.0	0.318	48.1	18213	37833	70
37	864.0	0.318	48.1	18178	37765	70
38	863.0	0.318	48.1	18139	37689	70
39	862.0	0.318	48.1	18109	37616	70
40	861.0	0.318	48.1	18080	37544	70
41	860.0	0.318	48.1	18045	37475	70
42	859.0	0.318	48.1	18012	37404	70
43	858.0	0.318	48.1	17984	37342	70
44	857.0	0.318	48.1	17955	37284	70

45	856.0	0.318	48.1	17934	37233	70
46	855.0	0.318	48.1	17913	37186	70
47	854.0	0.318	48.1	17894	37146	70
48	853.0	0.318	48.1	17877	37105	70
49	852.0	0.318	48.1	17867	37076	70
50	851.0	0.318	48.1	17856	37051	70
51	850.0	0.318	48.1	17847	37031	70
52	849.0	0.318	48.1	11553	23895	70
53	848.0	0.317	48.1	11556	23898	70
54	847.0	0.317	48.2	11563	23912	70
55	846.0	0.317	48.2	11569	23919	70
56	845.0	0.317	48.2	11579	23940	70
57	844.0	0.317	48.2	11588	23958	70
58	843.0	0.317	48.2	11603	23982	70
59	842.0	0.317	48.2	11618	24006	70
60	841.0	0.317	48.2	11631	24034	70
61	840.0	0.317	48.2	11652	24068	70
62	839.0	0.317	48.2	11671	24103	70
63	838.0	0.317	48.2	11688	24142	70
64	837.0	0.317	48.2	11714	24183	70
65	836.0	0.317	48.2	11736	24235	70
66	835.0	0.317	48.2	11766	24291	70
67	834.0	0.317	48.2	11794	24347	70
68	833.0	0.317	48.2	11827	24407	70
69	832.0	0.317	48.2	11864	24469	70
70	831.0	0.316	48.3	11897	24534	70
71	830.0	0.316	48.3	11932	24609	70
72	829.0	0.316	48.3	11971	24677	70
73	828.0	0.316	48.3	12006	24752	70
74	827.0	0.316	48.3	12051	24833	70
75	826.0	0.316	48.3	12087	24908	70
76	825.0	0.316	48.3	12135	24999	70
77	824.0	0.316	48.3	12183	25091	70
78	823.0	0.316	48.3	12227	25174	70
79	822.0	0.316	48.4	12286	25291	70
80	821.0	0.315	48.4	12344	25397	70
81	820.0	0.315	48.4	12396	25499	70
82	819.0	0.315	48.4	12449	25606	70
83	818.0	0.315	48.4	12506	25710	70
84	817.0	0.315	48.4	12562	25817	70
85	816.0	0.315	48.5	12623	25935	70
86	815.0	0.315	48.5	12680	26052	70
87	814.0	0.314	48.5	12745	26168	70
88	813.0	0.314	48.5	12810	26296	70
89	812.0	0.314	48.5	12881	26426	70
90	811.0	0.314	48.5	12953	26562	70
91	810.0	0.314	48.6	13025	26704	70
92	809.0	0.314	48.6	13096	26845	70
93	808.0	0.313	48.6	13168	26985	70
94	807.0	0.313	48.6	13242	27127	70
95	806.0	0.313	48.6	13317	27268	70

96	805.0	0.313	48.7	13392	27403	70
97	804.0	0.313	48.7	13465	27543	70
98	803.0	0.312	48.7	13539	27686	70
99	802.0	0.312	48.7	13615	27828	70
100	801.0	0.312	48.7	13692	27979	70
101	800.0	0.312	48.8	13775	28133	70
102	799.0	0.312	48.8	13854	28297	70
103	798.0	0.312	48.8	13948	28460	70
104	797.0	0.311	48.8	14028	28622	70
105	796.0	0.311	48.8	14116	28785	70
106	795.0	0.311	48.9	14203	28949	70
107	794.0	0.311	48.9	14287	29107	70
108	793.0	0.310	48.9	14371	29259	70
109	792.0	0.310	49.0	14455	29418	70
110	791.0	0.310	49.0	14539	29570	70
111	790.0	0.310	49.0	14623	29731	70
112	789.0	0.310	49.0	14709	29894	70
113	788.0	0.309	49.1	14800	30068	70
114	787.0	0.309	49.1	14896	30245	70
115	786.0	0.309	49.1	14990	30419	70
116	785.0	0.309	49.1	15083	30591	70
117	784.0	0.308	49.2	15177	30765	70
118	783.0	0.308	49.2	15268	30932	70
119	782.0	0.308	49.2	15357	31099	70
120	781.0	0.308	49.2	15442	31259	70
121	780.0	0.308	49.3	15528	31427	70
122	779.0	0.307	49.3	15621	31587	70
123	778.0	0.307	49.3	15707	31749	70
124	777.0	0.307	49.3	15799	31917	70
125	776.0	0.307	49.4	15892	32089	70
126	775.0	0.306	49.4	15985	32265	70
127	774.0	0.306	49.4	16083	32440	70
128	773.0	0.306	49.4	16175	32617	70
129	772.0	0.306	49.5	16270	32787	70
130	771.0	0.305	49.5	16360	32951	70
131	770.0	0.305	49.5	16447	33120	70
132	769.0	0.305	49.5	16537	33276	70
133	768.0	0.305	49.6	16622	33435	70
134	767.0	0.305	49.6	16700	33587	70
135	766.0	0.304	49.6	16787	33733	70
136	765.0	0.304	49.6	16866	33885	70
137	764.0	0.304	49.7	16951	34038	70
138	763.0	0.304	49.7	17036	34199	70
139	762.0	0.304	49.7	17138	34388	70
140	761.0	0.303	49.7	17205	34498	70
141	760.0	0.303	49.7	17300	34682	70
142	759.0	0.303	49.8	17416	34892	70
143	758.0	0.303	49.8	17500	35048	70
144	757.0	0.303	49.8	17582	35201	70
145	756.0	0.302	49.8	17662	35344	70
146	755.0	0.302	49.9	17745	35491	70

147	754.0	0.302	49.9	17820	35635	70
148	753.0	0.302	49.9	17903	35779	70
149	752.0	0.302	49.9	17984	35929	70
150	751.0	0.301	49.9	18067	36086	70
151	750.0	0.301	50.0	18146	36227	70
152	749.0	0.301	50.0	18225	36376	70
153	748.0	0.301	50.0	18305	36520	70
154	747.0	0.301	50.0	18382	36656	70
155	746.0	0.301	50.0	18454	36792	70
156	745.0	0.301	50.1	18523	36918	70
157	744.0	0.300	50.1	18590	37044	70
158	743.0	0.300	50.1	18657	37164	70
159	742.0	0.300	50.1	18725	37284	70
160	741.0	0.300	50.1	18792	37411	70
161	740.0	0.300	50.1	18861	37537	70
162	739.0	0.300	50.1	18926	37657	70
163	738.0	0.300	50.2	18989	37774	70
164	737.0	0.300	50.2	19054	37894	70
165	736.0	0.299	50.2	19117	38004	70
166	735.0	0.299	50.2	19172	38110	70
167	734.0	0.299	50.2	19228	38211	70
168	733.0	0.299	50.2	19278	38302	70
169	732.0	0.299	50.2	19330	38396	70
170	731.0	0.299	50.2	19373	38479	70
171	730.0	0.299	50.3	19415	38561	70
172	729.0	0.299	50.3	19467	38643	70
173	728.0	0.299	50.3	19509	38726	70
174	727.0	0.299	50.3	19554	38801	70
175	726.0	0.299	50.3	19591	38879	70
176	725.0	0.299	50.3	19624	38943	70
177	724.0	0.298	50.3	19657	39002	70
178	723.0	0.298	50.3	19693	39061	70
179	722.0	0.298	50.3	19717	39117	70
180	721.0	0.298	50.3	19735	39148	70
181	720.0	0.298	50.3	19757	39183	70
182	719.0	0.298	50.3	19766	39207	70
183	718.0	0.298	50.3	19786	39236	70
184	717.0	0.298	50.3	19800	39258	70
185	716.0	0.298	50.3	19812	39284	70
186	715.0	0.298	50.3	19815	39285	70
187	714.0	0.298	50.3	19813	39282	70
188	713.0	0.298	50.3	19814	39272	70
189	712.0	0.298	50.3	19798	39256	70
190	711.0	0.298	50.3	19782	39226	70
191	710.0	0.298	50.3	19764	39192	70
192	709.0	0.298	50.3	19745	39150	70
193	708.0	0.298	50.3	19718	39096	70
194	707.0	0.298	50.3	19691	39035	70
195	706.0	0.298	50.3	19653	38971	70
196	705.0	0.298	50.3	19614	38885	70
197	704.0	0.298	50.3	19569	38795	70

198	703.0	0.298	50.3	19514	38691	70
199	702.0	0.298	50.3	19452	38577	70
200	701.0	0.298	50.3	19389	38456	70
201	700.0	0.298	50.3	19319	38322	70
202	699.0	0.298	50.3	19247	38186	70
203	698.0	0.298	50.3	19173	38046	70
204	697.0	0.298	50.3	19099	37894	70
205	696.0	0.298	50.3	19014	37737	70
206	695.0	0.298	50.3	18932	37571	70
207	694.0	0.299	50.3	18845	37396	70
208	693.0	0.299	50.3	18746	37205	70
209	692.0	0.299	50.3	18638	37005	70
210	691.0	0.299	50.3	18525	36787	70
211	690.0	0.299	50.2	18405	36559	70
212	689.0	0.299	50.2	18283	36327	70
213	688.0	0.299	50.2	18161	36094	70
214	687.0	0.299	50.2	18041	35857	70
215	686.0	0.299	50.2	17921	35621	70
216	685.0	0.299	50.2	17799	35393	70
217	684.0	0.299	50.2	17677	35157	70
218	683.0	0.300	50.2	17561	34922	70
219	682.0	0.300	50.2	17437	34689	70
220	681.0	0.300	50.1	17310	34443	70
221	680.0	0.300	50.1	17184	34199	70
222	679.0	0.300	50.1	17052	33947	70
223	678.0	0.300	50.1	16926	33699	70
224	677.0	0.300	50.1	16798	33463	70
225	676.0	0.300	50.1	16681	33240	70
226	675.0	0.301	50.1	16568	33024	70
227	674.0	0.301	50.0	16461	32823	70
228	673.0	0.301	50.0	16360	32640	70
229	672.0	0.301	50.0	16268	32457	70
230	671.0	0.301	50.0	16180	32294	70
231	670.0	0.301	50.0	16094	32134	70
232	669.0	0.301	50.0	16016	31975	70
233	668.0	0.302	49.9	15931	31827	70
234	667.0	0.302	49.9	15856	31684	70
235	666.0	0.302	49.9	15785	31550	70
236	665.0	0.302	49.9	15722	31437	70
237	664.0	0.302	49.9	15665	31332	70
238	663.0	0.302	49.9	15611	31240	70
239	662.0	0.302	49.8	15569	31156	70
240	661.0	0.303	49.8	15529	31089	70
241	660.0	0.303	49.8	15497	31025	70
242	659.0	0.303	49.8	15464	30974	70
243	658.0	0.303	49.8	15433	30922	70
244	657.0	0.303	49.8	15408	30888	70
245	656.0	0.303	49.8	15388	30852	70
246	655.0	0.303	49.7	15369	30824	70
247	654.0	0.303	49.7	15357	30811	70
248	653.0	0.304	49.7	15349	30802	70

249	652.0	0.304	49.7	15340	30803	70
250	651.0	0.304	49.7	15341	30809	70
251	650.0	0.304	49.6	15339	30825	70
252	649.0	0.304	49.6	15352	30846	70
253	648.0	0.304	49.6	15361	30873	70
254	647.0	0.304	49.6	15373	30903	70
255	646.0	0.304	49.6	15388	30944	70
256	645.0	0.305	49.6	15404	30989	70
257	644.0	0.305	49.6	15429	31043	70
258	643.0	0.305	49.6	15454	31103	70
259	642.0	0.305	49.5	15476	31170	70
260	641.0	0.305	49.5	15509	31242	70
261	640.0	0.305	49.5	15541	31311	70
262	639.0	0.305	49.5	15573	31383	70
263	638.0	0.306	49.5	15602	31463	70
264	637.0	0.306	49.5	15636	31543	70
265	636.0	0.306	49.4	15672	31617	70
266	635.0	0.306	49.4	15708	31695	70
267	634.0	0.306	49.4	15745	31773	70
268	633.0	0.306	49.4	15780	31857	70
269	632.0	0.306	49.4	15816	31939	70
270	631.0	0.306	49.4	15859	32030	70
271	630.0	0.306	49.4	15894	32117	70
272	629.0	0.307	49.4	15935	32195	70
273	628.0	0.307	49.4	15966	32277	70
274	627.0	0.307	49.3	16003	32355	70
275	626.0	0.307	49.3	16036	32425	70
276	625.0	0.307	49.3	16071	32506	70
277	624.0	0.307	49.3	16104	32576	70
278	623.0	0.307	49.3	16137	32650	70
279	622.0	0.307	49.3	16166	32720	70
280	621.0	0.307	49.3	16207	32798	70
281	620.0	0.307	49.3	16241	32877	70
282	619.0	0.307	49.3	16282	32966	70
283	618.0	0.308	49.2	16318	33056	70
284	617.0	0.308	49.2	16359	33149	70
285	616.0	0.308	49.2	16402	33245	70
286	615.0	0.308	49.2	16453	33347	70
287	614.0	0.308	49.2	16499	33454	70
288	613.0	0.308	49.2	16552	33568	70
289	612.0	0.308	49.2	16612	33693	70
290	611.0	0.308	49.2	16677	33828	70
291	610.0	0.308	49.2	16748	33977	70
292	609.0	0.308	49.2	16830	34153	70
293	608.0	0.308	49.2	16923	34354	70
294	607.0	0.309	49.1	17030	34584	70
295	606.0	0.309	49.1	17147	34840	70
296	605.0	0.309	49.1	17277	35121	70
297	604.0	0.309	49.1	17417	35424	70
298	603.0	0.309	49.1	17577	35759	70
299	602.0	0.309	49.0	17746	36110	70

300	601.0	0.310	49.0	17930	36495	70
301	600.0	0.310	49.0	18128	36917	70
302	599.0	0.310	49.0	18344	37371	70
303	598.0	0.310	49.0	18583	37874	70
304	597.0	0.310	49.0	18859	38454	70
305	596.0	0.310	48.9	19171	39107	70
306	595.0	0.311	48.9	19513	39827	70
307	594.0	0.311	48.9	9929	20292	28
308	593.0	0.311	48.9	10123	20698	28
309	592.0	0.311	48.8	10318	21105	28
310	591.0	0.311	48.8	10509	21502	28
311	590.0	0.312	48.8	10681	21864	28
312	589.0	0.312	48.8	10826	22161	28
313	588.0	0.312	48.8	10926	22369	28
314	587.0	0.312	48.8	10963	22447	28
315	586.0	0.308	49.2	10918	22353	28
316	585.0	0.303	49.8	10761	22023	28
317	584.0	0.293	51.0	14698	27989	154
318	583.0	0.288	51.6	14294	27214	154
319	582.0	0.284	52.0	13744	26143	154
320	581.0	0.284	52.0	13101	24912	154
321	580.0	0.284	52.0	12465	23670	154
322	579.0	0.284	52.0	11881	22543	154
323	578.0	0.283	52.1	11390	21603	154
324	577.0	0.283	52.1	11006	20874	154
325	576.0	0.283	52.1	10731	20327	154
326	575.0	0.283	52.1	10548	19981	154
327	574.0	0.283	52.1	10454	19794	154
328	573.0	0.283	52.1	10433	19768	154
329	572.0	0.283	52.1	10510	19913	154
330	571.0	0.283	52.1	10656	20211	154
331	570.0	0.284	52.0	10880	20659	154
332	569.0	0.284	52.0	11181	21274	154
333	568.0	0.285	51.9	11595	22075	154
334	567.0	0.285	51.9	12231	23331	154
335	566.0	0.286	51.8	12862	24594	154
336	565.0	0.286	51.7	13376	25597	154
337	564.0	0.287	51.7	13854	26544	154
338	563.0	0.287	51.6	14306	27450	154
339	562.0	0.288	51.6	14741	28320	154
340	561.0	0.288	51.5	15155	29121	154
341	560.0	0.288	51.5	15488	29789	154
342	559.0	0.289	51.4	15672	30180	154
343	558.0	0.289	51.4	15657	30164	154
344	557.0	0.290	51.3	15400	29700	154
345	556.0	0.290	51.3	14923	28787	154
346	555.0	0.290	51.3	14276	27536	154
347	554.0	0.290	51.3	13563	26139	154
348	553.0	0.290	51.3	12832	24719	154
349	552.0	0.290	51.3	12140	23383	154
350	551.0	0.290	51.3	11521	22163	154



351	550.0	0.289	51.3	10981	21110	154
352	549.0	0.289	51.4	10522	20219	154
353	548.0	0.289	51.4	20250	38917	329
354	547.0	0.290	51.3	19626	37682	329
355	546.0	0.290	51.3	19112	36727	329
356	545.0	0.290	51.3	18712	36010	329
357	544.0	0.290	51.3	18441	35473	329
358	543.0	0.291	51.2	18256	35140	329
359	542.0	0.291	51.2	18418	35494	329
360	541.0	0.292	51.1	18626	35968	329
361	540.0	0.292	51.1	18728	36166	329
362	539.0	0.292	51.0	18733	36228	329
363	538.0	0.293	51.0	18720	36237	329
364	537.0	0.293	50.9	18693	36173	329
365	536.0	0.293	50.9	18614	36071	329
366	535.0	0.294	50.8	18521	35940	329
367	534.0	0.294	50.8	18416	35777	329
368	533.0	0.295	50.7	18303	35597	329
369	532.0	0.295	50.7	18190	35384	329
370	531.0	0.296	50.6	18068	35195	329
371	530.0	0.296	50.6	17951	34976	329
372	529.0	0.296	50.6	17850	34772	329
373	528.0	0.296	50.6	17720	34562	329
374	527.0	0.296	50.5	17607	34340	329
375	526.0	0.297	50.5	17468	34115	329
376	525.0	0.297	50.4	17334	33892	329
377	524.0	0.298	50.4	17214	33646	329
378	523.0	0.298	50.4	17074	33392	329
379	522.0	0.298	50.3	16946	33152	329
380	521.0	0.298	50.3	16807	32912	329
381	520.0	0.299	50.3	16677	32680	329
382	519.0	0.299	50.3	16561	32443	329
383	518.0	0.299	50.2	16423	32201	329
384	517.0	0.299	50.2	16316	31991	329
385	516.0	0.299	50.2	16201	31775	329
386	515.0	0.300	50.2	16074	31559	329
387	514.0	0.300	50.2	15969	31335	329
388	513.0	0.300	50.1	15844	31122	329
389	512.0	0.300	50.1	15725	30891	329
390	511.0	0.300	50.1	15605	30663	329
391	510.0	0.300	50.1	15482	30428	329
392	509.0	0.300	50.1	15368	30209	329
393	508.0	0.301	50.0	15248	29998	329
394	507.0	0.301	50.0	15145	29783	329
395	506.0	0.301	50.0	15040	29586	329
396	505.0	0.301	50.0	14934	29394	329
397	504.0	0.301	50.0	14851	29210	329
398	503.0	0.301	50.0	14740	29021	329
399	502.0	0.301	50.0	14637	28837	329
400	501.0	0.301	50.0	14560	28657	329
401	500.0	0.302	49.9	14453	28456	329

402	499.0	0.302	49.9	14342	28262	329
403	498.0	0.302	49.9	14242	28067	329
404	497.0	0.302	49.9	14150	27874	329
405	496.0	0.302	49.8	14032	27687	329
406	495.0	0.303	49.8	13935	27495	329
407	494.0	0.303	49.8	13825	27313	329
408	493.0	0.303	49.8	13740	27141	329
409	492.0	0.303	49.8	13658	26949	329
410	491.0	0.303	49.7	13555	26791	329
411	490.0	0.303	49.7	13469	26610	329
412	489.0	0.304	49.7	13364	26430	329
413	488.0	0.304	49.6	13263	26250	329
414	487.0	0.305	49.6	13152	26074	329
415	486.0	0.305	49.5	13054	25884	329
416	485.0	0.306	49.5	12942	25699	329
417	484.0	0.306	49.4	12822	25527	329
418	483.0	0.306	49.4	12753	25350	329
419	482.0	0.307	49.3	12644	25167	329
420	481.0	0.307	49.3	12542	25008	329
421	480.0	0.308	49.2	12453	24840	329
422	479.0	0.309	49.1	12347	24670	329
423	478.0	0.309	49.1	12260	24506	329
424	477.0	0.310	49.0	12152	24326	329
425	476.0	0.310	48.9	12036	24134	329
426	475.0	0.311	48.8	11909	23928	329
427	474.0	0.312	48.8	11797	23740	329
428	473.0	0.313	48.7	11678	23533	329
429	472.0	0.314	48.6	11563	23345	329
430	471.0	0.315	48.5	11434	23147	329
431	470.0	0.316	48.4	11319	22956	329
432	469.0	0.316	48.3	11203	22741	329
433	468.0	0.317	48.2	11099	22546	329
434	467.0	0.318	48.1	10969	22344	329
435	466.0	0.319	48.0	10856	22137	329
436	465.0	0.320	47.9	10716	21915	329
437	464.0	0.321	47.8	10575	21669	329
438	463.0	0.322	47.6	10420	21411	329
439	462.0	0.323	47.5	10270	21165	329
440	461.0	0.324	47.4	10111	20877	329
441	460.0	0.325	47.3	9975	20608	329
442	459.0	0.326	47.2	9808	20331	329
443	458.0	0.327	47.1	9653	20038	329
444	457.0	0.328	47.0	19021	39549	675
445	456.0	0.329	46.8	18713	38964	675
446	455.0	0.330	46.7	18377	38391	675
447	454.0	0.332	46.6	18060	37769	675
448	453.0	0.333	46.5	17710	37141	675
449	452.0	0.334	46.4	17385	36491	675
450	451.0	0.338	45.9	17003	35797	675
451	450.0	0.344	45.3	16675	35116	675
452	449.0	0.354	44.2	14286	32581	329

453	448.0	0.360	43.6	14703	33578	329
454	447.0	0.364	43.2	15078	34530	329
455	446.0	0.365	43.1	15447	35426	329
456	445.0	0.366	43.0	15776	36260	329
457	444.0	0.367	43.0	16084	37064	329
458	443.0	0.368	42.9	16390	37822	329
459	442.0	0.368	42.8	16672	38545	329
460	441.0	0.369	42.8	16940	39240	329
461	440.0	0.370	42.7	17202	39907	329
462	439.0	0.370	42.6	8715	20259	154
463	438.0	0.371	42.6	8810	20533	154
464	437.0	0.372	42.5	8911	20787	154
465	436.0	0.372	42.4	8991	20994	154
466	435.0	0.373	42.4	9062	21199	154
467	434.0	0.373	42.4	9134	21376	154
468	433.0	0.374	42.3	9184	21533	154
469	432.0	0.374	42.3	9243	21682	154
470	431.0	0.375	42.2	9287	21816	154
471	430.0	0.375	42.2	9318	21918	154
472	429.0	0.376	42.1	9349	22016	154
473	428.0	0.376	42.1	9379	22092	154
474	427.0	0.376	42.0	9391	22149	154
475	426.0	0.377	42.0	9396	22184	154
476	425.0	0.377	42.0	9397	22200	154
477	424.0	0.378	41.9	9382	22209	154
478	423.0	0.378	41.9	9375	22202	154
479	422.0	0.378	41.8	9356	22164	154
480	421.0	0.379	41.8	9321	22123	154
481	420.0	0.379	41.8	9293	22060	154
482	419.0	0.380	41.7	9250	21979	154
483	418.0	0.380	41.7	9193	21873	154
484	417.0	0.381	41.6	9142	21756	154
485	416.0	0.381	41.6	9072	21611	154
486	415.0	0.382	41.5	8979	21451	154
487	414.0	0.382	41.4	8902	21272	154
488	413.0	0.383	41.4	8808	21079	154
489	412.0	0.384	41.3	8714	20886	154
490	411.0	0.385	41.2	8609	20683	154
491	410.0	0.386	41.2	8505	20473	154
492	409.0	0.386	41.1	8411	20253	154
493	408.0	0.387	41.0	8300	20026	154
494	407.0	0.388	40.9	16406	39618	329
495	406.0	0.389	40.8	16160	39135	329
496	405.0	0.390	40.7	15919	38613	329
497	404.0	0.391	40.6	15644	38072	329
498	403.0	0.393	40.5	15369	37494	329
499	402.0	0.394	40.3	15069	36902	329
500	401.0	0.396	40.2	14774	36317	329
501	400.0	0.398	40.0	14483	35713	329
502	399.0	0.399	39.9	14205	35122	329
503	398.0	0.401	39.7	13907	34548	329

504	397.0	0.402	39.6	13640	33971	329
505	396.0	0.404	39.4	13362	33390	329
506	395.0	0.406	39.3	13082	32805	329
507	394.0	0.407	39.1	12794	32198	329
508	393.0	0.409	39.0	12500	31575	329
509	392.0	0.412	38.8	12176	30920	329
510	391.0	0.414	38.6	11859	30229	329
511	390.0	0.417	38.3	11517	29541	329
512	389.0	0.419	38.1	11204	28876	329
513	388.0	0.421	37.9	10905	28225	329
514	387.0	0.423	37.8	10610	27566	329
515	386.0	0.425	37.6	10334	26944	329
516	385.0	0.427	37.4	10047	26339	329
517	384.0	0.429	37.2	9785	25737	329
518	383.0	0.431	37.0	9520	25159	329
519	382.0	0.433	36.9	9268	24577	329
520	381.0	0.435	36.8	9022	23980	329
521	380.0	0.436	36.7	8777	23370	329
522	379.0	0.437	36.5	8515	22770	329
523	378.0	0.438	36.4	8301	22201	329
524	377.0	0.440	36.3	8079	21661	329
525	376.0	0.440	36.3	7881	21152	329
526	375.0	0.441	36.2	7694	20676	329
527	374.0	0.442	36.1	7517	20226	329
528	373.0	0.443	36.1	14745	39649	675
529	372.0	0.444	36.0	14416	38905	675
530	371.0	0.441	36.2	14147	38195	675
531	370.0	0.437	36.5	13865	37465	675
532	369.0	0.429	37.2	12359	27719	2778
533	368.0	0.426	37.5	12707	28645	2778
534	367.0	0.426	37.5	12887	29524	2778
535	366.0	0.428	37.3	13105	30220	2778
536	365.0	0.429	37.2	13266	30740	2778
537	364.0	0.429	37.2	13465	31019	2778
538	363.0	0.431	37.1	13481	31265	2778
539	362.0	0.433	36.9	13454	31459	2778
540	361.0	0.436	36.7	13407	31540	2778
541	360.0	0.438	36.5	13405	31532	2778
542	359.0	0.440	36.3	13258	31466	2778
543	358.0	0.442	36.2	13166	31276	2778
544	357.0	0.444	36.0	13105	31112	2778
545	356.0	0.445	35.9	12952	30876	2778
546	355.0	0.449	35.6	12685	30556	2778
547	354.0	0.451	35.4	12606	30151	2778
548	353.0	0.455	35.0	12309	29753	2778
549	352.0	0.459	34.7	12050	29247	2778
550	351.0	0.464	34.3	11766	28658	2778
551	350.0	0.469	34.0	11451	28140	2778
552	349.0	0.472	33.7	11200	27524	2778
553	348.0	0.476	33.4	10928	26836	2778
554	347.0	0.481	33.0	10578	26183	2778

555	346.0	0.487	32.6	10276	25525	2778
556	345.0	0.493	32.1	9916	24844	2778
557	344.0	0.498	31.7	9633	24139	2778
558	343.0	0.504	31.4	9329	23456	2778
559	342.0	0.510	30.9	9044	22875	2778
560	341.0	0.522	30.0	8746	22249	2778
561	340.0	0.539	28.9	8527	21752	2778
562	339.0	0.565	27.2	10111	36598	675
563	338.0	0.583	26.1	10051	37032	675
564	337.0	0.599	25.2	9984	37501	675
565	336.0	0.609	24.6	9881	37966	675
566	335.0	0.619	24.0	9772	38399	675
567	334.0	0.630	23.4	9643	38859	675
568	333.0	0.641	22.8	9541	39376	675
569	332.0	0.654	22.2	9411	39920	675
570	331.0	0.668	21.5	4628	20262	329
571	330.0	0.684	20.7	4527	20534	329
572	329.0	0.700	20.0	4404	20809	329
573	328.0	0.716	19.2	4338	21087	329
574	327.0	0.734	18.5	4232	21391	329
575	326.0	0.752	17.7	4119	21735	329
576	325.0	0.772	16.9	3997	22029	329
577	324.0	0.793	16.1	3886	22373	329
578	323.0	0.816	15.3	3760	22710	329
579	322.0	0.841	14.4	3626	23048	329
580	321.0	0.868	13.5	3470	23439	329
581	320.0	0.899	12.6	3291	23790	329
582	319.0	0.933	11.7	3117	24167	329
583	318.0	0.969	10.7	2935	24590	329
584	317.0	1.008	9.8	2743	24957	329
585	316.0	1.049	8.9	2563	25347	329
586	315.0	1.093	8.1	2371	25735	329
587	314.0	1.139	7.3	2197	26116	329
588	313.0	1.187	6.5	2025	26515	329
589	312.0	1.238	5.8	1859	26910	329
590	311.0	1.291	5.1	1712	27271	329
591	310.0	1.350	4.5	1543	27665	329
592	309.0	1.414	3.9	1394	28086	329
593	308.0	1.485	3.3	1240	28512	329
594	307.0	1.560	2.8	1113	28955	329
595	306.0	1.643	2.3	978	29388	329
596	305.0	1.726	1.9	870	29811	329
597	304.0	1.816	1.5	767	30226	329
598	303.0	1.903	1.3	711	30635	329
599	302.0	2.000	1.0	628	31030	329
600	301.0	2.098	0.8	561	31421	329
601	300.0	2.194	0.6	525	31784	329
602	299.0	2.288	0.5	489	32151	329
603	298.0	2.383	0.4	461	32493	329
604	297.0	2.489	0.3	435	32834	329
605	296.0	2.604	0.2	402	33176	329

606	295.0	2.718	0.2	385	33485	329
607	294.0	2.800	0.2	387	33785	329
608	293.0	2.901	0.1	365	34047	329
609	292.0	2.948	0.1	368	34282	329
610	291.0	3.000	0.1	358	34509	329
611	290.0	3.000	0.1	363	34748	329
612	289.0	3.000	0.1	365	34976	329
613	288.0	3.000	0.1	353	35232	329
614	287.0	3.000	0.1	364	35504	329
615	286.0	3.000	0.1	357	35811	329
616	285.0	3.000	0.1	357	36157	329
617	284.0	3.000	0.1	359	36516	329
618	283.0	3.000	0.1	345	36877	329
619	282.0	3.000	0.1	352	37218	329
620	281.0	3.000	0.1	354	37553	329
621	280.0	3.000	0.1	348	37886	329
622	279.0	3.000	0.1	358	38226	329
623	278.0	3.000	0.1	355	38560	329
624	277.0	3.000	0.1	348	38907	329
625	276.0	3.000	0.1	346	39297	329
626	275.0	3.000	0.1	352	39703	329
627	274.0	3.000	0.1	353	40173	329
628	273.0	3.000	0.1	167	20363	154
629	272.0	3.000	0.1	167	20678	154
630	271.0	3.000	0.1	170	21062	154
631	270.0	3.000	0.1	168	21468	154
632	269.0	3.000	0.1	166	21868	154
633	268.0	3.000	0.1	168	22262	154
634	267.0	3.000	0.1	167	22646	154
635	266.0	3.000	0.1	167	23275	154
636	265.0	3.000	0.1	165	23740	154
637	264.0	3.000	0.1	167	24160	154
638	263.0	3.000	0.1	167	24658	154
639	262.0	3.000	0.0	166	25212	154
640	261.0	3.000	0.0	165	25690	154
641	260.0	3.000	0.0	169	26218	154
642	259.0	3.000	0.0	166	26877	154
643	258.0	3.000	0.0	166	27484	154
644	257.0	3.000	0.0	167	28119	154
645	256.0	3.000	0.0	165	28801	154
646	255.0	3.000	0.0	164	29423	154
647	254.0	3.000	0.0	164	30020	154
648	253.0	3.000	0.0	166	30645	154
649	252.0	3.000	0.0	165	31264	154
650	251.0	3.000	0.0	169	31935	154
651	250.0	3.000	0.0	170	32607	154
652	249.0	3.000	0.0	166	33272	154
653	248.0	3.000	0.0	170	33980	154
654	247.0	3.000	0.0	166	34680	154
655	246.0	3.000	0.0	164	35391	154
656	245.0	3.000	0.0	167	36105	154

657	244.0	3.000	0.0	168	36750	154
658	243.0	3.000	0.0	167	37370	154
659	242.0	3.000	0.0	163	37941	154
660	241.0	3.000	0.0	167	38461	154
661	240.0	3.000	0.0	168	38918	154
662	239.0	3.000	0.0	165	39305	154
663	238.0	3.000	0.0	167	39623	154
664	237.0	3.000	0.0	166	39852	154
665	236.0	3.000	0.0	168	39987	154
666	235.0	3.000	0.0	164	40010	154
667	234.0	3.000	0.0	167	39898	154
668	233.0	3.000	0.0	168	39659	154
669	232.0	3.000	0.0	164	39361	154
670	231.0	3.000	0.0	168	38996	154
671	230.0	3.000	0.0	165	38599	154
672	229.0	3.000	0.0	166	38212	154
673	228.0	3.000	0.0	164	37815	154
674	227.0	3.000	0.0	169	37446	154
675	226.0	3.000	0.0	166	37073	154
676	225.0	3.000	0.0	164	36699	154
677	224.0	3.000	0.0	166	36321	154
678	223.0	3.000	0.0	168	35938	154
679	222.0	3.000	0.0	162	35549	154
680	221.0	3.000	0.0	165	35126	154
681	220.0	3.000	0.0	168	34671	154
682	219.0	3.000	0.0	164	34144	154
683	218.0	3.000	0.0	166	33530	154
684	217.0	3.000	0.0	166	32791	154
685	216.0	3.000	0.0	163	31838	154
686	215.0	3.000	0.0	166	30533	154
687	214.0	3.000	0.0	166	28605	154
688	213.0	3.000	0.0	166	26293	154
689	212.0	3.000	0.1	167	24926	154
690	211.0	3.000	0.1	164	23837	154
691	210.0	3.000	0.1	168	22080	154
692	209.0	3.000	0.1	168	20012	154
693	208.0	3.000	0.1	166	18693	154
694	207.0	3.000	0.1	343	35758	329
695	206.0	3.000	0.1	355	33695	329
696	205.0	3.000	0.1	354	31547	329
697	204.0	3.000	0.1	351	30401	329
698	203.0	3.000	0.1	355	29394	329
699	202.0	2.981	0.1	356	28239	329
700	201.0	2.938	0.1	361	26833	329
701	200.0	2.926	0.1	358	25692	329